Department of Chemical Engineering

Wavelet Based Dynamic Modelling of Simulated Moving Bed Chromatographic Processes

Hong Mei Yao

This thesis is presented for the Degree of

Doctor of Philosophy

of

Curtin University of Technology

May 2009

DECLARATION

To the best of my knowledge and belief this thesis contains no material previously published by any other person except where due acknowledgement has been made. This thesis contains no material which has been accepted for the award of any other degree or diploma in any university.

Signature:_____

Date:_____

ABSTRACT

Simulated moving bed chromatography process (SMBCP) is the technical realisation of a countercurrent adsorption process through the cyclic port switching. SMB technology reduces the cost of packing material with high loading capacity and provides high purity and high recovery in a very short time. Major commodity applications have been found in the petroleum, food, biotechnology, pharmaceutical and fine chemical industries. The industrial applications bring an emergent demand to improve the SMBCP operation for higher product quality, productivity, efficiency and robustness. However, for this particular process, we encounter several challenges. Firstly, the interplay of the effects of strong nonlinearities, competition of solutes, mass transfer resistance and fluid dynamic dispersion produces steep concentration fronts. Mathematical model accounted for this particular property constitutes a serious difficulty for the solution procedure. Secondly, a dynamic SMB model consists of a set of partial differential, ordinary differential and algebraic equations, which are highly coupled. The large size is a problem due to its intensive computation when on-line optimisation and real-time control are necessary. Thirdly, the SMB unit operation exhibits complex dynamics. Process metrics for design and operation can be determined only when a cyclic steady state is reached after a certain number of switching. Achieving this steady state by solving the PDE models cycle after cycle involves expensive calculation. Studies have been carried out to solve these problems through process analysis, investigation on spatial discretisation techniques, and development of an accelerated integration scheme.

Through a systematic study on the advances of SMB modelling, design and control, a set of functionally equivalent models for SMBCP are identified and summarized for their practical applications. The limitations of the existing modelling techniques in industrial applications are also identified. Furthermore, structural analysis of the existing models is conducted for a better understanding of the functionality and suitability of each model. Suggestions are given on how to choose an appropriate model with sufficient accuracy while keeping the computational demand reasonably low for real time control.

Effort is made on to the systematic investigation of different numerical methods for the solution of PDEs to circumvent the steep gradients encountered in chromatographic separation. Comprehensive studies are conducted on a single column chromatographic process represented by a transport-dispersive-equilibrium linear model. Numerical solutions from the upwind-1 finite difference, wavelet-collocation, and high resolution methods are evaluated by quantitative comparisons with the analytical solution for a range of Peclet numbers. It reveals that for a PDE system with a low Peclet number, all existing numerical

methods work well, but the upwind finite difference method consumes the most time for the same degree of accuracy of the numerical solution. The high resolution method provides an accurate numerical solution for a PDE system with a medium Peclet number. The wavelet collocation method is capable of catching up steep changes in the solution, and thus can be used for solving PDE models with high singularity.

The advantages and disadvantages of the wavelet based approaches are further investigated through several case studies on real SMBCP system. A glucose-fructose separation process is firstly chosen with its relatively simple isotherm representations. Simulations are conducted using both wavelet collocation and upwind finite difference methods. For more complicated applications, an enantiomers separation process is selected. As the PDEs model exhibit a certain degree of singularity, wavelet collocation and high resolution methods are adopted for spatial discretisation. It is revealed that both the wavelet based approaches and high resolution methods are good candidates in terms of computation demand and prediction accuracy on the steep front. This is the first time that these two frontier numerical methods are used for such a complex SMB system models and our results are encouraging for the development of model-based online control scheme.

In developing a new scheme to rapidly obtain the solution at steady state for any arbitrary initial condition, the concept of Quasi-Envelope (QE) is adopted under the consideration that a SMBCP can be treated as a pseudo-oscillatory process because of a large number of continuous switching. The scheme allows larger steps to be taken to predict the slow change of starting state within each switching. Combined with previously developed wavelet-based technique, this method is successfully applied to the simulation of a SMB sugar separation process. Investigations are also carried out on the location of proper starting point for the algorithm and on the effect of changing stepsize to the convergence of iteration method. It is found that if the starting state of Quasi-Envelope is chosen to be the same as the original function, the multivalue algorithm would require similar computational effort to achieve the steady state prediction, regardless of the integration stepsize. If using constant stepsize, launching QE later is helpful when quasi-envelope displays steep change at the start-up period. A changing stepsize produces slow convergence compared to the constant stepsize strategy, thus increasing the work load where the stepsize change is occurring. Other iteration method is required to be imposed to achieve faster convergence right from the beginning. Potential applications can be seen for other chemical engineering processes with inherent cyclic behaviour.

ACKNOWLEDGMENTS

Upon completion of this thesis, I would like to express my gratitude and appreciation to my principal supervisor Professor Moses Oludayo Tadé for his academic stimulation, constructive advice, and wonderful pastoral care throughout my entire research.

My sincere thanks are also extended to my co-supervisor Associate Professor Yu-Chu Tian of Queensland University of Technology. This research was inspired from his initiative. His vast experience in research and his technical insight have been the valuable source of guidance for this project.

I am also thankful to Dr. Tonghua Zhang for the open and helpful discussions on the numerical computing issues at various stages of this study.

This research is conducted with the support of the Australian Postgraduate Award (APA) and I would also like to acknowledge the support of the Department of Chemical Engineering, Curtin University of Technology.

Last but not least, this study would not have been possible without the support and understanding of my husband Charles Zhao and my two lovely children Sarah and Dennis. This dissertation is attributed to you all!

BIOGRAPHY AND PUBLICATIONS

Hong Mei Yao obtained her Bachelor of Engineering in 1988 and Master of Process Engineering in 1990 from East China University of Science and Technology, China. Then she worked as a process engineer and HR officer in Shanghai. She received her Master's degree in Chemical Engineering from Curtin University of Technology, Australia, in 1999. She commenced her PhD study at the Department of Chemical Engineering in February 2006.

Since 1995, she has been working in the Department of Chemical Engineering and Engineering Faculty in the capacity of tutoring various units and supervising research & design projects. Over the years she has also been a part-time Research Assistant in many funded projects. From October 2006, she has been serving as Editorial Assistant for the international journal: Asia-Pacific Journal of Chemical Engineering.

Her general areas of interests and research activities have covered a broad range of subject areas, including bioprocess (fermentation), combustion process, wastewater treatment, industrial waste management (refinery residue), and separation process (simulated moving bed chromatography). Her specific interests and expertise are in modelling, simulation, optimisation, and control design for industrial complex system using frontier mathematical tools (wavelets, high resolution, adaptive discretisation, neural networks, component analysis, and cluster analysis).

Papers in Support of This Thesis

Yao, H M, Zhang, T H, Tadé, M O and Tian, Y C (2008): Book Chapter - Wavelet Based Approaches and High Resolution Methods for Complex Process Models, Computational Chemistry – Frontier, in press.

Yao, H M, Tian, Y C and Tadé, M O (2008): *Using Wavelets for Solving SMB Separation Process Models*, Industrial & Chemical Engineering Research, 47, 5585-5593.

Yao, H M, Tadé, M O and Tian, Y C (2008): *Transit and Steady State Prediction by Wavelet: Application to the SMB Separation Process*, APCChE '2008, The 12th Asia-Pacific Congress of Chemical Engineering, Dalian, China, August.

Yao, H M, Tadé, M O and Tian, Y C: *Accelerated Computation of Cyclic Steady State for Simulated-Moving-Bed Processes*, submitted.

Yao, H M, Tadé, M O and Tian, Y C: *Integrated Solution Strategy for Fast and Accurate Simulation of Cyclic Processes*. in preparation.

TABLE OF CONTENTS

4. SPATIAL DISCRETISATION FOR SINGLE COLUMN MODEL

5. NUMERICAL SOLUTION OF SMBCP MODEL

6. ACCELERATING THE STEADY STATE DETERMINATION

7. CONCLUSIONS AND RECOMMENDATIONS

REFERENCES

LIST OF FIGURES

LIST OF TABLES

CHAPTER 1
INTRODUCTION

1.1 Background of SMB Chromatographic Separation Processes

Separation processes are significant in various industries. They have been estimated as accounting for 40% to 70% of the capital and operating costs in chemical industries (Spear, 2006). Energy-intensive separation processes like distillation are facing increasing challenges from other alternative technologies. Just like membrane technologies are offering a viable alternative to some traditional separation processes, so is the simulated moving bed (SMB) chromatography.

Chromatography is typically used in laboratories for efficient separation of mixtures of chemical compounds using the phenomenon of adsorption. The basic principle is the use of the different adsorption behaviour of components in the milieu of solvent and adsorbent. The specific separation method of "Column Chromatography" uses a glass column filled with adsorbent through which passes a composite liquid mixture. The technique operates such that each component will form in a different section of the column arranged by colour according to the adsorption affinity of each material. If appropriate desorbent is poured into the column, the components that have been adsorbed on the adsorbent dissolve into the desorbent and start moving downwards in the column with different migration rates. The components in the lower layers move faster. The liquids can then be collected from the bottom of the column as they drip out.

Strictly speaking, a chromatographic process requires that (1) the adsorbent is contained within a fixed bed; and (2) the mixture to be separated is introduced as a pulse into a flowing stream of a carrier fluid. In broader sense, the term chromatography is used to include any separation process that depends on partition between a flowing fluid and a solid adsorbent (Ruthven, 1984). Chromatography was initially developed for extraction and purification of complex mixtures of vegetal origin; and later it achieved rapid growth and has now become a ubiquitous analytical method. The strengths of the technique are especially manifested in the separation of isomers and natural materials.

SMB chromatography is the technical realisation of a countercurrent adsorption process, approximating the countercurrent flow by a cyclic port switching. It consists of a certain

number of chromatographic columns connected in series; and the countercurrent movement is achieved by sequentially switching the inlet and outlet ports of one column downwards in the direction of the liquid flow after a certain period of time. This mechanism is illustrated in Figure 1.1.

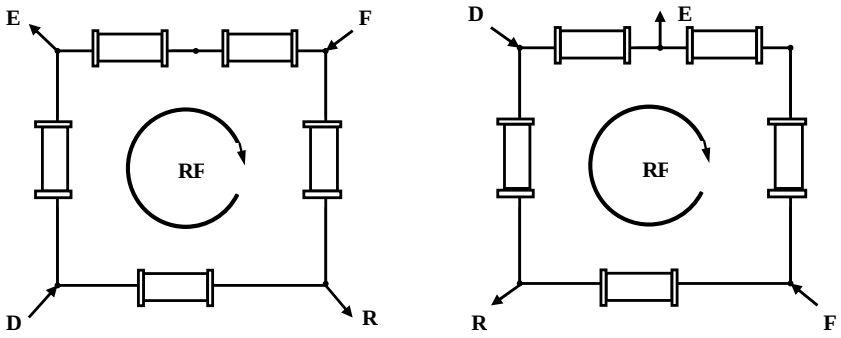

(a) Current switching period (b) Next switching period

Figure 1.1 *An SMB unit with 5 columns in 4 sections configuration of 1/2/1/1 (RF: direction of fluid flow and port switching).*

Compared with the conventional fixed-bed operation, the SMB technology has many advantages:

- Countercurrent flow enhances the potential for separation and continuous feeding improves the throughput of the equipment.
- By reducing the required volumes of stationary and mobile phase, SMB processes can achieve higher productivities with lower solvent consumption, implying that the products are less diluted and consequently the product recovery step is easier and cheaper.
- Another great advantage of the SMB chromatography is its capacity to scale up linearly. A pilot scale process can be reproduced quickly at production scale without sacrificing the purity and production rate.

The chromatographic separation technique used in industry for purification and separation of materials can be traced back to as early as in the 1950s, when it was evaluated for production of chemicals. Industrial scale preparative separations took a giant step in the 1960s when UOP (Universal Oil Products) introduced and commercialised the Sorbex family of SMB processes for petroleum refining and petrochemical. Since then, major commodity applications have been found in the petroleum industry, e.g., separation of xylene isomers (Minceva & Rodrigues, 2002, 2005; Jin & Wankat, 2005), food industries, e.g. separation of sugars (Saska et al., 1992; Azevedo & Rodrigues, 2000; Molnar et al., 2005; Lu et al., 2006)

or amino acid (Xie et al., 2005), and others (Ruthven & Ching, 1989; Francotte & Richert, 1997; Lehoucq et al., 2000; Borges da Silva et al., 2005).

In the 1990s, the use of chromatography in biotechnology, pharmaceutical and fine chemical industries (Pais et al., 1998, 2000; Schulte, 2001; Wongso et al., 2004; Wang & Ching, 2004; Wei et al., 2006) had a significant explosion fuelled by the market trend toward chirally pure therapeutic compounds, which was driven by competitive advantages achieved by patents on chirally pure materials and regulatory pressure.

During the last decade, chromatography was recognised by the pharmaceutical industry as the key general separation method for the purification of the drug intermediates and pharmaceuticals. The motivation for these advances was that the SMB technology reduces the cost of packing materials with high loading capacity and could also provide high purity and high recovery in a very short time. It has been considered for the enantiomer purification, chiral separation, diastereoismers separation and removing small amount of a single impurity (e.g. purification of Paclitaxel from its closely related impurities). Furthermore, the pharmaceutical industry is also attracted by its easy scale up to reduce the time from laboratory to market. The SMB technology has been recognised to be the technique best suitable for a two-cut fractionation of the feed stream, and can be used at all scales of the development of some drugs from the early tests to commercial production.

1.2 Motivations for This Work

The industrial applications of the SMB technology require a good design of the SMB systems and effective control of the system operation. It is an emergent requirement to improve the SMB chromatographic process (SMBCP) operation for higher product quality, productivity, efficiency, and robustness. Optimisation of this operation can be achieved through optimising a performance index (or multiple indices) with respect to the manipulated process variables. It requires accurate process models as constraints and powerful numerical solver for complex model solutions. In addition, process modelling is also necessary for scale-up from laboratory to industrial sale, for prediction of process dynamics, and for on-line process control.

However, for this particular process, we encounter at least the following challenges:

1) An adsorption column has several features that make the modelling task particularly challenging. These include: strong nonlinearities in the adsorption equilibrium isotherms, interference effects due to the competition of solutes for adsorbent sites, mass

transfer resistances between the fluid and solid phases, and fluid-dynamic dispersion phenomena. The interplay of these effects produces steep concentration fronts, which move along the column during the process. This particular property, if accounted for by the mathematical model, constitutes a serious difficulty for the solution procedure.

2) As far as a SMB system is concerned, the model consists of a set of partial differential equations (PDEs) for mass balance over the column, ordinary differential equations (ODEs) for parabolic intraparticle concentration profile, and algebraic equations (AEs) for equilibrium isotherms and node mass balances. These equations are highly coupled, making it very difficult, if not impossible, to be solved analytically. Finite discretisation of the PDEs gives rise to dynamic systems of a very high order. Problems with sharp variations of solutions require even larger discretisation models. The CPU time required for the simulation of a SMB chromatography largely depends on how many ODEs need to be solved. Systems with more components and stiff concentration profiles require more ODEs. The large size is a problem due to its intensive computation when on-line optimisation and real-time control are necessary.

3) The SMB unit operation exhibits complex dynamics because an SMB process never reaches a steady state, implying that all process variables do not reach time-invariant profiles. The stationary regime of this process is a cyclic steady-state (CSS), in which the state of the spatially distributed concentration at the certain time of last switching is identical to the state at that time instant of the next switch. It is also indicated by the convergent time profiles of concentration at the withdrawing ports. Process metrics for design and operation are determined only after the system reaches a CSS. Generally speaking, the PDE models can be solved cycle after cycle until it converges to the CSS. Since this procedure is repeated sufficiently for a large number of cycles (more than 10 cycles), the calculations are expensive. The challenge relates to a fast integration of the SMB cycles while capturing the process dynamics.

These challenges leave us the following open questions:

- How to choose an appropriate model with sufficient accuracy while keeping the computational demand reasonably low for real-time control
- What kind of discretisation technique is more suitable to circumvent the steep change encountered in chromatographic separation
- How to rapidly obtain the solution at stationary state for any arbitrary initial condition.

This thesis provides practical solutions to these questions.

1.3 Research Methodology

The overall aim of this project is to develop and apply frontier techniques for process modelling and advanced control of SMB chromatographic processes, to optimise SMBCP operation and consequently to enhance the economic growth of the industries based on the SMBCPs. To achieve this, the following studies were carried out:

- SMBCP dynamics analysis and model selection: to identify various SMBCP models and their dynamic properties in representing adsorption process, ultimately, to develop control-relevant models for real-time applications;
- Numerical solution: to investigate a powerful numerical computing framework for solutions of complicated SMBCP model using frontier spatial discretisation techniques.
- Fast simulation: to develop an effective integration procedure for the simulation of cyclic operation of SMBCP with sufficient stability and robustness.

The detailed research methodology to target the above objectives are outlined below.

(1) *Process Analysis and Modelling*

This involves the investigation of the structure of the existing models for structural insight and it is aimed to find the "simplest" possible model for the given modelling goal, the real time control. To fully understand the model mechanism, a good knowledge of the complex process dynamic behaviour is required. Through a systematic study on the advances of SMB modelling, design and control, a set of functionally equivalent models - candidate models - for SMBCP will be identified and summarized for their practical applications. Based on the notions of performance and quality indices and measures, an appropriate model type should be chosen that on one hand is detailed enough to describe the complexity of the process dynamics and on the other hand is suitable for simulation and real time control.

(2) *Spatial Discretisation Techniques for Solving PDEs with Singularity*

The major technique under consideration for transforming PDEs to ODEs is the wavelet based methods. We aim at promoting this recently developed approach in numerically solving chemical engineering process models represented by a series of PDEs. To evaluate the computing power of wavelet based methods, other discretisation algorithms are also involved, such a, upwind finite difference and high resolution methods.

In chromatographic separation, the concentration fronts experience steep changes. Such sharp transitions are typically moving with time along a spatial coordinate. Wavelets play a role for efficient and fully adaptively solving this kind of problems. In the developed wavelet method,

- Trial functions are chosen to be a class of interpolating functions generated by the autocorrelation of the usual compactly supported Daubechies scaling functions.
- The original function can be represented as wavelet expansion function and operations will be performed using the corresponding wavelet coefficients only. Wavelet properties will lead to very sparse matrices and this sparse coding will significantly reduce the number of function evaluations in generating the Jacobian and accelerate the integration.
- The treatment of the boundary conditions will be based on some modified interpolating functions constructed to achieve an interpolating operator at the interval of the same accuracy as the counterpart on the line.

The wavelet-collocation method will be used to derive a nonlinear and possibly high-order ordinary differential equation (ODE) system that accurately reproduces the SMBCP dynamics.

Studies will be conducted firstly on a single column chromatographic process represented by a transport-dispersive-equilibrium linear model. Numerical solutions from finite difference, wavelet-collocation, and high resolution methods are evaluated by quantitative comparisons with analytical solution for a range of Peclet numbers.

(3) *Applications to SMB Dynamic Models*

First of all, a dynamic SMB system model will be established. Then, a complete model solution algorithm is developed and implemented. The advantages and disadvantages of the wavelet based approaches are demonstrated through several case studies:

- A glucose-fructose separation process is firstly chosen with its relatively simple isotherm representations. Simulations are conducted using both wavelet collocation and upwind finite difference methods. Quantitative evaluations are made on product purity and yield. Computer elapsed time is compared with those reported in open literature.
- For more complicated applications, an enantiomers separation process is selected. As the PDEs model present a certain degree of singularity, wavelet collocation and high resolution methods will be adopted for spatial discretisation. Apart from the

computational time, a specifically defined relative error will be used as criteria to evaluate the convergence performance of proposed algorithms.

(4) *Fast Steady State Determination*

Although direct substitution approach mimics the start-up of the cycle accurately, it is time consuming and expensive. In this research, we will introduce the concept of "quasi-envelope" (QE) to accelerate the achievement of steady state for a SMB process.

QE is initially introduced for solving highly oscillatory ordinary differential equations. It is based on the observation that when a nearly periodic function is sampled at multiples of the period of the oscillation, the resulting sequence of points changes slowly. If the oscillation is very fast compared to the underlying slowly-varying function, a smooth curve (the QE) which passes through these points can be defined. Larger steps can be taken over several (possibly many) cycles to predict the slow change quasi-envelope, and from which the solution to the original system can be recovered.

The idea is adopted under the consideration that the SMBCP can be treated as a pseudo-oscillatory process because of a large number of continuously switching. Starting from its multi-step representation, some implementation issues will be considered in terms of its generalisation and accomplishing the variable step size. After successful application to our SMB process, investigations will be carried out to further improve of the algorithm.

1.4 Research Contributions

This thesis makes significant contribution to numerical solution and simulation of SMBCP models through developing a systematic, unified, and powerful tool using wavelets. It also contributes to the development of model based control and optimal operation of SMBCP.

The first contribution lies in the systematic model analysis to characterise their complexity and dynamic behaviours so that a proper model type can be selected to meet particular application requirement.

Another contribution is the comprehensive investigation of different numerical methods for the solution of PDEs with singularity. This has been a largely ignored area and little work has been done in this aspect. Especially, PDE model for diffusion-dispersion process presents very different dynamic behaviour when model parameters changed. This work set an example on how to choose suitable numerical methods to solve particular problems.

This is also the first time to apply wavelet based approaches, as well as high resolution methods, to solving SMBC models. The widely used numerical solver using finite difference, finite element or orthogonal collocation methods leads to very complex models with an enormous need for computational power. The use of non-uniform grids or moving elements that dynamically adapt to the changes in the solution has the difficulty in determining the mobility of the grid and in the accurate definition of the function when a new grid point or element is added between two existing grid points or elements. Because of the inherent characteristics of wavelet, it becomes possible to use a basic method with less resolution level to reach our simulation goal.

The fourth contribution goes to the development of effective integration techniques for fast steady state determination of SMBC operation. This is the first time that a completely new concept is introduced to avoid the direct substitutions traditionally used in the simulation of SMB process. The success will see its application to other similar chemical engineering process, such as, cyclic catalytic reactor or distillation columns. It will benefit the further development of nonlinear model predictive control to optimise those operations with sufficient stability and robustness.

In general, the project addresses a significant industrial problem at the frontier of engineering research by application of the leading edge research techniques in applied mathematics, process modelling, and advanced control. The results of this project will directly contribute to a better understanding and implementation of the optimal SMBCP operation to achieve efficient and high purity separations. The outcomes of this research are generic with applications to many complex industries.

1.5 Outline of the Thesis

The structure of the thesis is summarised in the attached diagram (Figure 1.2). The three columns with borders correspond to the three challenges and questions outlined before. From Chapter 3 to Chapter 6, each Chapter covers one of the four research contributions. Boxes in blue contain background information or mathematical theory. Boxes in yellow are the work carried out in this research. The interactions of sections are indicated by arrows. In total, the thesis is organised into seven chapters.

Chapter 1 provides introductory material giving the perspective of SMB industrial applications and motivations of the study. The challenges in the SMB design and operation are discussed; and research problems to be investigated in this work are highlighted. This

leads to the research methodology to target those problems. The contributions of this thesis are outlined.

Chapter 2 covers literature review on various methods of chromatographic separation operation, advances in SMB modelling, and various numerical methods for solving complex PDEs represented models.

Column modelling and proposed spatial discretisation techniques are presented in ***Chapter 3***. Mathematical theory emphasises the basic concepts of wavelets and wavelet collocation methods. As a comparative technique, high resolution method is also briefly introduced because it is relatively new.

Investigation on spatial discretisation methods are presented in ***Chapter 4*** for a single column model. Comprehensive studies are carried out to the processes with a range of Peclet numbers, using finite difference, wavelet collocation and high resolution methods to transform PDEs to ODEs. Comparisons are made among those methods both quantitatively and qualitatively in terms of computational time, the prediction accuracy and algorithm convergence.

In ***Chapter 5***, principle of dynamic modelling of SMBCPS is given. Two case studies on the separation of fructose-glucose and bi-naphthol enantiomers are conducted in very detail.

Chapter 6 deals with a fast integration technique for the simulation of cyclic processes. The results from previous chapters provide useful guide to the selection of proper spatial discretisation methods. Application to SMB process uses one of the cases studied in Chapter 5. Further investigations are conducted on the performance of the algorithm.

In ***Chapter 7***, conclusions are drawn and recommendations are made based on this study.

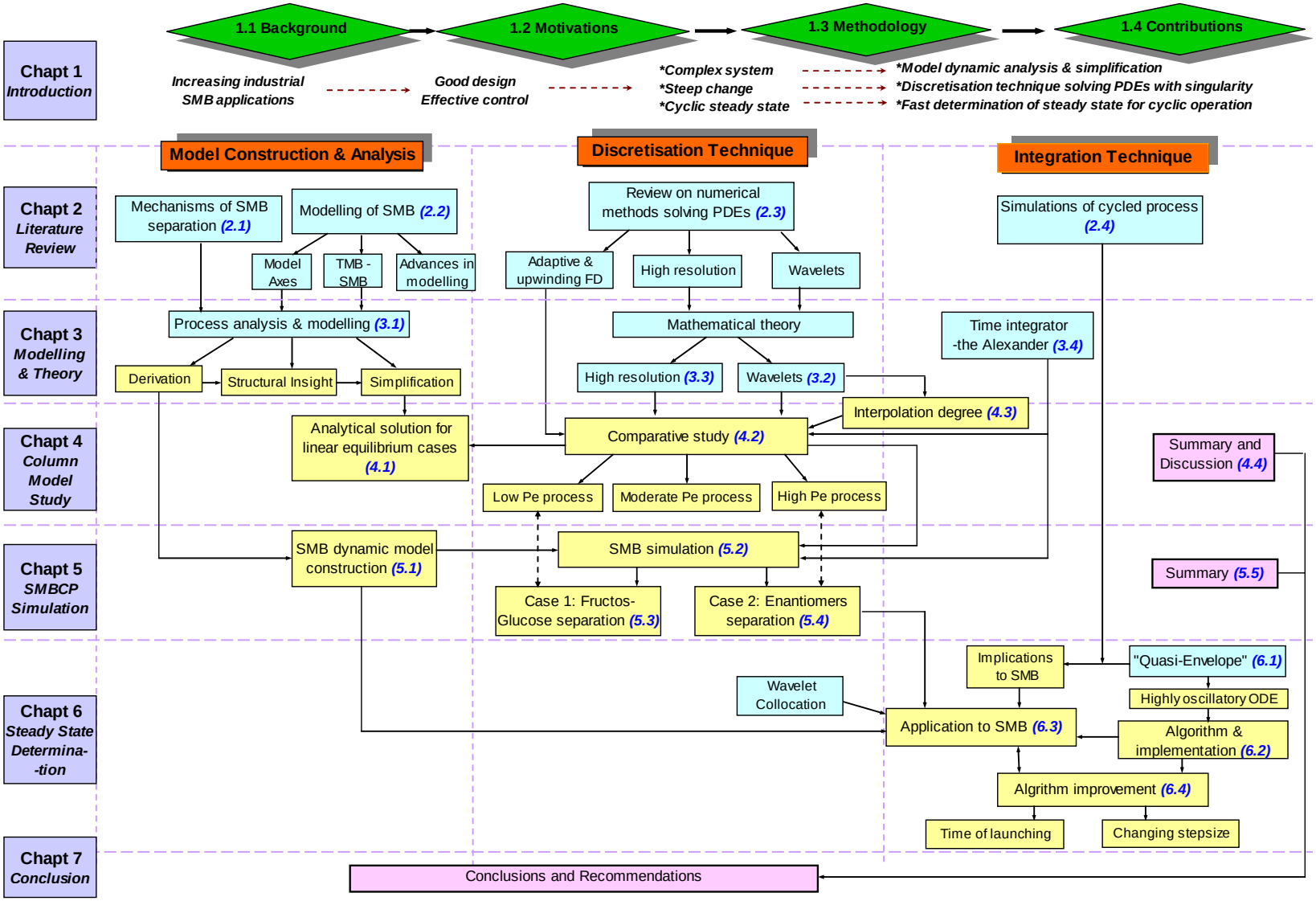
1.1 Background
1.2 Motivations
1.3 Methodology
1.4 Contributions
Chapt 1 Introduction
Increasing industrial SMB applications
Good design Effective control
*Complex system
*Steep change
*Cyclic steady state
*Model dynamic analysis & simplification
*Discretisation technique solving PDEs with singularity
*Fast determination of steady state for cyclic operation
Model Construction & Analysis
Discretisation Technique
Integration Technique
Chapt 2 Literature Review
Mechanisms of SMB separation (2.1)
Modelling of SMB (2.2)
Model Axes
TMB - SMB
Advances in modelling
Review on numerical methods solving PDEs (2.3)
Adaptive & upwinding FD
High resolution
Wavelets
Simulations of cycled process (2.4)
Chapt 3 Modelling & Theory
Process analysis & modelling (3.1)
Derivation
Structural Insight
Simplification
Mathematical theory
High resolution (3.3)
Wavelets (3.2)
Time integrator -the Alexander (3.4)
Interpolation degree (4.3)
Chapt 4 Column Model Study
Analytical solution for linear equilibrium cases (4.1)
Comparative study (4.2)
Low Pe process
Moderate Pe process
High Pe process
Summary and Discussion (4.4)
Chapt 5 SMBCP Simulation
SMB dynamic model construction (5.1)
SMB simulation (5.2)
Case 1: Fructos-Glucose separation (5.3)
Case 2: Enantiomers separation (5.4)
Summary (5.5)
Chapt 6 Steady State Determina--tion
Wavelet Collocation
Implications to SMB
"Quasi-Envelope" (6.1)
Highly oscillatory ODE
Application to SMB (6.3)
Algorithm & implementation (6.2)
Algrithm improvement (6.4)
Time of launching
Changing stepsize
Chapt 7 Conclusion
Conclusions and Recommendations

CHAPTER 2
LITERATURE REVIEW

In this chapter, an introduction to the operation of chromatographic separation is presented followed by a review of the modelling of simulated moving bed for the purpose of giving a fundamental knowledge of the process and some modelling related issues. Subsequently, the numerical methods for solving complex models represented by partial differential equations are overviewed. Frontier spatial discretisation techniques are emphasised. Literature review is also conducted on the simulation of cycled processes.

2.1 The Methods of Chromatographic Separation Operation

In order to help with a good understanding of the mechanisms of Simulated Moving Bed Chromatographic Processes (SMBCPs), we will give a technical introduction of the three basic modes of chromatographic separation operation: fixed-bed chromatography, moving-bed chromatography and the simulated moving-bed chromatography.

2.1.1 Fixed-Bed Chromatography

This chromatographic technique is essentially the same as the method used in laboratory analysis. By having the targeted composite substance absorbed into the adsorbent, the chromatographic process divides the mixed substance into its parts. Now let us suppose that the adsorption affinity of substances A, B are as follows, A<B, and the velocities of components A and B in the fixed-bed mode are $U_A > U_B$.

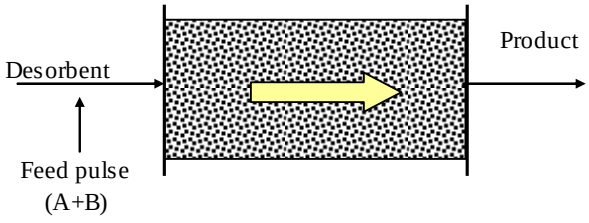

Figure 2.1 *Fixed bed chromatography*

A column as shown in Figure 2.1 is packed with adsorbent, and then filled with liquid desorbent. A fixed amount of the sample liquid is fed in at one end of the column. If we continually feed in liquid desorbent, each component of the sample (A and B) will move in the adsorbent layers at the migration rates U_A and U_B, determined by their individual adsorption affinity. Thus, if there is a difference between these rates, as component A and component B move through the adsorbent layers they will separate from each other. In this way, by collecting the liquids as they successively drip out of the column, the mixture can be separated into fractions each abundant with one of the component materials.

Fixed-bed adsorption systems are typically operated in a cyclic manner with each bed repeatedly undergoing a sequence of steps, such as pressurization, adsorption, blowdown, and desorption. Since the types and densities of the desorbent can be easily changed, fixed-bed chromatography can be applied to the separation of many types of useful substances.

However, the fixed-bed chromatographic process results in a material with a low concentration, in cases where a more precise separation is required, higher costs are required in raising the material's concentration.

There are some additional deficiencies when this method is used on a large scale:

- The entire adsorbent bed is not efficiently utilized.
- A large quantity of desorbent is consumed, and the separated components are obtained in a diluted state.
- In order to obtain a successful separation, a sufficiently large difference in the adsorption affinities of the adsorbates is required.
- The operation is not continuous.

Due to these deficiencies, there have been many innovative attempts to improve the fixed-bed mode so that it can be used on an industrial scale.

2.1.2 Moving-Bed Chromatography

The moving-bed method is one of the ways to make the fixed-bed system continuous. If the adsorbent in Figure 2.1 is forced to move in the opposite direction of the desorbent and sample mixture, at a migration rate U_S between the velocities of components A and B, i.e. ($U_A > U_S > U_B$), this would be the situation in Figure 2.2, where the desorbent is continuously fed into one end of the column, the adsorbent is made to move in the opposite direction, and the feed mixture is supplied at the middle of the bed.

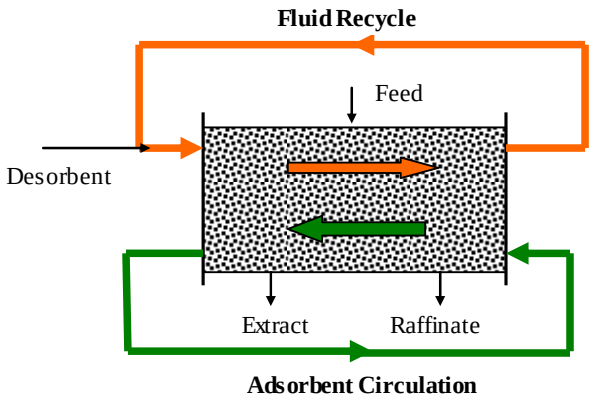

Figure 2.2 *Moving bed chromatography*

In such a situation, components A and B will move within the column at the speeds, $U_A - U_S$ (>0) and $U_B - U_S$ (<0), respectively. Thus, starting from the point where the feed mixture is fed, components A and B will move in opposite directions from one another within the column. If the mixture is continuously fed into such a device, components A and B will be continuously separated to both ends of the column.

With a device such as the one described above, a mixture can be separated in a continuous manner using the principle of the moving-bed mode. The benefits are less desorbent and less adsorbent than those used for fix-bed chromatography. There are some unusual characteristics of moving bed technology that cannot be accomplished with batch chromatography. For example, there is a useful path length effect. A longer path length will generally improve the chromatographic separation because additional equilibrium steps, or "theoretical plates' will be available. With moving bed technology the path length of adsorbent which interacts with the feed mixture can be increased beyond the length of the adsorbent in the system by increasing its internal flow rate. Increasing internal flows in both directions means the entering mixture will contact with a much longer path of resin before exiting. Instead of being constrained to path length as in batch chromatography, the moving bed system can increase path length without increasing the amount of adsorbent used. The adsorbent can be regenerated as soon as its role in the adsorption step has been completed.

Another advantage of moving bed technology is that heat transfer in moving bed system is better than in fixed bed system.

However, in a large industrial device, it is extremely difficult to uniformly move the adsorbent without disturbing the absorption band. Moving the column is mechanically

complex. The equipment required will inevitably be more expensive and need to cope with attrition of the adsorbent.

The simulated moving-bed mode described in the following section is a chromatographic separation method invented so as to obtain the same level of separation as the moving-bed mode, without having to actually move the adsorbent.

2.1.3 Simulated Moving-Bed Chromatography

Instead of physically moving the adsorbent, countercurrent flow may be simulated by switching adsorbent columns in sequence. As shown in Figure 2.3, the bed can be divided into relatively small number of columns with the ends of each column connected to form a circular loop. Four ports are opened for the feeding of mixture, desorbent and drawing of fluids. The introduction of the feed mixture is moved successively along in the direction of the flow of the desorbent.

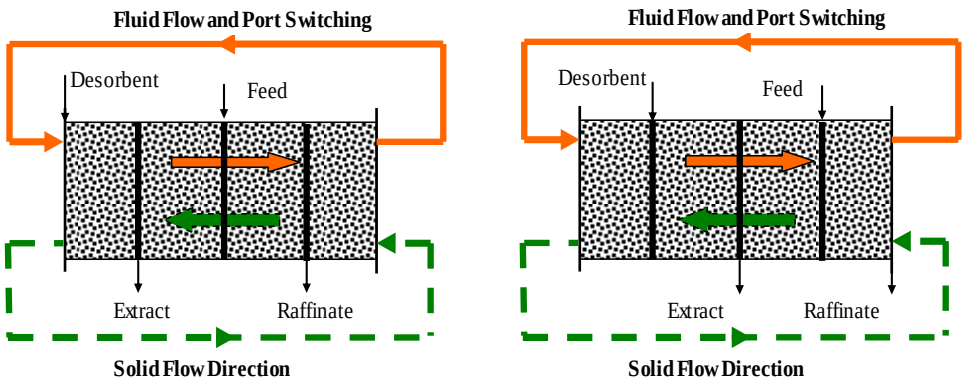

Figure 2.3 *Simulated moving bed chromatography*

While the fluids are circulating inside the column, assume that feed mixture, desorbent, extract, and raffinate are continuously allowed to enter or leave the column from each of the openings. Then, successively for the length of one full column at a time, the positions of the openings for these four outlet streams are changed in the direction of the circular flow at a regularly fixed time point. Here the migration rate at each opening is set so that it will be smaller than component A's migration rate, U_a, and larger than component B's migration rate, U_B.

By operating the device under these conditions, it seems as if the adsorbent moved at a migration rate, in the opposite direction to the flow of the fluids. Therefore, components A

and B move in the opposite direction from the feed mixture introduction point, and each component can be removed in a continuous manner from its respective withdrawal point.

This is how the simulated moving-bed chromatographic separation system works. A well known application of this principle is the SORBEX system, where a rotatory valve controls the motion of the ports along the column. The same result can be achieved by connecting each section of the column with many on-off valves; each of these is in turn a feed point or draw off point or simple connection depending on the particular role of the section at a particular time. Typically, four-section cascade SMB is the usual process scheme adopted for commercial applications and academic research.

SMB operation is not a perfect simulation of true moving bed (TMB) operation. The adsorbent movement simulation by valve switching is not accomplished in a continuous manner, but rather, jumps intermittently between columns. This means that as more columns are added to an SMB, a true moving bed is closely simulated. An infinite number of columns and infinitely short switching periods would be needed for an exact simulation. With sharp mass transfer zones or when high purity products are not required, one column per zone is satisfactory. When sharper separations are required, several segments per zone are needed. 4 to 12 columns are typically enough to obtain most of the benefits of a TMB.

2.1.4 Economical Advantages of SMB

The SMB process provides the advantages of a continuous countercurrent unit operation while avoiding the technical problems of a true moving bed. Economically, it has the flowing advantages:

A SMB process can use a higher concentration of solute in the feed than a batch process and the total concentration of products are much higher. The savings in solvent consumption from using a SMB process typically range from a factor of 3-10 when compared to batch chromatography (Pynnonen, 1998).

For a conventional SMB, the feed is continuous as well as the product withdraw flows. The process runs and produces the desired product continuously without significant operator interventions. This maximises the production capacity and minimizes the labour cost.

The nature of SMB operation in fact “stretches” the separation column. The average molecule inside the process loop passes through each section several times. Higher internal recirculation rate reduces the volume of stationary phase required. The increased mass

transfer driving force results in minimization of the adsorbent and eluent requirements for a given separation duty.

The SMB process was first developed to separate isomeric mixtures such as xylenes and sugars using resins or zeolites. Today it is successfully used in various areas. Figure 2.4 is a statistical analysis of the SMB separation related publications during the past 30 years. The figure clearly shows the significantly increasing interest in this area.

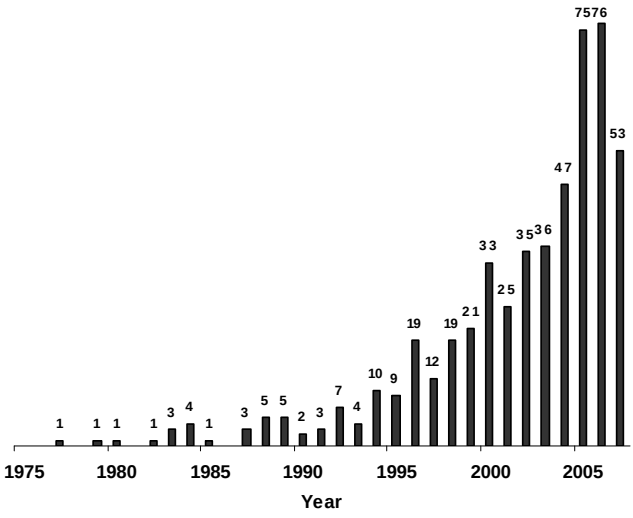

Figure 2.4 *Total number of publications related to SMB separation (extracted from EngineeringVillage2 database on May 1, 2008)*

2.2 Overview: Modelling of SMBCPs

A useful and comprehensive review of adsorption technology was given by Wankat (1986). For more fundamental texts, readers can refer to the books of Ruthven (1984) and Crittenden and Thomas (1998). This section will introduce some of the key concepts arisen in modelling of chromatography and overview the advances of SMB modelling during the last two decades.

2.2.1 Model Axes

Modelling of chromatography developed along three different axes, leading to the following three broad classes of models (Guiochon, 2002):

- **Plate Model** (**Stage model or Tank in Series model**) *(Guiochon & Ghodbane, 1988; Ruthven & Ching, 1989; Ernst & Hsu, 1989; Lee et al., 1993; Zhang et al. 2003a; Biressi et al., 2000; Wongso et al., 2004)*

  The method is to divide the column into a number of identical equilibrium stages that are placed in series. The mobile phase percolates from one plate to the next after equilibrium is achieved between the mobile and stationary phases. Approximate models because they depict a continuous column of length L as an arbitrary discrete number of well-mixed cells in series. By nature empirical model cannot be related to first principles and have no predictive value.

- **The Statistical Models** *(Gridding, 1960; Ruthven, 1984; Dondi et al., 1986, 2000)*

  It was used for simple calculation of estimates of the variance of chromatographic band profiles and to study the mechanism of band broadening.

- **Rate Equation Models**

  Rate models refer to models containing a rate expression, which describes the interfacial mass balance and the mass transfer kinetics. The modelling involves the solutions of systems of those differential equations. In principle, such model can take into account any kind of equilibrium isotherm and mass transfer effect and intraparticle gradients. Provided proper parameters are available (isotherm and mass transfer kinetics models and their parameters, experimental conditions), the solution of these models have great predictive value, which is useful for model predictive control. More details will be discussed in Chapter 3.

2.2.2 Advances in SMB Modelling

Mathematical modelling and simulation of SMBCP is widely documented in the literature (Hu & Sun, 1987; Chu & Hashim, 1995; Hassan et al., 1995; Kaczmarski et al., 1997; Pais et al., 1998; Strub & Schmidt-Traub, 1998; Henke et al., 2008; Barreto et al., 2008; Yao et al., 2008). As a consequence of application interests, a great amount of work has been devoted to the analysis and modelling of chromatographic processes. Researchers from disciplines of Chemical Engineering, Process Engineering, Chemistry, and even Bio-molecular Engineering are all involved. In the following, we will summarise the advances in SMB modelling by reviewing some of the most active research groups in terms of peer reviewed

publications and the significant impact of those publications. An overview of those previous works will enable us to identify our position and future directions.

Earlier contributions to the development of the first-principle models of countercurrent and simulated countercurrent separation systems were made by Ruthven and Ching (Ruthven, 1984; Ching, 1998; Ruthven & Ching, 1989). Most of their publications have become the guide for later SMB model development. The proposed **Node Model** is still adopted for modelling SMB systems nowadays. These researchers and colleagues have also explored industrial applications of those systems.

Since the 1980s, a large number of papers have been published on chromatographic separation from an interdisciplinary group of Mazzotti, Morbidelli, Storti, and colleagues. Their investigation in the optimisation of the operation parameters was conducted mainly on the operational region plane. They derived a graphical short-cut design methodology, the so-called **Triangle Theory**, and extended the theory to systems with nonlinear adsorption isotherms (Mazzotti et al., 1994, 1996, 1997; Storti et al., 1993, 1995). This methodology has once been widely used for an initial guesses of a feasible operating point of the process. It is also used as a tool for manually tuning the suboptimal operating conditions. More recently, work has been conducted on process control (Biressi et al., 2000; Abel et al., 2004; Strohlein et al., 2005; Erdem et al., 2006; Song et al., 2006). Other than the optimisation of traditional SMB systems (fixed feed rate and simultaneous port switching), Varicol processes (non-simultaneous and unequal shifts of ports) and PowerFeed operation (changing flow rates during the switching interval) have also been studied (Zhang et al., 2003a, 2003b). The On-line optimisation based SMB control scheme using repetitive model predictive control method (Natarajan & Lee, 2000) have been applied to different cases through simulations and experimental implementation.

Some fundamental issues such as column dynamics and thermodynamics, retention mechanisms and isotherm effects were addressed by Guiochon, Zhong and their collaborators (Zhong & Guiochon, 1994, 1996, 1997a, 1997b; Zhong et al., 1997c; Guiochon & Ghodbane, 1998). Especially, Guiochon's work has great impact on the separation science through development of new theory and shows how theory can guide the practical application of separations (Schure and Katti, 2006). Undoubtedly, through investigating the effect of the different parameters on the band profiles and the effect of the concentration histories on its two outputs, their work will help understand the SMB behaviour in detail.

Since late 1990s, Dünnebier and Klatt have also studied SMB processes from process control engineering point of view with the focus on process modelling for optimal design and

model-based control purpose (Dünnebier et al., 1998, 2000a, 2000b; Klatt et al., 2002). Earlier work was on the comparison of different modelling approaches. This led to their later proposal on process optimisation and design. From a thorough review of previous design methods, they put forward a new model-based optimisation strategy from the selection objective function, the degrees of freedom, constraints and the optimisation problem description. They proposed a two-layer control architecture in which the optimal operating trajectory was calculated off-line by dynamic optimisation based on a rigorous process model. The low-level control task was to keep the process on the optimal trajectory despite disturbances and plant model mismatch. Effort was also made to use neural networks for process identification (Wang et al., 2003).

Enantiomers and p-xylene separation processes have been studied by the Research of Laboratory of Separation and Reaction Engineering (LSRE) at University of Porto, Portugal, for the investigation of SMB transient and steady-state behaviour (Pais et al., 1998; Minceva & Rodrigues, 2002, 2005; Leão & Rodrigues, 2004). Different strategies for numerical solution of model and approaches on the determination of cyclic steady state were compared. The developed simulation software will be useful for the future development of efficient numerical algorithms for the solution of SMB model and for the fast prediction of cyclic steady state.

2.2.3 Equivalent -TMB versus Dynamic - SMB

Generally, the SMB modelling approach can be classified as:

- The system is represented in terms of an equivalent true moving bed model (E-TMB)
- The system is assembled by the models of single chromatographic columns under explicit consideration of the cyclic switching operation (D-SMB).

The main difference between equivalent TMB and dynamic SMB is their stationary regime to be considered. The TMB represents the traditional concept of steady state operation while modelling using D-SMB deal with its cyclic steady state. Practically, when increasing the number of columns and decreasing column length, the SMB will approach the TMB system.

When the cyclic port switching is neglected, the E-TMB model is simplified and can be solved very efficiently. It has been shown that the steady-state solution of a detailed TMB model reproduces the solution of a SMB model reasonably well under certain circumstances (Hashimoto et al., 1983; Storti et al., 1988; Pais et al., 1998). However, E-TMB is a rather severe idealization of the simulated countercurrent process, it is restricted to the case of three

or more columns per zone with linear isotherms and no reaction is involved (Dunnebier et al., 2000a). Research has shown that, in the case of the three-section process, the TMB approach is of limited quantitative value (Chu & Hashim, 1995) thus need to be treated with caution. Comparative simulations (Strube & Schmidt-Traub, 1998) also suggested that since E-TMB models do not include the transient regime of the quasi-stationary, periodic steady state of SMB processes and not consider the upper and lower bounds of the retention time, an SMB optimisation based on E-TMB model will lead to a miscalculated operating condition.

Earlier applications of SMB were large separation units used in food and petrochemical industries, which operated under nearly linear behaviour of the equilibrium isotherm. Most of the recent applications are in the area of fine chemicals and pharmaceutical products, which operated with nonlinear adsorption behaviour and in a high purity range. Figure 2.5 indicates that, among three major applications, chiral separation is growing rapidly.

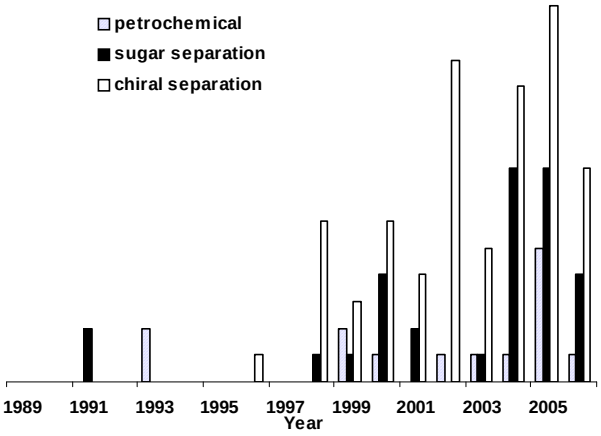

Figure 2.5 *The distribution of the research interest (extracted from EngineeringVillage2 database on May 1, 2008)*

SMB modelling through dynamic simulation gives essential information for a better understanding of chromatographic processes. It is a crucial aid to develop control strategies and to analysis the stability of SMB processes concerning malfunctions.

In this project, we will use the dynamic simulated moving bed modelling method and the rate equation models for our study.

2.3 Numerical Methods for Solving Partial Differential Equation Models

Typically, a dynamic SMBCP model is described by a set of partial differential equations (PDEs), ordinary differential equations (ODEs) and algebra equations (AEs). The most comprehensive model: the general rate model, consider axial dispersion, interfacial mass transfer between the mobile and the stationary phases, intraparticle diffusion, and multi-component isotherms. The number of model equations is enlarged in folder with the number of columns involved and the components to be separated. Only for specific cases, there exist analytical solutions for single column model (Ruthven, 1984; Zhong et al., 1996; Guiochon, 2002).

The methods of finite difference, finite element or finite volume are traditionally employed to solve PDEs numerically. Among those, solution of finite difference approximation is only acceptable for single component profile under linear conditions (Lu, 2004). Most existing research employs the finite element method (FEM) to discretise the convection-dominated parabolic PDEs of the liquid phase and orthogonal collocation for diffusion-dominated PDEs of the solid phase (Yu & Wang, 1989; Gu, 1995; Kaczmarski et al., 1997; Leão & Rodrigues, 2004; Araújo et al., 2006). The resulting ODE system is in general very complex and with an intensive need for computational power. Other methods developed for single column (or fixed-bed adsorption) model are not always extended for solving SMB model due to the complexity of the resulting modelling system.

2.3.1 Adaptive Grid Algorithm and Upwinding Scheme

In general, the two-stage method of lines (MOL) is popularly adopted for the discretisation of time-dependent PDEs. First, the space variables are discretised on a selected space mesh, using FD or FE approximation, to convert the PDE problem into a system of ODEs with time as an independent variable. The discretisation in time is then applied to complete the scheme. Effort has been made either on the development of spatial discretisation technique or on the improvement of integration performance. Because the well-known stiff ODE solver, e.g. Gears method, can provide very good temporal performance, we will focus on the various spatial discretisation techniques.

For chromatographic separation, travelling wave front posses sharp moving spatial transitions. In order to fully capture the steep front, peak, and tail, the space grid has to contain a large number of mesh points. Finite discretisation of the PDEs usually gives rise to dynamic systems of a very high order. Problems with sharp variations of solutions even demand larger discretisation models. The CPU time required for the simulation of a SMB

system highly depends on how many ODEs need to be solved. Systems with more components and stiff concentration profiles require more ODEs. The large size is a problem due to its intensive computation when on-line optimisation and real-time control are necessary.

Here comes the demand of using non-uniform grids or moving elements, such as, adaptive finite differences or moving finite elements that dynamically adapt to the changes in the solution. Early in 1990, Furzeland (1990) conducted an evaluation and comparison of three moving-grid methods for one dimensional PDEs problem. Later in the work of Wouwer et al. (1998), five adaptive grid methods were examined. These two publications provided a comprehensive review and theoretical explanations on the moving grid technique, and could also be applied to the recent works in this area.

According to Furzeland (1990), the moving grid approach has three directions:

- The finite-difference method proposed by Petzold (1987). It involves two steps, a moving Lagrangian step and a regridding step. The moving Lagrangian step applies a stiff ODE solver to an augmented semi-discrete system, while in the regridding step a redistribution of points at the forward time level is carried out through a De Boor-type equidistribution algorithm.
- The finite-difference method based on the ideas from Dorfi and Drury (1987). The grid movement is regularised by employing a smoothing technique in both space and time. An implicit equation is used which underlines a spatial equidistribution transformation based on an arc-length monitor function.
- The finite-element method of Miller and co-workers (1981). It generates a system of continuous time ODEs for mesh points. Grid movement is regularised by using penalty functions.

Both finite-difference moving-grid methods are based on the equidistribution principle. The idea of the equidistribution principle is to equally distribute a given mesh function in space, placing more nodes where the spatial error is large.

Wouwer et al. (1998) classified adaptive grid based on the method of line (MOL) into two categories: the local refinement algorithms and moving grid algorithms. The former involves local addition or removal of nodes as needed, while the latter moves a fixed number of nodes to the regions of rapid solution variation. The details of the classification and test results on Burgers' equation are summarised in Table 2.1.

Table 2.1 *Summary of various adaptive grid algorithms (Wouwer et al., 1998)*

Adaptive Grid Algorithm		**Representing Author (apart from Wouwer et al.)**	**Grid Placement Criterion**	**Test on Burgers' Equation**
Local Refinement		Hu and Schiesser (1981)	Second-order derivative	Simple concept; technically complicated for implementation; substantial parameter tunning may be required
		Eigenberger and Butt (1976)	Error estimation procedure	
Moving Grid (equidistribution principle)	Static Regridding	Sanz-Serna and Christie (1986); Revilla (1986)	Equidistribute a pre-defined function based on solution curvature	Competitive with all the adaptive solvers
	Dynamic Regridding	Huang and Russell (1996)	Movement of nodes is governed by a moving mesh PDE.	Reduced nodes; robust; high computational expense (require large number of time steps)
		Blom et al. (1994)	Nonlinear Galerkin discretisation ; Smoothed equidistribution principle using regularization technique of Dorfin and Drury	Very good temporal performance; robust and reliable

Furzeland's three moving grid methods could be fitted into Wouwer's dynamic regridding algorithm. The largest difficulty with adaptive grid method is to determine the mobility of the grid (or the elements) and the accurate definition of the function when a new grid point (or element) is added between two existing grid points (or elements).

Another technique tracking shook or steep wave in solving PDEs is the Upwinding schemes. It has been found that for reaction-convection-diffusion equations, which represent many chemical engineering problems, central difference discretisation is unstable because it gives spurious oscillatory profiles (Gibbs phenomena) near the shock. Upwinding schemes are introduced to overcome the drawback from central discretisation used in most of the moving mesh software. Upon which, the schemes of Essentially Non-Oscillatory (ENO) and Weighted ENO (WENO) have been developed for the discretisation of first-order derivative term. The combination of moving mesh with adaptive Upwinding schemes (e.g. ENO, WENO, Flux-Limited and Piecewise Hyperbolic Method (PHM)) on uniform (Jiang and Shu, 1996; Lim et al., 2001a) or non-uniform grid (Li and Petzold, 1997) have been studied to track the rarefaction as well as the shock for problems with nonconvex flux. A review of

recently developed spatial discretisation methods can be found in Lim et al. (2001b). All the above mentioned Upwinding schemes have been tested on convection-dominated problems with moving shock results.

Effort has also been made to investigate alternative and more effective numerical solvers for PDEs with Algebraic Equations (AEs). As in our example, the packed-bed chromatographic separation is described by convection-dominated parabolic PDEs for mass conservation in the mobile and solid phase, and AEs for the adsorption isotherm between the two phases. The iterative space-time Conservation Element/Solution Element (CE/SE) method was initially proposed by Chang and To (1991) and later adopted by Lim & Jorgensen (2004b) to solve chromatographic adsorption problems. The CE/SE method enforces both local and global flux conservation in space and time by using the Gauss's divergence theorem. Application to the SMBCPs provided non-dissipative and accurate solutions and fast calculation was achieved (Lim and Jorgensen, 2004b). However, it remains an important area worthy to be explored in order to improve computational efficiency, etc.

2.3.2 Using Wavelet for Solving PDEs with Singularity

Since the early 1800s, approximation using superposition of functions has existed. Joseph Fourier discovered that any periodic function can be represented as a sum of sines and cosines (Fourier series). The trick is to multiply the sines and cosines by a coefficient to change their amplitude (the height of their waves) and to shift them so that they either add or cancel. This is the well-known Fourier Transform. Certain non-periodic functions (finite) can also be treated in this way. However, a Fourier Transform hides information about time. It proclaims how much of each frequency a signal contains, but is secretive about when these frequencies were emitted. The lack of time information makes a Fourier Transform vulnerable to errors. It is poorly suited to very brief signals, or signals that change suddenly and unpredictably.

Wavelets are an extension of Fourier analysis. The goal is to turn the information of a signal into numbers and coefficients, that can be manipulated, stored, transmitted, analysed, or used to reconstruct the original signal. Compared against the "one size fits all" mentality of older Fourier series, wavelets supply both the big picture and fine detail at the same time. In another words, Fourier analysis is suited to very regular periodic signals, while wavelets transform is suited to highly non-stationary signals with sudden peaks or discontinuities.

Wavelets were developed independently in the fields of mathematics, quantum physics, electrical engineering, and seismic geology. Interchanges between these fields during the last

ten years have led to many new wavelet applications such as image compression, turbulence, human vision, radar, and earthquake prediction. Applying wavelets to discretise differential equations appears to be a very attractive idea. In finite element type methods, piecewise polynomial trial functions may be replaced by wavelets. Such an idea was explored by Glowinski, Lawton, Ravachol and Tenenbaum (1990). Many interesting numerical examples in their paper suggest that wavelets have great potential in the application to the numerical solution of differential equations.

In the seeking of numerical solution, wavelets have been used either directly as bases or for algebraic manipulations to simplify the results using existing discretisation methods (Nikolaou & You, 1994). There are two commonly used wavelet methods, the Wavelet-Galerkin and Wavelet-Collocation. In the Wavelet-Galerkin method, the solution is approximated by linear combinations of wavelets or scaling functions. The same base is used as weighting functions to calculate the unknown coefficients. In the Wavelet-Collocation method, the solution is evaluated at dyadic points by using the interpolating wavelet as the weighting function. The computations are performed in the physical space with redefined grid.

Orthogonality, compact support, and multi-level structure of the basis make wavelets well-suited for approximating functions with abrupt change, such as a shock wave or a sharp spike. In the case of moving steep front, using the wavelet transform one can track its position and increase the local resolution of the grid by adding higher resolution wavelets in that region. On the other hand, the resolution level in the smoother regions can be appropriately decreased, avoiding an unnecessarily dense grid (Cruz et al., 2001).

Applications of wavelet transformation to the solution of partial differential equation arising in the chemical engineering process is limited (Bertoluzza, 1996; Bertoluzza et al. 2000; Cruz et al. 2001, 2002; Liu et al. 2001; Bindal et al. 2003; Briesen & Marquardt, 2005). The majority of papers look at solving Burger's equation. Nikolaou and You (1994) used Daubechies' orthonormal wavelet and Chui-Wang's semi-orthogonal B-spline wavelet as basis, together with Galerkin's method to solve Initial Value problem and Two Point Boundary Value problems. For Burger's equation, wavelets were also compared with those using Chebyshev polynomials as the basis functions. It was pointed out that for differential equations with solutions that exhibit local irregularities, wavelets have a distinct potential.

Vasilyev et al. (1995) developed a multilevel wavelet collocation method based on the wavelet interpolation technique for solving PDEs. They suggested two different approaches to treat general boundary conditions. Their method was also tested on the one-dimensional

Burger's equation with small viscosity. Comparisons with other numerical algorithms (Fourier Galerkin, Fourier pseudospectral, Chebyshev collocation, spectral element, finite difference, wavelet Galerkin) have shown the competitiveness and efficiency of the proposed method.

More recently, Cruz et al. (2001, 2002) and Liu et al. (2001) exemplified the Wavelet-Collocation application in a fixed-bed adsorption model to simulate the propagation of a concentration peak along a chromatographic column with axial dispersion and linear/nonlinear adsorption isotherm. Both adaptive grid and constant grid methods were investigated. However, applications of the wavelet technique for solving an SMB system model, which is much more complicated than a single column model, have not been found in the open literature except by our recent work (Yao et al., 2008).

2.3.3 The High Resolution Method

Another method we will pay special attention as one of the comparative tool is the high resolution methods (HR). High resolution was originally proposed by Koren in 1993 for numerically solving advection-diffusion equations with source term. Based on the so-called centred finite-volume discretisation technique, the scheme for dealing with the one-dimensional problem was introduced first, and then it was expanded to solve the multi-dimensional problem. Later, this method was introduced into chemical engineering applications by Gunawan et al. (2004) and Qamar et al. (2006) to solve the multi-dimensional population equations in crystallization. The numerical results obtained in the above papers show the advantage of this new scheme.

Furthermore, a modified HR scheme, Adaptive High Resolution Scheme, was proposed by Qamar et al. (2006) for numerically solving multi-dimensional population balance models in crystallization processes. The application of the adapted scheme demonstrates its generality, efficiency and accuracy. It is noticed that both the original HR scheme and the adaptive HR scheme were designed for solving the partial differential equations with Dirichlet boundary conditions.

In order to employ this powerful scheme to solve the problems arising from a much wider range of industrial processes that can be modelled by partial differential equations with other boundary conditions, Zhang et al. (2008) extended the original HR scheme to solve the PDEs with Cauchy or Neumann boundary conditions. They also compared the HR method with the wavelet based scheme for numerically solving PDEs, and concluded that the HR scheme outperforms the wavelet based method for certain types of applications.

2.4 Simulation of Cyclic Process

In the mathematical modelling of SMBC process, numerical procedure can be investigated from two aspects. In the first place is the discretisation technique to circumvent the steep gradients encountered. The second is how to rapidly obtain the solution at stationary state for any arbitrary initial condition.

SMBCP unit operation is a typical cyclic or periodical process. The Cyclic Steady State (CSS) is practically reached after a certain number of valves switches, but the system states are still varying over time because of the periodic movement of the inlet and outlet ports along the columns. Generally speaking, the PDE models will be solved cycle after cycle until it converges to the CSS. Since this procedure is repeated sufficiently for a large number of cycles (more than 10 cycles, or over 100 switching), the calculations are expensive. Over the past decade, very rare simulation strategies have been investigated for the SMB chromatographic systems (Kloppenburg & Gilles, 1999; Minceva et al., 2003; Nilchan & Pantelides, 1998). The difference among those methods lies in the way of iteration for the whole cycle or just one switching time, starting from given initial conditions or using the CSS profile from previous simulation. This direct substitution approach mimics the start-up of the cycle accurately, but can also be time consuming and expensive.

Through our literature survey for the simulation of cyclic process, limited efforts have been made to the cyclic operation of catalytic reactors by periodic flow reverse. The exploration in developing a more rapid solution strategy is based on the observation that in cyclic operation, stationary conditions prevail when the cycle time is much less than the characteristic process time (Bhatia, 1991). In this work, a perturbation solution is developed to obviate the need of repeatedly solving the transient equations. The cyclic catalyst temperature profile is expressed as the sum of initial profile and a time-varying increment. As a result, the computational time is reduced by a factor of almost 10. In the further research by Gupta and Bhatia (1991), the initial value problem was treated as a boundary value problem in time, with the stationary catalyst temperature profiles at the beginning and the end of the half cycle being mirror images of each other. This allows direct solution of the cyclic profiles independent of the initial conditions. Because boundary value problem approach uses Newton's method for convergence promotion, it is more rapid than successive substitutions.

However, efforts made on the numerical method for highly oscillatory ordinary differential equations have attracted our attention. One of them is the "quasi-envelope" (QE) method proposed by Petzold (1981). It is based on the observation that when a nearly periodic

function is sampled at multiples of the period of the oscillation, the resulting sequence of points changes slowly. If the oscillation is very fast compared to the underlying slowly-varying function, a smooth curve (the QE) which passes through these points can be defined. Larger steps can be taken over several (possibly many) cycles to predict the slow change quasi-envelope, and from which the solution to the original system can be recovered. Applications of this method can be found for a binary separation in a controlled distillation column (Toftegard & Jorgensen, 1989) and the catalytic reactor with periodic flow reversal (Santiago & Jorgensen, 1995). The computing time expenditure of about 12% of the time required to evaluate all cycles individually were reported.

2.5 Summary

The complexity of SMB operation results in various modelling strategies and model representations. Although different numerical methods have been developed for the solution of PDEs, publications can be hardly seen on the discussion of their suitability for different situations. Dynamic SMB model is necessary for better design and optimisation; however, it requires significant computational effort. Traditional direct substitution is not effective in terms of fast determination of steady state. In this study, we conduct a systematic research to obtain a structural insight of those models so that a unified framework for accurate, yet computationally efficient modelling of general SMBCPs can be developed. Effort is also made in the comprehensive study on frontier numerical techniques for the solution of SMB models under a range of parameters. Furthermore, a brand new approach is proposed to quickly obtain the cyclic steady state of SMB operation.

In the next chapter, detailed column modelling and basic concept on the relevant mathematical methods will be presented together with the algorithms for numerically solving such a model.

CHAPTER 3
COLUMN MODELLING AND NUMERICAL METHODS

In order to optimise SMBCPs, it is necessary to describe the exact position and shape of the transient concentration fronts as a function of fluid velocity and component concentrations. Mathematical models of varying complexity have been used to investigate the performance and design of SMB processes to separate different mixtures. Mathematical modelling and simulation play a very important role in developing and studying SMB separation processes.

Starting from the mechanisms of mass transfer and mass exchange in a separation column, we will develop a column model from mass balance, which takes into account all the possible phenomena. Then, these equations will be progressively simplified for specific situations.

3.1 Analysis and Modelling of Adsorption Processes

Dynamic SMB model consists of two main parts: single chromatographic column model describing the kinetics of adsorption and node balances model describing the connection of the columns combined with the cyclic switching (Araujo et al., 2006). Since the behaviour of equilibrium isotherm determines the character of chromatography being linear or non-linear, the models of chromatography column are not specific to the components being separated. It is the combination of generally formatted equations with any possible isotherm expression. The level of mathematical difficulty encountered depends much on the nature of equilibrium relationship, the concentration level, and the choice of flow mode.

According to Ruthven (1984: Chapter 8), model complexity should be analysed from the following classification:

- Nature of Equilibrium Relationship (Linear isotherm, Favourable isotherm, or unfavourable isotherm).
- Isothermal (Heat transfer resistance can be neglected) or Near Isothermal
- Concentration level of mixed components
    1) Trace systems – component with low concentration
    2) Nontrace systems - high concentration (usually for gaseous systems)
- Flow Model
    1) Plug flow (neglect axial dispersion), or

2) Dispersed Plug flow

- Complexity of Kinetic Model
  1) Negligible mass transfer resistance (equilibrium condition)
  2) Single mass transfer resistance (either external film control or intraparticle diffusion control)
  3) Two mass transfer resistance (External film + intraparticle diffusion or macropore-micropore internal diffusion resistance)
  4) Three mass transfer resistance (External film + two internal diffusion)

In the following subsection, we will summarise the models available from literature in a systematic way to help the understanding of their suitability.

3.1.1 Derivation of General Rate Model

In a separation column, the mobile phase containing the solvent and components flows through the solid phase, the package of fine, globular and porous particles (adsorbent). As shown in Figure 3.1, the particle consists of a solid part, a liquid pore phase and surrounded by a film. The affinity of the component to the adsorbent leads to the transport of the component from the solvent to the particles. The driving force of this transport is the tendency of equilibrating the molecular load, between the solvent and the surface of the particles.

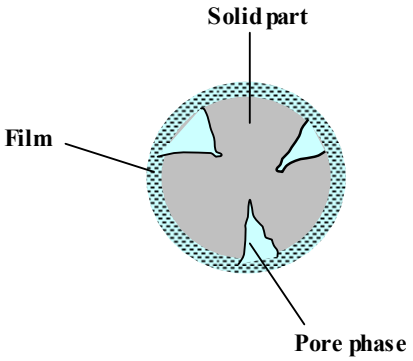

Figure 3.1 *Adsorbent particle*

The mass transfer between the two phases is dominated by three phenomena: convection, diffusion, and dispersion. Convective and dispersive mass transfers are present in the mobile phase. The mass exchange between the mobile and solid phase takes place by diffusion through the film of solvent surrounding the particle. In principle, adsorptive exchange takes

place all over the particle surface; however, for ease of modelling, only the pore phase is supposed to be in exchange with the particle surface, and the exchange between the pore phase and the mobile phase occur through the film. The mechanism is illustrated in Figure 3.2.

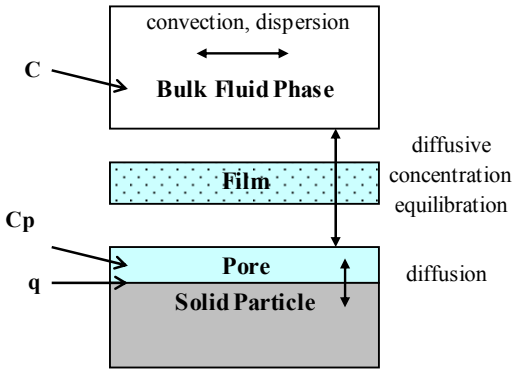

Figure 3.2 *Mass transfer and mass exchange in separation process*

From fluid dynamics and mass transfer, mathematical descriptions are available for the above three phenomena. Several assumptions are made for the application to the adsorptive chromatographic separation process:

- Isothermal (constant temperature during a run)
- Homogeneous package porosity
- Homogeneous particle size and porosity
- Constant radial distribution of the mobile phase concentration
- Neglect of column wall effects
- Local equilibrium is established within the pores
- The film mass transfer can be used to describe the interfacial mass transfer between the bulk-fluid and particle phases.
- The diffusion and mass transfer parameters are constant

The general rate model attempts to account for all the possible contributions to the mass transfer kinetics arising in chromatography by including the axial dispersion, external film mass transfer resistance, the intraparticle pore diffusion. Because this model considers the stagnant mobile phase inside the particle and the percolating mobile phase outside the particle, two types of mass balance equations are needed. This allows the coexistence of a

homogeneous stream of mobile phase and a non-homogeneous particle bed. The concentration in the particles increases from the surface to the centre when the front of the peak passes, and decreases on the peak tail. Although there are several versions of general models (Dünnebier et al., 2000a; Guiochon, 2002; Toumi & Engell, 2003; Lu, 2004), the following basic form of equations are recognised to be essential.

Mass balance in the mobile phase (or bulk-liquid phase)

This mass balance is written for a fluid percolating through a bed of spherical particles with radius of R_p in the column:

$$\frac{\partial C}{\partial t} + u\frac{\partial C}{\partial x} = D_{ax}\frac{\partial^2 C}{\partial x^2} - \frac{1-\varepsilon_b}{\varepsilon_b}\frac{\partial \overline{q}}{\partial t} \tag{3.1a}$$

Mass balance in the solid phase

Assume the solid phase consists of porous, uniform and spherical particles with void fraction ε_p and local equilibrium is established within the pores. The mass balance inside the particles is written as:

$$\frac{\partial C_p}{\partial t} + \frac{1-\varepsilon_p}{\varepsilon_p}\frac{\partial q}{\partial t} = D_p\frac{1}{r^2}\frac{\partial}{\partial r}(r^2\frac{\partial C_p}{\partial r}) \tag{3.1b}$$

For the fluid film resistance: $\frac{\partial \overline{q}}{\partial t} = \frac{3k_{ext}}{R_p}(C - C_p\,|_{r=R_p})$

And the solid film resistance: $\frac{\partial q}{\partial t} = k_{\text{int}}(q^* - q)$

Equations (3.1a) and (3.1b) are also called "Distributed Plug-flow Model" (Strube & Schmidt-Traub, 1998).

The boundary conditions

There are two flux boundary conditions, one at the column inlet and the other at the column exit:

The condition for $x = 0$ at $t > 0$ is: $$\frac{\partial C}{\partial x} = \frac{u}{D_{ax}}(C - C^{in}) \quad (3.1c)$$

The condition for $x = L$ at $t > 0$ is: $$\frac{\partial C}{\partial x} = 0 \quad (3.1c')$$

For Equation (3.1b), the boundary conditions are:

$$\frac{\partial C_p}{\partial r} = 0; \quad \text{at } r = 0 \quad (3.1d)$$

$$\frac{\partial C_p}{\partial r} = \frac{k_{ext}}{\varepsilon_p D_p}(C - C_{p|_{r=R_p}}); \text{ at } r = R_p \quad (3.1d')$$

The initial conditions

The initial conditions describe the status of the column at the start of mixture injection,

$$C(0, x) = C^{in}; \quad C_p = C_p(0, r, x) \quad (3.1e)$$

The Adsorption Isotherm Model

An isotherm model relates the component concentration in solid phase to the one in mobile phase. It describes the thermodynamic behaviour of the modelled system. The type of adsorption isotherms is a key to distinguish different chromatographic process by influencing the structure of the resulting mathematical expression. Process with linear isotherms are most applied for sugar separation processes and can be modelled and simulated much easier than those with nonlinear isotherms, e.g., enantiomers separation.

The relationship of adsorption equilibrium isotherm can be expressed in a general form:

$$q_i^* = f_i(C_1, C_2, \cdots C_N)$$

N stands for the total number of components in feeding mixture. The following are some of the equilibrium isotherm models reported in literature.

Freundlich: $$q_i^* = KC_i^{1/n}$$

Langmuir: $$q_i^* = \frac{bC_i}{1+bC_i}$$

Extended Langmuir: $$q_i^* = \frac{a_i C_i}{1+\sum_{n=1}^{N} b_n C_n}$$

For ion-exchange: $$q_i^* = \frac{a_i C_i}{\sum_{n=1}^{N} b_n C_n}$$

Langmuir-Freundlich: $$q_i^* = \frac{a_i C_i^{m_i}}{1+\sum_{n=1}^{N} b_n C_n^{m_n}}$$

Modified Competitive Langmuir: $$q_i^* = \lambda_i C_i + \frac{a_i C_i}{1+\sum_{n=1}^{N} b_n C_n}$$

Thus, a chromatographic column model is represented by Equations (3.1a-e) plus any of the isotherm models. A simulated moving bed separation process model is a combination of several such column models with additional material balance equations at each column connection point. It is further enlarged by the number of components being separated and the time axial will be extended for hundreds of switching. The increasing of model complexity is always challenging for online model based optimisation and control. In the following subsection, we will conduct the analysis of this general rate model to see how it can be further simplified to suit various application requirements.

3.1.2 Existing Model Structural Insight and Simplification

(I) ***The Pore Model***

This is a simplified version of the general rate model. It is suitable for the situation when the mass transfer kinetics is moderately fast. It assumes homogeneous particles. The diffusive effects in the pore phase and on the surface can be neglected. The concentration of the pore phase can be assumed equal to the concentration in the film. Mass exchange is present between the mobile phase and the film. Average particle $\overline{q}$ and pore concentrations $\overline{C}_p$ are

used, which simplified the pore diffusion term in Equation (3.1b), leading to Equations (3.2a) and (3.2b).

$$\frac{\partial C}{\partial t} + u\frac{\partial C}{\partial x} = D_{ax}\frac{\partial^2 C}{\partial x^2} - \frac{1-\varepsilon_b}{\varepsilon_b}\frac{3k_T}{R_p}(C - \overline{C}_p) \tag{3.2a}$$

$$\frac{\partial C_p}{\partial t} + \frac{1-\varepsilon_p}{\varepsilon_p}\frac{\partial \overline{q}}{\partial t} = \frac{3k_T}{\varepsilon_p R_p}(C - \overline{C}_p) \tag{3.2b}$$

with the film resistance: $\dfrac{\partial \overline{q}}{\partial t} = k_{\text{int}}(q^* - \overline{q})$; $\quad q^* = F(\overline{C}_p)$

where the overall mass transfer coefficient k_T is governed by both the external and the internal mass transfer coefficients: $k_T = \left[\dfrac{1}{k_{ext}} + \dfrac{1}{k_{\text{int}}}\right]^{-1}$

The "Lumped Parameter Mass Transfer Model" (Natarajan & Lee, 2000) contains the same equations.

(II) ***Dispersive Model***

It assumes mass transfer kinetics between the mobile phase and pore phase percolating across the column and particles is infinitely fast. Local mass transfer resistance can be neglected, thus $C \approx \overline{C}_p$. This gives the following single equation of dispersive model.

$$\frac{\partial C}{\partial t} + u_T\frac{\partial C}{\partial x} = D_T\frac{\partial^2 C}{\partial x^2} - \frac{1-\varepsilon_T}{\varepsilon_T}\frac{\partial \overline{q}}{\partial t} \tag{3.3}$$

This model contains only one of the equations from General Rate Model. However, it has lumped coefficients to account for both the external and internal effects, where, the total porosity: $\varepsilon_T = \varepsilon_b + (1-\varepsilon_b)\varepsilon_p$; $u_T = \dfrac{\varepsilon_b}{\varepsilon_p}u$ and $D_T = \dfrac{\varepsilon_b}{\varepsilon_p}D_{ax}$.

To complete Equation (3.3), there are two ways of expressing mass transfer resistance $\dfrac{\partial \overline{q}}{\partial t}$, the Transport-Dispersive and Equilibrium-Dispersive Model.

(III) ***Transport-Dispersive Model***

In cases where the mass transfer resistance is not large, but cannot be entirely neglected, a Linear Driving Force (LDF) Model will commonly be used to describe the kinetic effect of mass transfer.

$$\frac{\partial \overline{q}}{\partial t} = k_T (q^* - \overline{q}) \tag{3.4}$$

Combined with the appropriate isotherm equation $q^* = F(C)$, it is the most popular model in the literature for various applications, e.g., Lumped Solid Diffusion Model (Song et al., 2006); Non-equilibrium Model (Lim, 2004c).

(IV) ***Equilibrium-Dispersive Model***

Assuming mass transfer equilibrium, where $\overline{q}$ is directly given by the isotherm equation, we have:

$$\overline{q} = q^* = F(C) \tag{3.5}$$

This simplification will give us a useful model after rearrangement of Equation (3.3). For any given adsorption isotherm $q^* = F(C)$, there is (Dünnebier et al., 1998):

$$\frac{\partial C}{\partial t} = \frac{1}{1 + \dfrac{1-\varepsilon_T}{\varepsilon_T}\dfrac{\partial q^*}{\partial C}} \left(-u_T \frac{\partial C}{\partial x} + D_T \frac{\partial^2 C}{\partial x^2}\right) \tag{3.6}$$

It is seen that the right hand side includes the convective and dispersive terms, both of which are weighted by a factor containing the phase relation and the slope of the isotherm $\dfrac{\partial q^*}{\partial C}$. It also implies that the effect of axial dispersion and mass transfer are additive. This approach is valid when the column efficiency is high, but is questionable in most cases of enantiomeric separation or for the elution of many proteins.

(V) ***The Lumped Kinetic Model***

It has been found that the axial dispersion, mass transfer resistance and particle diffusion effect can be lumped into a single parameter. By adjusting the corresponding parameters, one can simplify the dispersive model by considering only one of the effects. There are two types of lump models found in the literature:

1. Lumped mass transfer resistance to D_{ap} (axial dispersion coefficient). Under linear condition, it is also under the name of "Dispersive Model for Linear Isotherms) (DLI-model) (Klatt et al., 2002) when applied to the separation of fructose and glucose). For a process with linear adsorption equilibrium, the DLI-model is shown to provide a very accurate and computationally efficient simulation model (Dünnebier et al., 1998).

$$\frac{\partial C}{\partial t} + u\frac{\partial C}{\partial x} = D_{ap}\frac{\partial^2 C}{\partial x^2} \tag{3.7}$$

2. Lumped the axial dispersion to effective mass transfer coefficient k_{ap} in LDF model, which leads to Equation (3.5b) (Dünnebier & Klatt, 2000)

$$\frac{\partial C}{\partial t} + u\frac{\partial C}{\partial x} = \frac{1-\varepsilon_b}{\varepsilon_b}k_{ap}(q^* - \overline{q}) \tag{3.8}$$

(VI) ***The Ideal Model (Equilibrium Plug-Flow)***

The simplest model is the idea model, which neglect all non-ideal effects and assume overall equilibrium (Dünnebier & Klatt, 2000; Dünnebier et al., 1998). It assumes that the column has an infinite efficiency, mass transfer between mobile and stationary phase is instantaneous and there is no axial dispersion.

$$\frac{\partial C}{\partial t} + u_T\frac{\partial C}{\partial x} = -\frac{1-\varepsilon_T}{\varepsilon_T}\frac{\partial \overline{q}}{\partial t} \tag{3.9}$$

When assuming mass transfer equilibrium $q = q^*$ with the isotherm represented in a general form by $q^* = F(C)$, Equation (3.9) can be transformed into

$$\frac{\partial C}{\partial t} = -\frac{u_T}{1+\dfrac{1-\varepsilon_T}{\varepsilon_T}\dfrac{\partial q^*}{\partial C}}\frac{\partial C}{\partial x} \tag{3.10}$$

This model has the advantage of simplicity and can be solved analytically for most of the adsorption isotherms.

3.1.3 Choosing the "Simplest" Model For Given Modelling Goal

The derivation of each successive model is illustrated in the Figure 3.3, where assumptions are outlined helping the development of next stage model, from the complicated one to the simplified ones.

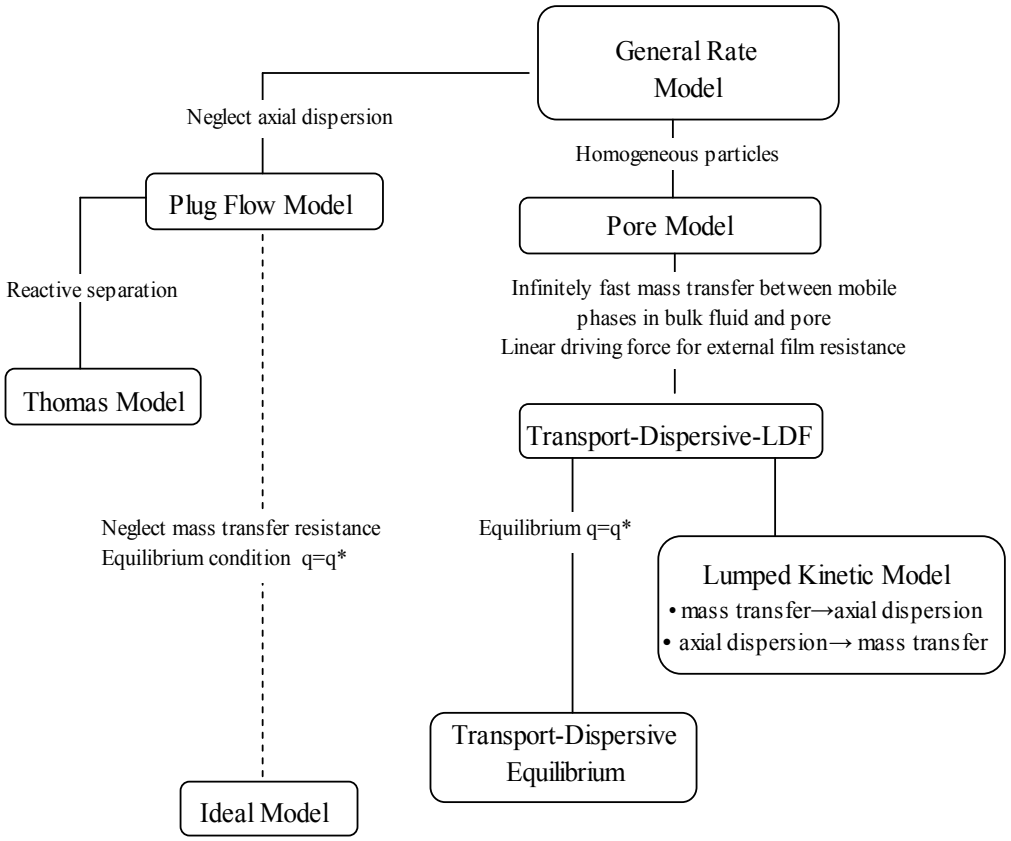

Model Type	Mass Transfer Resistance	Mass Transfer interface	Dimension of Variables
General Rate	External film pore diffusion	C - $C_p\|_{r=R_p}$ - C_p - q^* - q	$C(t,x)$, $C_p(t,r,x)$, $q(t,r,x)$
Pore Model	External film pore diffusion	C - $\overline{C}_p$ - q^* - q	$C(t,x)$, $\overline{C}_p(t,x)$, $q(t,x)$
Transport-Dispersive LDF	External film	C - q^* - q	$C(t,x)$, $q(t,x)$
Transport-Dispersive Equilibrium	Negligible	C - q $(q^* = q)$	$C(t,x)$, $q(t,x)$

Figure 3.3 *Column Model development chart and illustration.*

One may find other model names in the literature, such as: **Equilibrium Transport, Equilibrium Transport Dispersive, Lumped Model, Equilibrium Model, Dispersed Plug Flow, Distributed Plug Flow, Lumped Solid Diffusion, Diffusion Model, and Nonequilibrium Model,** etc. All these mentioned models can more or less be fitted into our classification.

The ways of describing mass transfer resistance between the mobile phase and the solid phase make a big contribution to the complexity of the model. It may be treated either according to equilibrium theory or by including an appropriate rate expression to account for mass transfer resistance, generally in terms of LDF model or diffusion model, or their combination. All equilibrium models assume $q = q^*$, using isotherm equation directly to represent the relationship between the concentration on particle surface and in bulk fluid phase. While the linear driving force (LDF) model is the application of the first Fick's law of mass transport and is an equation of equilibrium isotherm.

As the basis of process analysis, control, and operational optimisation, modelling of SMBCPs has been paid increased attention in the open literature (Dünnebier et al., 2000a). Being the major part of the SMBCP model, selection of an appropriate column model becomes critical. It determines the complexity of the model representation and, thereafter, the computational intensity. In summary, a column model can be chosen from the following three types:

(1) ***Ideal model***. Both mass transfer resistance and axial dispersion are neglected.
(2) ***Dispersive model***. Mass transfer resistance and axial dispersion are modelled. The model has a compromise between the accuracy and computational efficiency (Abel et al., 2004).
(3) ***General rate model***. The following effects are modelled (Toumi & Engell, 2004): convection, axial dispersion, pore diffusion, solid and liquid phase mass transfer, multi-component adsorption, and homogenously/heterogeneously catalysed reactions.

A fundamental question to be addressed is: which model should be chosen that on one hand is detailed enough to describe the complexity of the process dynamics and on the other hand is suitable for simulation and real time control? Most existing SMBCP models use an equilibrium transport dispersive column model based on the absorption equilibrium isotherm and a linear driving force approach for mass transfer from bulk to solid phase. LDF model offers a realistic representation of industrial processes and provides a good compromise between accurate and efficient solutions of these models (Biegler et al., 2004), thus has been widely used in modelling many adsorption processes due to its remarkable simplicity and good agreement with experimental results (Ching, 1997). From our model structural analysis

in the last few subsections, a dispersive model expressed by Equation (3.3) and Equations (3.4) and (3.5) will be adopted to represent the column dynamics in all of the separation cases under study.

3.2 Wavelets Methods for Solving PDEs

In this study, we will promote wavelet collocation methods for solving chromatographic column models numerically in view of its advantage in the approximating functions with abrupt change. The effectiveness of these methods will be discussed through a special case, where analytical solution is also available for comparison purpose. For completeness, in this section we will introduce the basic concepts and definitions of wavelet, followed by the two methods based on the previous work of Koren (1993), Bertoluzza (1996), Qamar et al. (2006) and Zhang et al. (2008). Although finite difference method is also used in this research for comparison purpose, its mathematical theory will not be presented here. For fundamentals of finite discretisation, readers can refer to the book of "Numerical Methods and Modelling for Chemical Engineers" by Mark E. Davis (1984).

3.2.1 Basic Concepts and Definitions

Wavelets are functions that have compact support, i.e. non-zero only on a finite interval, and used in representing data or other functions. Wavelets literally mean "small waves" - they oscillate, their curves yield zero net area, and they are localized in time. This leads to the possibility that wavelets are better suited to represent functions that are localized both in time and frequency. In particular, wavelets enable us to represent functions with sharp spikes or edges.

Wavelets are defined by the wavelet function $\psi(x)$, i.e., the mother wavelet, and scaling function $\phi(x)$, i.e., father wavelet. One starts from the mother wavelet and generates the basis by dilation (scaling) and translation operations, $\psi(ax-b)$. For discrete wavelets, the parameters by which one translates, b, and dilates, a, are restricted to a discrete set, usually $a=2^j$, $b=k$ where j and k are integers. In the so-called multiresolution analysis, which we will discuss in the next section, details or fluctuations at different levels of resolution are represented by wavelets at different scales and positions. In formal terms, this representation is a wavelet series representation of a square-integrable function with respect to either a complete, orthonormal set of basis functions, or an overcomplete set of frame of a vector space (also known as a Riesz basis), for the Hilbert space of square integrable functions.

Multiresolution Analysis

Approximation of a function can be conducted at different resolution levels. We define a sequence of resolutions such that all details of the function on scales smaller than 2^j are suppressed at resolution j. Denote that subspace by V_j. A multiresolution analysis of $L^2(R)$ is a nested sequence of subspaces $\{V_j\}$ such that

(i) $V_j \subset V_{j+1}$

(ii) $\bigcap_j V_j = \{0\}, \overline{\bigcup_j V_j} = L^2(R) \subset V_{j+1}$

(iii) $f(x) \in V_j \Leftrightarrow f(2x) \in V_{j+1}$

(iv) $f(x) \in V_0 \Leftrightarrow f(x-k) \in V_0$

(v) There exists a function $\phi(x)$, such that $\phi(x-k)$ is an orthonormal basis of V_0.

Multiresolution analysis explains how wavelets work for processing data. The first point requires that any subspace be contained in all the higher subspaces. The second requirement is that all square integrable functions be included at the finest resolution and only the zero function at the coarsest level. As the resolution gets coarser and coarser, more and more details are removed, and in the limit $j \to -\infty$, only a constant function survives and since it has to be square integrable, it can only be the zero function. Therefore, we demand that $\lim_{j\to-\infty} V_j = \{0\}$. On the other hand, when we increase the resolution, more details are included and as the resolution goes to infinity, we should recover, crudely speaking, the entire initial space $L^2(R)$, that is, $\lim_{j\to\infty} V_j \to L^2(R)$.

The third condition is the key requirement of scale or dilation invariance. If $f(x)$ is in V_j, that is, $f(x)$ contains no details or fluctuations at scales smaller than $1/2^j$, then $f(2x)$ is a function obtained by squeezing $f(x)$ by a factor of 2 and contains no details at scales smaller than $1/2^{j+1}$. Therefore, $f(2x)$ is in V_{j+1}. The fourth condition is the requirement of translation or shift invariance of the space V_j. The third and fourth requirements of dilation and translation invariance yield the result that if $f(x) \in V_0$, $f(2^j x - k) \in V_j$.

The final definition introduces the scaling function $\phi(x)$, which generates the basis functions for all the spaces. Through translations (shifting) of the scaling function, a Riesz basis of

subspace is formed. Furthermore, through translation of $\phi(x)$ by a factor of 2^j and dilation by a factor of k, a Riesz basis, $\{\phi_{j,k}(x)\}$ is obtained for the subspace $V_j \subset L^2(R)$, where

$$\phi_{j,k}(x) = 2^{j/2}\phi(2^j x - k) \tag{3.11}$$

which is corresponding to resolution level of j.

To find the relationship between scaling functions in different spaces, we will look at the following operation. Since $V_0 \subset V_1$, any function in V_0 can be expanded in terms of the basis functions of V_1. In particular, the scaling function can also be expanded in terms of $\{\phi_{1,k}(x)\}$:

$$\phi(x) = \sum_k p(k)\phi_{1,k}(x) = \sqrt{2}\sum_k p(k)\phi(2x - k) \tag{3.12}$$

This is called the dilation equation. This equation relates the scaling function at two successive scales, x and $2x$, and, hence, it is also referred to as the two-scale equation or refinement equation. Using the fact that $\{\phi_{1,k}(x)\}$ are orthonormal, the coefficients $p(k)$ can be obtained by computing the inner product:

$$p(k) = \langle \phi_{1,k}(x), \phi(x) \rangle = \sqrt{2}\int_{-\infty}^{\infty} \phi(x)\phi(2x - k)dx \tag{3.13}$$

It is obvious that there is some information lost when the approximation goes from level $j+1$ to level j. Let the orthogonal complement of V_j to V_{j+1} be W_j, such that, $V_j \oplus W_j = V_{j+1}$. W_j is called the detail space at resolution level j and is orthogonal to V_j. This means the inner product between any element in W_j and any element in V_j vanishes. We can continue the decomposition and obtain

$$V_{j+1} = W_j \oplus_j V_j = W_j \oplus W_{j-1} \oplus V_{j-1} = \cdots = W_j \oplus W_{j-1} \oplus W_{j-2} \oplus \cdots \oplus W_{j-J} \oplus V_{j-J} \tag{3.14}$$

It turns out that for a multiresolution analysis, the detail space W_j has an orthonormal basis $\{\psi_{j,k}(x)\}$. Each wavelet is generated from a single function $\psi(x)$ by translation and dilation.

The function $\psi(x)$ that generates all the basis functions of the W space is referred to as the mother wavelet or the basic wavelet.

Let us see how the mother wavelets and scaling functions relate to each other. Since $\{\psi(x)\}$ is in W_0, and, $W_0 \subset V_1$, $\psi(x)$ can be written as a superposition of the basis functions for V_1, $\{\phi_{1,k}(x)\}$. In particular, we have

$$\psi(x) = \sum_k q(k)\phi_{1,k}(x) = \sqrt{2}\sum_k q(k)\phi(2x-k) \tag{3.15}$$

Where $q(k)$ are a set of coefficients for the two-scale relationship of wavelet basis.

Note the similarity between this equation and the dilation equation. This is an equation relating the mother wavelet to the scaling function at the next finer scale. Again, using the fact that $\{\phi_{1,k}(x)\}$ are orthonormal, the coefficients $\{q(k)\}$ can be obtained by computing the inner product:

$$q(k) = \langle \phi_{1,k}(x), \psi(x) \rangle = \sqrt{2}\int_{-\infty}^{\infty} \psi(x)\phi(2x-k)dx \tag{3.16}$$

A Riesz basis for the subspace W_j is given by $\{\psi_{j,k}(x)\}$, where

$$\psi_{j,k}(x) = 2^{j/2}\psi(2^j x - k) \tag{3.17}$$

We give Table 3.1 as a summary of different wavelets representation.

Table 3.1 *Wavelets representation*

	Approximation Space	**Detailed Space**
Space Notation	V_j	W_j
Space Property	$V_j \subset V_{j+1}$	$W_j \perp W_k$ for $j \neq k$
Basis function	Scaling function $\phi(x)$	Mother wavelet $\psi(x)$
Refinement equation	$\phi(x) = \sqrt{2}\sum_k p(k)\phi(2x-k)$	$\psi(x) = \sqrt{2}\sum_k q(k)\phi(2x-k)$
Orthonormal basis	$\phi_{j,k}(x) = 2^{j/2}\phi(2^j x - k)$	$\psi_{j,k}(x) = 2^{j/2}\psi(2^j x - k)$

It is seen that wavelets constitute a special class of basis functions for $L^2(R)$. Different choices for the mother wavelet yield different wavelet bases. One could also start from the scaling function of a multiresolution analysis since the mother wavelet can be obtained through refinement equations.

Wavelet Transform

Using scaling functions as basis, an approximate solution to function $f(x)$, at resolution level j can be expressed as,

$$f(x) \approx I_j f_j(x) = \sum_k p_j(k)\phi_{j,k}(x) \tag{3.18}$$

where $p_j(k)$ is given by the inner product of $f_j(x)$ and $\phi_{j,k}(x)$,

$$p_j(k) = \left\langle f_j(x), \phi_{j,k}(x) \right\rangle = \int_{-\infty}^{\infty} f_j(x)\phi_{j,k}(x)dx$$

On the other hand, we can also use both scaling functions and wavelet functions to approximate $f(x)$. By multiresolution analysis, the space of square-integrable functions can be decomposed into a direct sum of orthogonal subspaces, e.g., decomposition of the space V_j into $W_{j-1} \oplus V_{j-1}$. In particular, any function in $L^2(R)$ can be expanded in terms of $\{\phi_{j,k}(x)\}$ and $\{\psi_{j,k}(x)\}$, the orthonormal bases of V_j and W_j, respectively.

$$f(x) \approx f_{j-1}(x) + d_{j-1}(x) \tag{3.19}$$

The part containing fluctuations is given by wavelet functions,

$$d_{j-1}(x) = \sum_k q_{j-1}(k)\psi_{j-1,k}(x)$$

3.2.2 Wavelet Based Collocation Methods

There are two methods for the solution of partial differential equations.

Collocation methods: the solution is obtained in the physical space over a dynamically adapted grid. Each wavelet is univocally associated with a collocation point and the grid adaptation is based on the analysis of the wavelet coefficients.

Galerkin methods: obtain the solution in the wavelet coefficient space and in general can be considered gridless methods.

In the collocation method proposed by Bertoluzza and Naldi (1994), trial functions are a class of interpolating functions generated by autocorrelation of the usual compactly supported Daubechies scaling functions.

$$\theta(x) = \int_{-\infty}^{\infty} \phi(y)\phi(y-x)dy \tag{3.20}$$

Where: $\phi(x)$ is the Daubechie's wavelet with compact support $[0.L]$, and $\theta(x)$ plays the role of scaling function. It can be verified that the linear span of $\left\{\theta_{j,k} = \theta(2^j x - k), k \in Z\right\}$ forms a multiresolution analysis and the function defined by Equation (3.20) satisfies the interpolation properties for integer k

$$\theta(k) = \begin{cases} 1, k = 0 \\ 0, k \neq 0, k \in Z \end{cases} \tag{3.21}$$

In order to take advantage of the interpolating function defined by Equation (3.20) to numerically solve differential equations, the interpolation operator,

$$I_j f_j(x) = \sum_k p_j(k)\theta_{j,k}(x) \tag{3.22}$$

is introduced (Bertoluzza, 1994, 1996) to approximate the unknowns in the PDEs. For the interpolation operator, we have the following error estimate, which guarantees the convergence of the numerical method.

$$\left\| f - I_j f \right\|_r \leq C 2^{-j(s-r)} \left\| f \right\|_s \tag{3.23}$$

Now let us see how to apply the above to our problem. Consider the following chromatographic separation model defined on a bounded interval $x \in [0,1]$

$$\frac{\partial u(x,t)}{\partial t} = f(x,t,u,\frac{\partial u}{\partial x},\frac{\partial^2 u}{\partial x^2}) \tag{3.24}$$

The original function can be represented in terms of a wavelet expansion, using coefficients in a linear combination of the basis.

$$u(x,t) \approx u_J(x,t) = \sum_{k=0}^{2^J} p_J(x_k,t)\theta_{J,k}(x) \tag{3.25}$$

$k = 0,1,\cdots,2^J$; $x_k = k/2^J$

$p_J(x_k,t)$ are the 2^J+1 unknown wavelet coefficients. In the collocation method, these coefficients are determined by satisfying the boundary value problem exactly at collocation points. Substituting (3.25) to (3.24), the PDEs can then be discretised into a set of ODEs by using the dyadic points in the spatial dimension.

$$\frac{du_J(x_k,t)}{dt} = f(x_k,t,u_J(x_1,t),\cdots u_J(x_k,t)) \tag{3.26}$$

To deal with boundary conditions, we will adopt one of the schemes proposed by Bertoluzza (1996) for the construction of interpolating function. This is a relatively mature method for numerically solving the pure mathematical problems, though only limited work addresses its application in engineering. It is based on the following modified interpolation functions (Donoho, 1992), where $\{\theta^l_{j,k}\}$ and $\{\theta^r_{j,k}\}$ are defined basis for the left and right boundaries.

$$\theta^l_{j,k} = \theta_{j,k} + \sum_{n=-L}^{-1} a_{n,k}\theta_{j,n} \tag{3.27a}$$

$$\theta^r_{j,k} = \theta_{j,k} + \sum_{n=2^j+1}^{2^j+L} b_{n,k}\theta_{j,n} \tag{3.27b}$$

with

$$a_{n,k} = \prod_{\substack{i=0 \\ i\neq k}}^{2M-2} \frac{x_n - x_i}{x_k - x_i} \quad ; \qquad b_{n,k} = \prod_{\substack{i=2^j-2M+2 \\ i\neq k}}^{2^j} \frac{x_n - x_i}{x_k - x_i}$$

M is the number of interpolating points in the neighbourhoods of the endpoints of the interval in question. It can be verified that the modified interpolation functions defined in Equation (3.27) have similar properties as Equation (3.20). Substituting Equation (3.27) into Equation (3.22), we can have the modified interpolation operator, which will be used in this study, as the following

$$I_j f_j = \sum_{k=0}^{L} p_j(k)\theta_{j,k}^{l} + \sum_{k=L=1}^{2^j-L-1} p_j(k)\theta_{j,k} + \sum_{k=2^j-L}^{2^j} p_j(k)\theta_{j,k}^{r} \tag{3.28}$$

Applying Equation (3.28) to PDE and evaluating it at the dyadic point yields a set of ODEs. The resulting ODEs can be solved by using any of the time integrator schemes.

3.3 High Resolution

As one of the relative new techniques for solving PDEs, the high resolution algorithms will also be investigated, which will be taken for comparison purpose while conducting this investigation on wavelet based methods. Consider the following PDE with appropriate boundary and initial conditions,

$$\frac{\partial u}{\partial t} + \frac{\partial f(u)}{\partial x} + \beta \frac{\partial^2 u}{\partial x^2} = 0, x \in [a,b] \tag{3.29}$$

In wavelet collocation method, the concerned interval is discretised by using the dyadic points, which can take advantage of the interpolation property of the interpolating wavelet. For high resolution method, we will divide the concerned interval into a number of subintervals uniformly. For instants N subintervals Ω_i. Let $d = (b-a)/N$, $x_{1/2} = a$ and $x_{N+1/2} = b$, we have $\Omega_i = [x_{i-1/2}, x_{i+1/2}]$, $i = 1, \cdots, N$, with $x_{i-1/2} = a + (i-1)d$. Denotes the approximation of the unknown u in Ω_i by y_i. Then, by using the way proposed in Qamar et al. (2006), we have

$$y_i = \frac{1}{d}\int_{x_{i-1/2}}^{x_{i+1/2}} u(x,t)dx, i = 1, \cdots, N \tag{3.30}$$

Substituting Equation (3.30) into Equation (3.29) gives,

$$\frac{dy_i}{dt} + \frac{1}{d}(f_{i+1/2} - f_{i-1/2}) + \frac{1}{d}\beta\left(\frac{\partial y}{\partial x}\Big|_{x_{i+1/2}} - \frac{\partial y}{\partial x}\Big|_{x_{i-1/2}}\right) = 0 \tag{3.31}$$

The function $f_{i+1/2}$ can be approximated by using one of the two schemes proposed in (Koren, 1993).

(1) Upwinding scheme

$$f_{i+1/2} = f_i, \qquad i = 1, \cdots, N \tag{3.32}$$

(2) κ – flux *interpolation scheme*

$$f_{i+1/2} = f_i + \frac{1+\kappa}{4}(f_{i+1} - f_i) + \frac{1-\kappa}{4}(f_i - f_{i-1}) \tag{3.33}$$

$$\kappa \in [0,1],\ i = 2,\cdots,N-1$$

For function $\left.\frac{\partial y}{\partial x}\right|_{x_{i+1/2}}$, there is

$$\left.\frac{\partial y}{\partial x}\right|_{x_{i+1/2}} = \frac{y_{i+1} - y_i}{d} \tag{3.34}$$

Different boundary conditions will be treated for function $f_{i+1/2}$ and $\left.\frac{\partial y}{\partial x}\right|_{x_{i+1/2}}$ by using the methods proposed in (Koren, 1993; Zhang et al., 2008).

(1) ***PDEs with Dirichlet boundary conditions (Koren, 1993)***

Dirichlet boundary conditions have the following format:

$$u(t,a) = u_{in}\ ;\quad u(t,b) = u_{out} \tag{3.35}$$

On the boundary of the spatial variable, we have

$$f_{1/2} = f(u_{in}) \tag{3.36a}$$

$$f_{1+1/2} = f\left(\frac{y_1 + y_2}{2}\right) \tag{3.36b}$$

$$f_{N+1/2} = f(y_{out}) \tag{3.36c}$$

$$\left.\frac{\partial y}{\partial x}\right|_{1/2} = \frac{-8u_{in} + 9y_1 - y_2}{3d} \tag{3.36d}$$

$$\left.\frac{\partial y}{\partial x}\right|_{N+1/2} = \frac{8u_{out} - 9y_N + y_{N-1}}{3d} \tag{3.36e}$$

(2) ***PDEs with Cauchy boundary condition (Zhang et al., 2008)***

If the boundaries are represented by the following Cauchy conditions:

$$u(t,a)+\varphi\frac{\partial u}{\partial x}\Big|_{x=a}=u_{in}\ ;\ \frac{\partial u}{\partial x}\Big|_{x=b}=u_{out} \tag{3.35'}$$

Equations (3.36a), (3.36c), (3.36d) and (3.36e) will respectively become:

$$f_{1/2}=f(y(t,a))+\frac{1}{2}(f(y_1)-f(y(t,a))) \tag{3.36a'}$$

$$f_{N+1/2}=f(y_N)+\frac{1}{2}(f(y_N)-f(y_{N-1}) \tag{3.36b'}$$

$$\frac{\partial y}{\partial x}\Big|_{1/2}=\frac{-8u_{in}+9y_1-y_2}{3d-8\varphi} \tag{3.36d'}$$

$$\frac{\partial y}{\partial x}\Big|_{N+1/2}=u_{out} \tag{3.36e'}$$

where

$$y(t,a)=\frac{3du_{in}-9\varphi y_1+\varphi y_2}{3d-8\varphi}$$

3.4 Time Integrator - the Alexander Method

The time integrator used for the study on temporal discretisation technique is the Alexander method. It will also serve as the inner integrator in Chapter 6 for the simulation of cycled process. This is a third-order semi-implicit Runge-Kutta method, which requires several implicit equations to be solved in series. The Alexander method has 3 stage equations with the order of 3. The stability of this method is L-stable, which means it not only has the whole negative half plane as stability regions, but also be capable of dampening out possible oscillation in the numerical solution even for very large negative eigenvalues. The good stability of the method makes it particularly well-suited for stiff problems.

Its Butcher block looks like:

η	**η**	**0**	**0**
c	**c- γ**	**η**	**0**
1	**b1**	**b2**	**η**
1	**b1**	**b2**	**η**

where η = 0.4358665, c = (1+ η)/2, b1 = – (6 η ^{2} -– 16 η + 1)/4, b2 = (6 η ^{2} – 20 η + 5)/4.

The information contained in this block can be translated by the following representations. For simplicity, we define the following general form of ordinary differential equation after spatial discretisation. For a specific point along the column length x_i, the PDE becomes:

$$\frac{dC(x_i,t)}{dt} = f(t, C(x_i,t))$$

Discretisation along time axis with step size of h, the estimation of $C(x_i,t_{k+1})$ at t_{k+1} will be calculated through the following equations. Denote y the estimated value, $y(x_i,t_k) \approx C(x_i,t_k)$; $y_k = y(x_i,t_k)$.

The stage times are:

$$t_{k,1} = t_k + \eta h$$

$$t_{k,2} = t_k + ch \tag{3.37}$$

$$t_{k,3} = t_k + h$$

And the stage values are calculated from the equations:

$$y_{k,1} = y_k + \eta h K_1; \qquad K_1 = f(t_{k,1}, y_{k,1})$$

$$y_{k,2} = y_k + (c-\eta)hK_1 + \eta h K_2; \qquad K_2 = f(t_{k,2}, y_{k,2}) \tag{3.38}$$

$$y_{k,3} = y_k + b_1 hK_1 + b_2 hK_2 + \eta h K_3; \qquad K_3 = f(t_{k,3}, y_{k,3})$$

The overall slope estimation:

$$K^* = b_1 K_1 + b_2 K_2 + \eta K_3 \tag{3.39}$$

New point for the next time step is given as:

$$y_{k+1} = y_k + hK^* \tag{3.40}$$

It is seen that relations in Equation (3.38) are implicit equations. Newton's iteration method will be used as implicit equation solver to estimate each stage values. A step in the Newton iteration for the first stage estimation is:

$$y_{k,1}^{m+1} = y_{k,1}^{m} - (1 - \eta h \left.\frac{\partial f}{\partial y}\right|_{y_{k,1}^{m}})^{-1} (y_{k,1}^{m} - y_k - \eta h f(t_{k,1}, y_{k,1}^{m})) \tag{3.41}$$

where m is the iteration step

3.5 Summary

In this Chapter, a systematic study on the advances of SMB modelling, design and control is carried out. A set of functionally equivalent models for SMBCP are identified and summarized for their practical applications. The limitations of the existing modelling techniques in industrial applications are also identified. Furthermore, structural analysis of the existing models is conducted for a better understanding of the functionality and suitability of each model. Suggestions are given on how to choose an appropriate model with sufficient accuracy while keeping the computational demand reasonably low for real time control.

In the next Chapter, we will present our investigation on the spatial discretisation techniques mentioned here to numerically solve a single column model.

Nomenclature

C: fluid phase concentration

C_p: concentration in the pores of the particle

$\overline{C_p}$: average concentration in the pores of the particle

D_{ax}: axial dispersion coefficient of the bulk fluid phase

D_p: diffusion coefficient within the pores

D_T: lumped dispersion and diffusion coefficient $D_T = \frac{\varepsilon_b}{\varepsilon_p} D_{ax}$

D_{ap}: axial dispersion coefficient taking into account of mass transfer resistance effect

J: wavelet resolution level

k_{ext}: fluid film mass transfer resistance

k_{int}: solid film mass transfer resistance

k_T: overall mass transfer coefficient

k_{ap}: mass transfer coefficient taking into account of axial dispersion

M: interpolation degree of boundary treatment in wavelet-collocation method

q: concentration of component in the solid phase

$\overline{q}$: average solid phase concentration

$q*$: equilibrium concentration in interface between two phases

R_p: particle radius

r: radial coordinate for particle

t: time coordinate

u: interstitial velocity

u_T: overall interstitial velocity $u_T = \frac{\varepsilon_b}{\varepsilon_p} u$

V_j: wavelet subspace

x: axial coordinate

$\psi(x)$: wavelet function

$\phi(x)$: scaling function

ε_b: void porosity of the mobile phase

ε_p: internal porosity of the particles

ε_T: total porosity $\varepsilon_T = \varepsilon_b + (1-\varepsilon_b)\varepsilon_p$

CHAPTER 4
SPATIAL DISCRETISATION FOR SINGLE COLUMN MODEL

Among the column models for chromatography, the Transport-Dispersive Linear Driving Force (LDF) models have been widely used in modelling many adsorption processes due to their simplicity and good agreement with experimental results (Ching, 1997). LDF is the application of the first Fick's law of mass transport and is an equation of equilibrium isotherm. It offers a realistic representation of industrial processes and is shown to be a good compromise between accurate and efficient solutions of these models (Biegler et al., 2004). In this study, we will use the following typical expression of Transport-Dispersive-LDF model to describe the kinetics of each column.

$$\frac{\partial C}{\partial t} + u\frac{\partial C}{\partial x} = D\frac{\partial^2 C}{\partial x^2} - \frac{1}{\alpha}\frac{\partial q}{\partial t} \tag{4.1}$$

$$\frac{\partial q}{\partial t} = k_{eff}(q^* - q) \tag{4.2}$$

where: $\alpha = \frac{\varepsilon_T}{1-\varepsilon_T}$; $\varepsilon_T = \varepsilon_b + (1-\varepsilon_b)\varepsilon_p$ is the fractional void volume and $D = \frac{\varepsilon_b}{\varepsilon_p} D_{ax}$ is the total diffusion coefficient in the solution.

4.1 Analytical Solution for Linear Equilibrium Case

In order to evaluate the performance of wavelet-collocation method, we will consider a simple linear equilibrium case. Under this assumption, an analytical solution is given by Lapidus and Amundson (1952) for any time at any point in the column. In the case where equilibrium is established at each point in the bed, $q = q^*$, Equation (4.1) can be transformed into:

$$\frac{\partial C}{\partial t} = \frac{1}{1 + \frac{1}{\alpha}\frac{\partial q^*}{\partial C}}\left(-u\frac{\partial C}{\partial x} + D\frac{\partial^2 C}{\partial x^2}\right) \tag{4.3}$$

For a linear equilibrium isotherm, $q^* = kC$, so that , $\frac{\partial q^*}{\partial C} = k$

We consider a pulse injection with a concentration of C_0 and duration of t_0, and specify constant concentration as boundary conditions:

$$C(0,t) = \begin{cases} C_0 & \text{at } t \le t_0 \\ 0 & t > t_0 \end{cases} \quad \text{and initial conditions of: } C(x,0) = 0;$$

Using dimensionless transformation, let:

$$\tau = ut\alpha / L; \qquad Pe = uL / D; \qquad z = x / L; \qquad c = C / C_0; \quad \tilde{q} = q / C_0$$

Then, according to Lapidus and Amundson (1952), the model's analytical solution is:

$$c(z,\tau) = \begin{cases} H(\tau) & \text{at } \tau \le \tau_0 \\ H(\tau) - H(\tau - \tau_0) & \tau > \tau_0 \end{cases} \tag{4.4}$$

with

$$H(\tau) = \frac{1}{2}[1 + erf\left(\sqrt{\frac{\tau Pe}{4(\alpha + k)}} - z\sqrt{\frac{Pe(\alpha + k)}{4\tau}}\right) + e^{zPe}\, erfc\left(\sqrt{\frac{\tau Pe}{4(\alpha + k)}} + x\sqrt{\frac{Pe(\alpha + k)}{4\tau}}\right)]$$

where $erf()$ and $erfc()$ are the error and complementary error functions, respectively:

$$erf(x) = \frac{2}{\sqrt{\pi}}\int_0^x e^{-t^2} dt; \qquad erfc(x) = \frac{2}{\sqrt{\pi}}\int_x^\infty e^{-t^2} dt$$

Calculations are conducted by assuming a column with infinite extent (so the end boundary condition is not included). We will look at the concentration profiles at column length of L. Figure 4.1 depicts an example of the concentration propagation along the column, which is the exact solution of this problem.

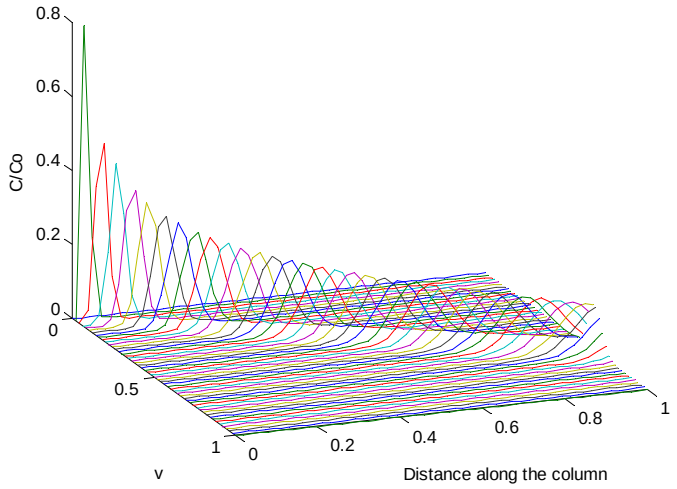

Figure 4.1 *Analytical solution:* $Pe = 500$, $(\alpha + k) = 20$

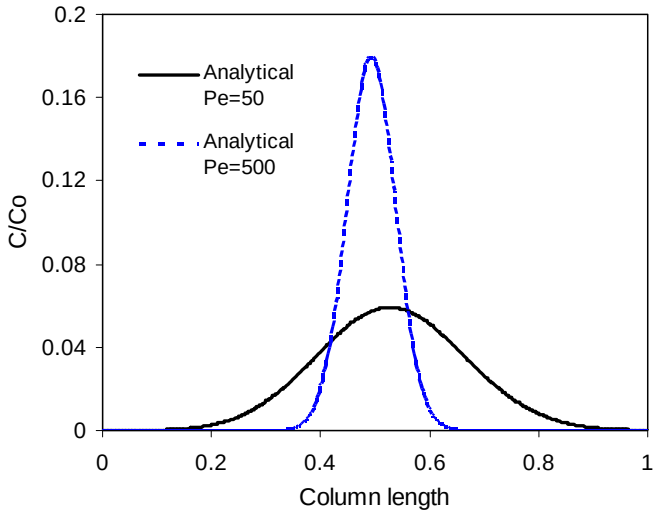

Figure 4.2 *The effect of Peclet number for a pulse injection.* $(\alpha + k) = 20, \tau = 10, \tau_0 = 0.4$

Figure 4.2 shows the shape of the wave, at certain time instant, for different Peclet number Pe. It is seen that with the increasing of Pe, the shape of wave gets steeper. In another words, large Pe values contributes to stiff concentration profiles. In fluid dynamics, the Péclet number is a dimensionless number relating the rate of advection of a flow to its rate of diffusion. For theoretical studies, it is not necessary to run very stiff cases. However, in engineering applications the Péclet number is often very large. In fact, in common axial flow chromatography, the Péclet numbers for axial dispersion often run into the thousands or higher (Gu, 1995). From this observation, we will consider three cases with Pe being set up as *50* (low), *500* (moderate) and *5000* (high).

This solution is limited to a chromatography in an equilibrium situation with linear isotherm. Most separation processes are more complicated than this. However, it appears useful when exact solution is needed in order to compare the accuracy of solution obtained by a numerical method.

4.2 Comparative Study on Numerical Solutions

Numerical simulations have been performed using the finite difference, wavelet collocation, and high resolution methods for spatial discretisation. The resulting ordinary equations transformed from partial differential equations using these three methods are given below.

(1) For the ***finite difference*** method, we use Upwind-1 for discretisation. The advantage of upwinding scheme has been outlined in Chapter 2.

Let $y(z,\tau) \approx C(z,\tau)$, an approximation of the concentration ratio, the resulting ODEs for each spatial mesh point are:

$$\frac{dy(z_i,\tau)}{d\tau} = \frac{1}{(\alpha+k)\Delta z}[\frac{1}{Pe\Delta z}y(z_{i+1},\tau) - (1+\frac{2}{Pe\Delta z})y(z_i,\tau) + (1+\frac{1}{Pe\Delta z})y(x_{i-1},\tau)] \quad (4.5)$$

$$y(z_1,\tau) = \begin{cases} 1 & \text{at} \quad \tau \le \tau_0 \\ 0 & \qquad \tau > \tau_0 \end{cases}$$

where: $i = 2\cdots N$, $\Delta z = z_{i+1} - z_i$, N is the number of mesh points.

(2) To solve this problem using the ***wavelet-collocation*** method, an approximation of the concentration ratio is expressed by a compactly supported orthonormal wavelets:

$$\frac{dy(z_i,\tau)}{d\tau} = \frac{1}{\alpha+k}[\frac{1}{Pe}\sum_{j=1}^{2^J+1} y(z_j,\tau)T_{i,j}^{(2)} - \sum_{j=1}^{2^J+1} y(z_j,\tau)T_{i,j}^{(1)}] \quad (4.6)$$

where $i = 2\cdots 2^J+1$; $T_{i,j}^{(1)}$ and $T_{i,j}^{(2)}$ are the first- and second-order derivatives, respectively, for the interpolating function. The boundary condition imposes one more constraint in an additional equation for the first spatial point:

$$y(z_1,\tau) = \sum_{j=1}^{2^J+1} y(z_j,\tau)T_{1,j} = \begin{cases} 1 & \text{at} \quad \tau \le \tau_0 \\ 0 & \qquad \tau > \tau_0 \end{cases}$$

(3) Applying the ***high resolution*** method to the model equation gives the following ODEs:

$$\frac{dy(z_i,\tau)}{d\tau} = \frac{1}{(\alpha+k)\Delta z Pe}\left(\frac{\partial y}{\partial z}\Big|_{z_{i+1/2}} - \frac{\partial y}{\partial z}\Big|_{z_{i-1/2}}\right) - \frac{1}{\Delta z}[y(z_{i+1/2},\tau) - y(z_{i-1/2},\tau)] \quad (4.7)$$

where $i = 1 \cdots N$. The expression of each component is defined in Section 3.3; and $z_{1/2}$ is the Dirichlet left boundary defined in Equation (3.35).

4.2.1 Finite Difference and Wavelet Collocation for Process with Low Pe

As shown in Figure 4.2, at $Pe = 50$, the wave front and tail are all relatively flat. We choose finite difference and wavelet-collocations for this study. Starting with standard finite difference method, the number of mesh point are chosen to be 65 (equivalent to *J=6*), *257* (equivalent to *J=8*), and *500*, respectively. Figure 4.3 depicts the numerical solutions of the model using the finite difference method. It is seen from the figure that for low Pe, the finite-difference method can eventually handle the problem if the number of mesh points is sufficiently high (over 500 in this example).

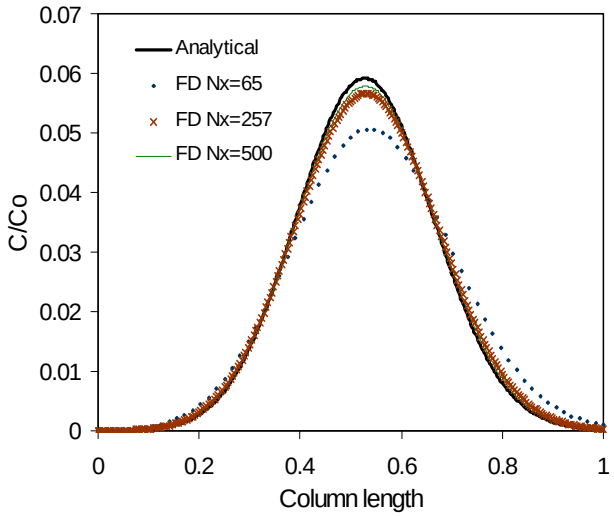

Figure 4.3 *Numerical solutions from the Finite Difference method.*
$(\alpha + k) = 20$; $\tau = 10$; $\tau_0 = 0.4$; $Pe = 50$

The next trials are carried out using wavelet collocation method. Simulations are conducted on the levels *J = 6*, *7*, and *8*,. Such wavelet levels represent the total collocation points of *65*, *129*, and *257*, respectively. Figure 4.4 is the numerical solutions. Level 7 upwards start to produce some sort of overshooting. This phenomenon is also observed by other researchers and needs further investigation. However, this could be easily avoided by choosing a higher minimum wavelet level to give acceptable numerical solutions.

For comparisons of finite difference and wavelet collocation methods, the absolute error between the numerical and analytical solutions has been calculated. This is displayed in Figure 4.5.

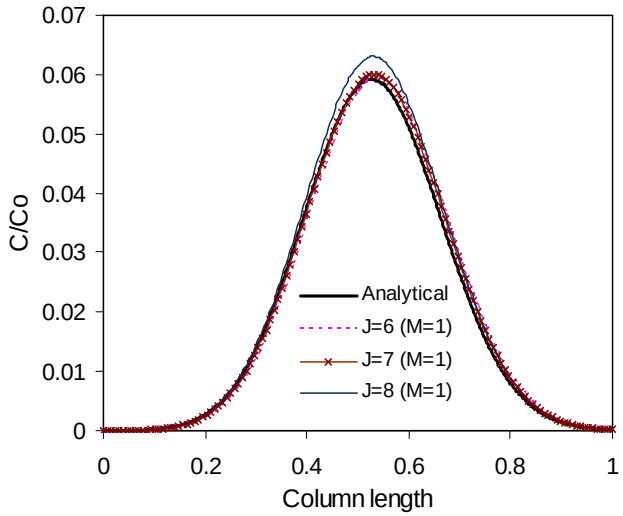

Figure 4.4 *Numerical solutions from Wavelet Collocation*
$(\alpha + k) = 20$; $\tau = 10$; $\tau_0 = 0.4$; $Pe = 50$

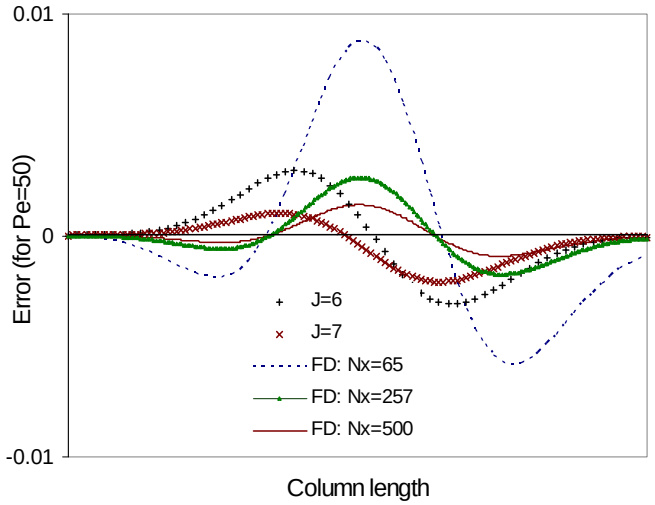

Figure 4.5 *Comparison of prediction errors.*
$(\alpha + k) = 20, \tau = 10, \tau_0 = 0.4,$ $Pe = 50$

For similar degree of discretisation, wavelet does show its advantage of using less collocation points to obtain a reasonable prediction. The error distributions are quite different for these two methods. For the finite difference method, the error exists at every section of the wave, e.g., front, peak and tail, especially; the peak presents the largest error. For the wavelet method, the error is located at the front and tail, but not around the peak, which is

actually the turning point of error sign. This reflects the capability of the wavelet method in capturing steep change very well.

4.2.2 Finite Difference, Wavelet Collocation and High Resolution for Process with Moderate Pe

When *Pe* is moderate, we will look at the numerical solutions using all of the three methods. For finite difference, the number of mesh point has been increased up to *1000*, above this, the computer indicated out of memory. For wavelet collocation, the resolution level has been set up as *J = 6, 7, 8, 9, 10*. For high resolution method, we choose *Nz = 65*, *129*, *257*, and *513*. The temporal integration has 500 points for all the trials. We will evaluate their performance both quantitatively and qualitatively through a series of figures and table.

At first, Figure 4.6 is the numerical solution obtained by finite difference method.

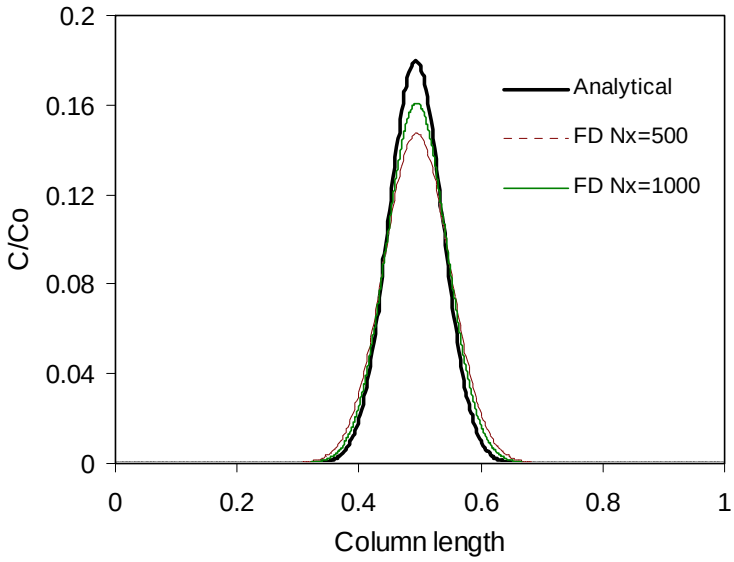

Figure 4.6 *Numerical solutions from finite difference at* $Pe = 500$

It can be seen that with the increasing of steepness as a result of higher Peclet number selected, the finite difference method can no longer accurately predict the peak value. It appears very reluctant to climb up the peak even with such a large number of mesh points.

However, as shown in Figure 4.7, using wavelet-collocation method, the numerical solutions catch up with the real steep change very well. It is noticed that resolution level 8 does not display any overshoot in this situation. However, a higher level still produces overestimation as displayed in Figure 4.7b for *J = 9*, and *J = 10*.

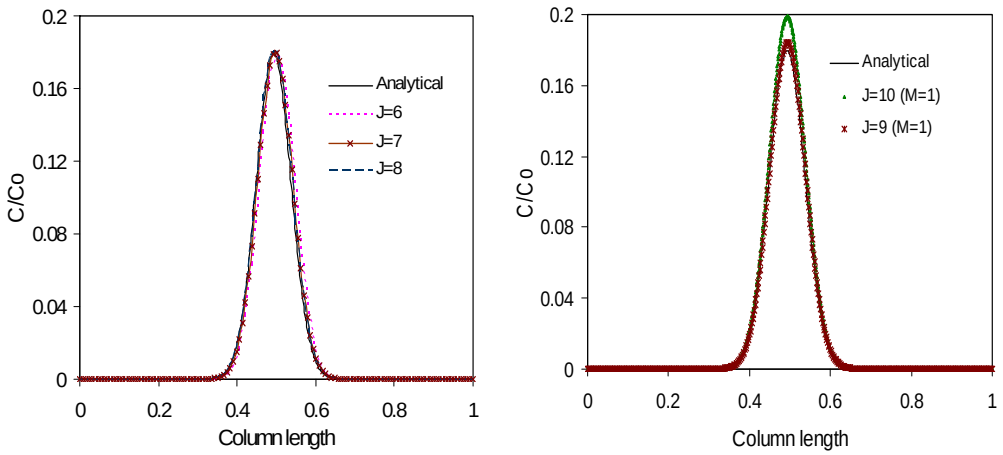

Figure 4.7 *Numerical solutions from Wavelet collocation at* $Pe = 500$

For a broad picture of how wavelet tackle the steep front problem, we will give the peak track for different *J* levels in Figure 4.8, which are drawn against the analytical solution representing wave propagation with time.

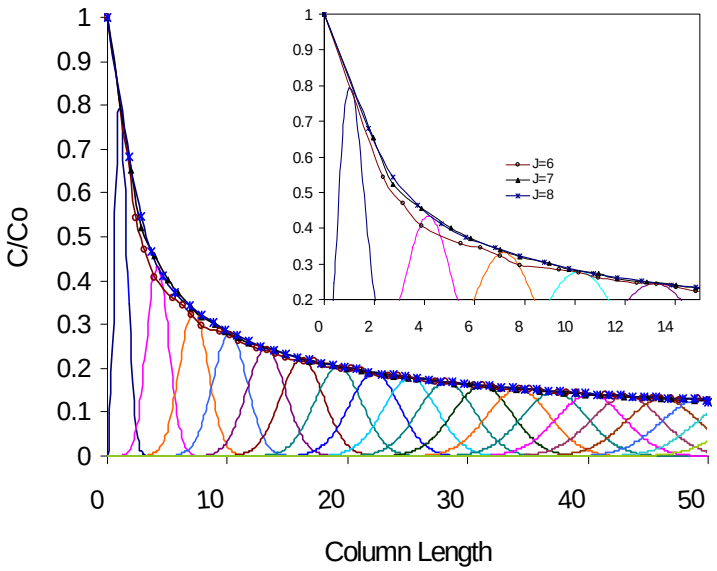

Figure 4.8 *Predicted concentration peak (in line).*

Trials are also conducted using the high resolution approach. Results are shown in Figure 4.9. When the number of mesh point increases to a certain level (e.g. 513), the high resolution method can approximate the true result very well. On the other hand, one does not need to worry about the overestimation problem arising from the wavelet approximation.

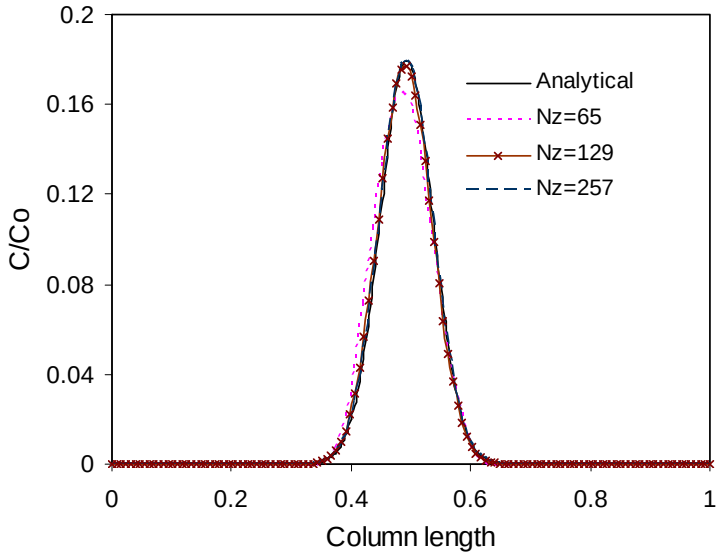

Figure 4.9 *Numerical solutions from High Resolution* $Pe = 500$

The performance of PDEs solver using different spatial discretisation algorithms is summarised in Table 4.1. Comparisons can be made on their approximation accuracy and computing time. Wavelet has remarkable advantage against finite difference if a proper resolution level is chosen, while high resolution also produces acceptable approximation with a relatively low computational demand. Further discussion can be found in Section 4.4.

Table 4.1 *Performance of discretisation methods at Pe=500*

Spatial Discretisation		**Absolute Error at Peak**	**Elapsed Computing Time* (sec)**
Finite Difference	Nx=500	0.03229	106.4
	Nx=1000	0.01868	299.4
Wavelet Collocation	J=6	0.00184	2.0
	J=7	0.00000	6.9
	J=8	0.00118	37.1
	J=9	0.00458	363.4
High Resolution	Nz=65	0.01417	11.8
	Nz=129	0.00285	28.8
	Nz=257	0.00050	72.3
	Nz=513	0.00023	213.0

**the temporal mesh number is 500 for all trials; conducted on a personal computer with an Intel's Pentium IV 3.00GHz processor*

Furthermore, when the distribution of absolute error along the column length is studied, it is interesting to see from the figures below, that the error distribution from the high resolution method (Figure 4.10a) has adverted shape from the wavelet collocation method (Figure 4.10b). This phenomenon may be explained from the mechanisms of these two different methods. However, this observation also leads to a useful assumption that, if two methods are combined, the developed algorithm could be very powerful.

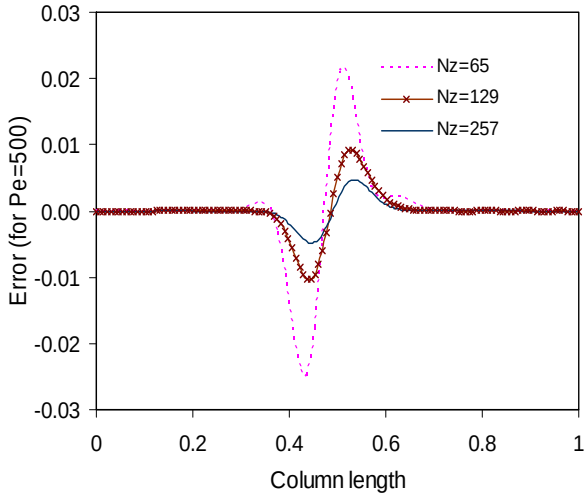

(a)

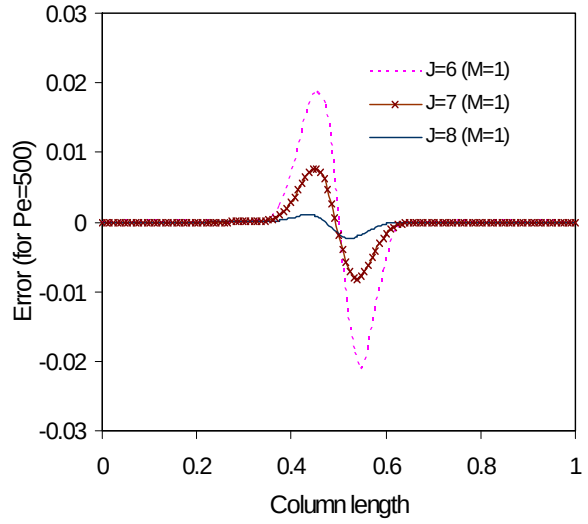

(b)

Figure 4.10 *Error distributions from (a) High resolution (b) Wavelet collocation*

4.2.3 Wavelet Collocation and High Resolution for Processes with Higher Pe

Wavelet-collocation and high resolution methods are investigated for processes with high *Pe*. Finite difference method is no longer considered here because the previous case shows it is not suitable for the model with even higher Peclet number. Comparisons are made for the concentration profile at certain point along the column length. As well as the illustration in Figure 4.11, prediction analysis results are also tabulated in Table 4.2.

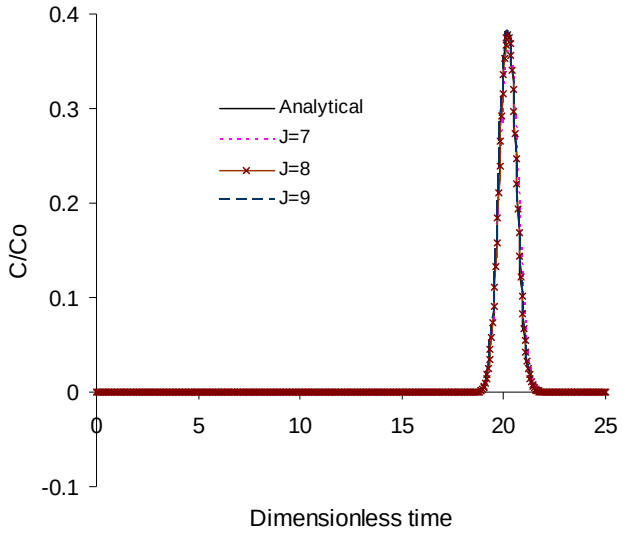

(a) Wavelet collocation

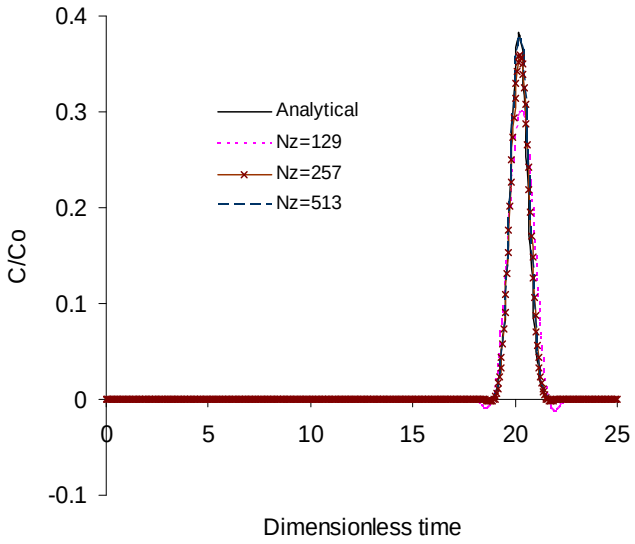

b) High resolution.

Figure 4.11 *Calculated concentration peak at certain column position (* $Pe = 5000$ *)*

Table 4.2 *Performance of discretisation methods at higher Pe=5000*

Spatial Discretisation		**Absolute Error at Peak**	**Elapsed Computing Time* (sec)**
Wavelet Collocation	J=7	0.0202	6.7
	J=8	0.0040	34.0
	J=9	0.0001	322.0
High Resolution	Nz=129	0.0815	28.7
	Nz=257	0.0222	65.8
	Nz=513	0.0048	188.5

**the temporal mesh number is 500 for all trials.*

For the wavelet collocation method, the resolution level can be up to *9* without overestimation, although the cost of computation increases significantly. It is concluded that high resolution method is still a potential candidate for solving PDEs with such a degree of singularity.

4.3 The Interpolation Degree of Boundary Treatment in Wavelet Collocation Method

Section 3.2 introduced the basic concept of the wavelet collocation method. The general expression of Equation (3.28) contains three parts. Apart from classical interpolating functions, two polynomials are defined with the degree of (2*M*-1) to interpolate the original problem at the left and right boundaries. The selection criterion of *M* is not reported in any of the previous literature. We did conduct several trails for the determination of a best value of *M*. From Figures 4.12, 4.13, and 4.14, it is seen that, for this specific problem, *M*=1 seems to be the most reliable choice and it has been used for all our study on wavelet method.

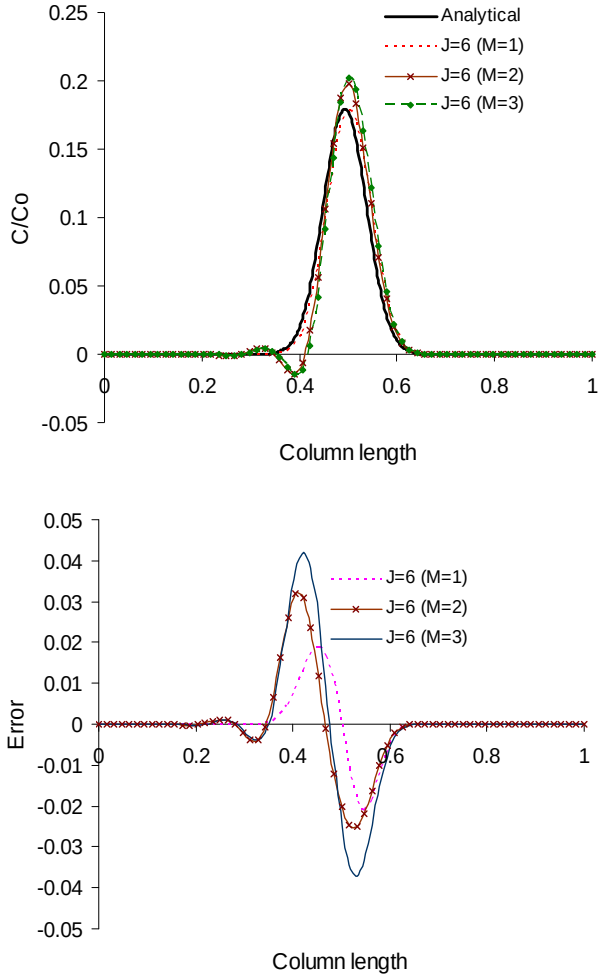

Figure 4.12 *The effect of M on the simulation performance (J=6)*

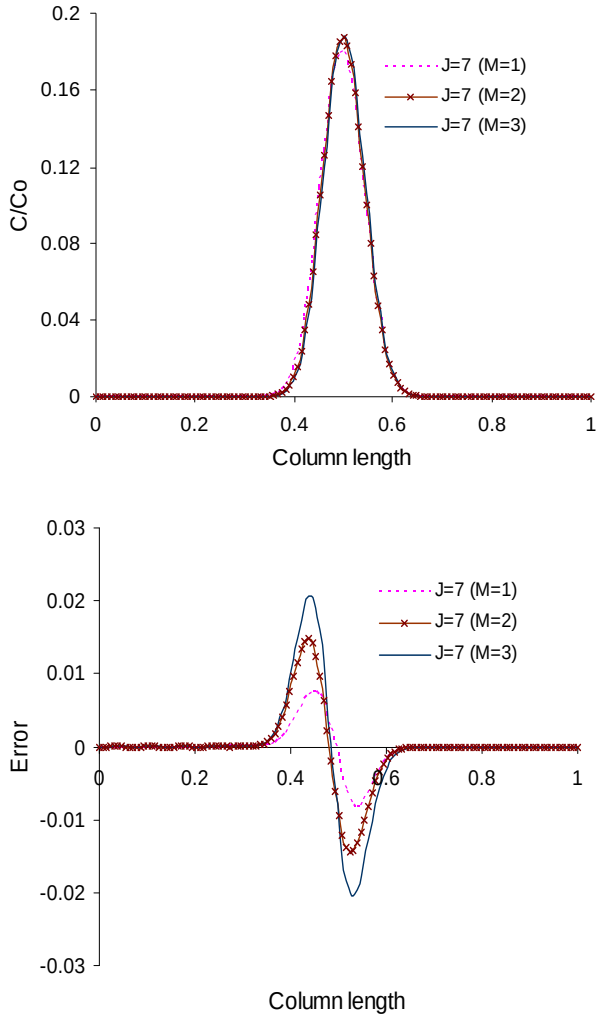

Figure 4.13 *The effect of M on the simulation performance (J=7)*

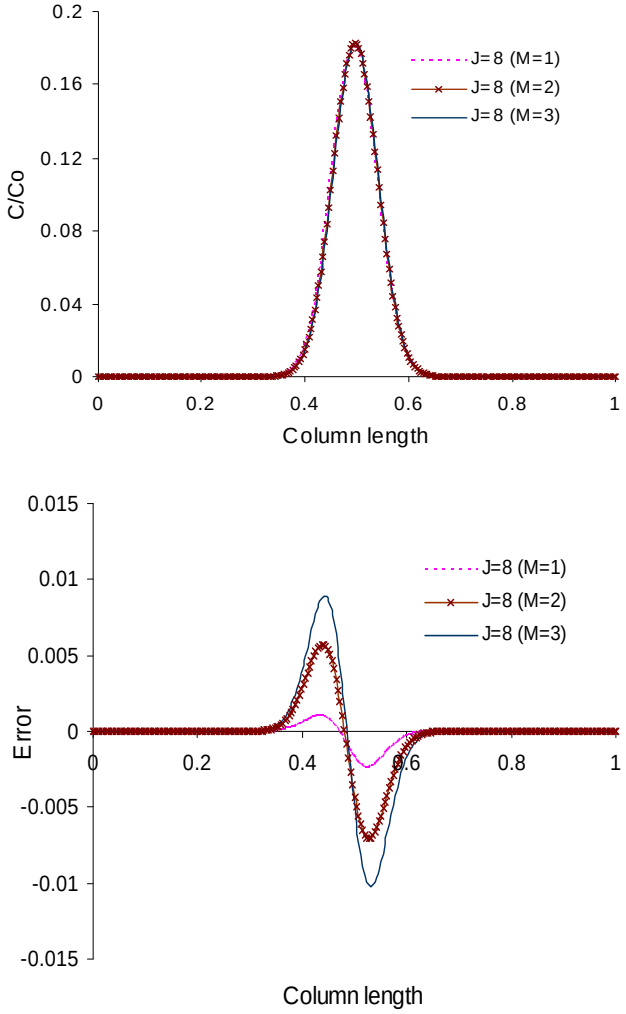

Figure 4.14 *The effect of M on the simulation performance (J=8)*

4.4 Summary and Discussion

In summary, this chapter has explored some upfront discretisation techniques for the solution of partial differential equations with singularity. The solution of a single column chromatographic process represented by a Transport-Dispersive-Equilibrium linear model was used to investigate the numerical power of proposed methods on the prediction of transit behaviour of wave propagation. Comparisons of the solutions from finite difference, wavelet and high resolution methods with the analytical one were conducted on a range of Peclet numbers. For the simulation results from Section 4.2.1, we can see that all the proposed methods work well when the PDEs system has low Peclet number, especially the upwind finite difference method, which can offer good numerical solution but with most computing time. The high resolution method provides an accurate numerical solution for the PDEs in question with moderate value of Pe. The wavelet collocation method is capable of catching up with the steep changes in the solution, and thus can be used for numerically solving PDEs with high singularity.

Generally, in terms of the two approaches (wavelet collocation and high resolution) mainly investigated here, wavelet based methods offers a better solution to PDEs with high singularity, however, prior knowledge of wavelet is required in order to take advantage of this kind of method. High resolution method is easy for implementation and can offer reasonable result with reasonable computing time.

Nevertheless, some issues need to be pointed out from this research.

(1) The wavelet collocation method should be used with caution because overestimation is observed in our simulation results and the previous work as well. Unlike the finite difference and high resolution methods, it is not a one way convergence method. The selection of resolution level is highly related to specific problem, such as, the most accurate results are from $J = 6$ for $Pe = 50$, $J = 7$ for $Pe = 500$, and $J = 9$ for $Pe = 5000$, respectively.

(2) We have also observed that the selection of the value of the number of interpolating points, M, is very important since it could affect the numerical solution significantly. No report has been found on this issue so far in the open literature.

(3) The results from this comprehensive study are encouraging for applications to more complicated model systems.

Nomenclature

C: fluid phase concentration

C_0: concentration in pulse injection

c: dimensionless concentration $c = C / C_0$

D: total diffusion coefficient of the bulk fluid phase

J: wavelet resolution level

L: column length

M: interpolation degree of boundary treatment in wavelet-collocation method

N_x: number of mesh points in finite difference method

N_z: number of subintervals in high resolution method

k_{eff}: effective mass transfer coefficient

k: parameter for linear isotherm

Pe: Peclet number $Pe = uL / D$

q: concentration of component in the solid phase

$\tilde{q}$: dimensionless concentration in the solid phase $\tilde{q} = q / C_0$

$q*$: equilibrium concentration in interface between two phases

$T_{i,j}^{(1)}, T_{i,j}^{(2)}$: first- and second-order derivatives for the interpolating function associated with wavelet-collocation method

t: time coordinate

t_0: pulse injection duration

u: interstitial velocity

V_j: wavelet subspace

v: volume of solution $v = ut\alpha$

x: axial coordinate

y: approximation of concentration

z: dimensionless axial coordinate $z = x / L$

α: fractional void volume $\alpha = \varepsilon_T / (1 - \varepsilon_T)$

ε_T: total porosity

τ: dimensionless time $\tau = ut\alpha / L$

CHAPTER 5
NUMERICAL SOLUTION OF SMBCP MODEL

Our investigation in the last chapter has shown that recent advances in wavelet based approaches and high resolution methods have the potential to be adopted for solving more complicated dynamic system models. This chapter will highlight the successful applications of these methods in solving complex models of simulated-moving-bed (SMB) chromatographic processes. The advantages of the wavelet based approaches and high resolution methods are further demonstrated through applications to dynamic SMB models for sugar and enantiomers separation processes.

5.1 Dynamic Modelling of SMBCPs

The simulated moving bed chromatographic process is the technical realisation of a countercurrent adsorption process, approximating the countercurrent flow by a cyclic port switching. It consists of a certain number of chromatographic columns in series while the countercurrent movement is achieved by sequentially switching the inlet and outlet ports one column downwards in the direction of the liquid flow after a certain time period. The stationary regime of this process is cyclic steady-state (CCS), in which in each section an identical transient during each period between two valve switches takes place. The CSS state is practically reached after a certain number of valves switches, but the system states are still varying over time because of the periodic movement of the inlet and outlet ports along the columns.

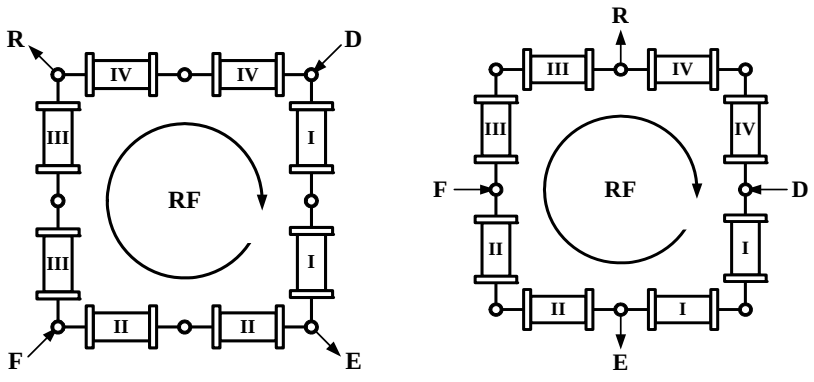

(a) Current switching period (b) Next switching period

Figure 5.1 *An SMB unit with 2 columns in each of the 4 sections (RF: direction of fluid flow and port switching)*

Dynamic SMB model mainly consists of two parts: a single chromatographic columns model, and the node balances model describing the connection of the columns combined with the cyclic switching. The switching operation can be represented by a shifting of the initial or boundary conditions for the single columns. After a relatively brief start-up period, the adsorption beds will reach the cyclic steady state (CSS). Normally, CSS is determined by solving the PDE system repeatedly for each step of the cyclic process in sequence, using the final concentration profile for each step as the initial condition for the next step in the cycle.

A schematic description of the modelling system is depicted in Figure 5.2.

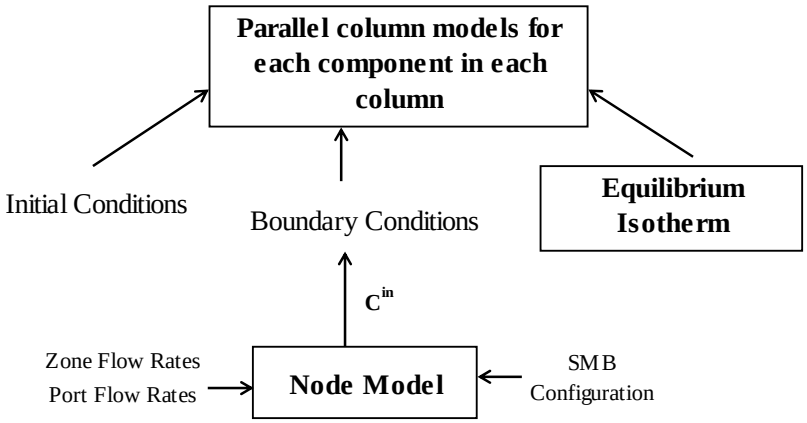

Figure 5.2 *SMB dynamic modelling system*

In the following we will give detailed model equations.

- **Column Model for Chromatography**

The selected column model structure is the same as that described in Chapter 4, the transport-dispersive-LDF model. We will expand the model to describe a multi-columns binary separation process. The mass balance of component *i* in the mobile phase (or bulk-liquid phase) is,

$$\frac{\partial C_{i,j}}{\partial t} + u_j \frac{\partial C_{i,j}}{\partial x} = D_T \frac{\partial^2 C_{i,j}}{\partial x^2} - \frac{1-\varepsilon_T}{\varepsilon_T} \frac{\partial q_{i,j}}{\partial t} \tag{5.1}$$

A simple Linear Driving Force model is used to represent the overall mass transfer kinetics for the adsorption phase:

$$\frac{\partial q_{i,j}}{\partial t} = k_{eff,i}(q_{i,j}^{*} - q_{i,j}) \tag{5.2}$$

And the equilibrium isotherms:

$$q_{A,j}^{*} = F_A(C_{A,j}, C_{B,j}); \qquad q_{B,j}^{*} = F_B(C_{A,j}, C_{B,j}) \tag{5.3}$$

where, $i = A, B$; $j = 1 \cdots N_{column}$; N_{column} denotes total number of columns.

To complete the dynamic modelling system, apart from the column model described in Equation (5.1), (5.2) and (5.3), initial conditions and boundary conditions are also essential.

Initial Condition:

$$C_{i,j}^{[s]}(0, x) = C_{i,j}^{[s-1]}(t_s, x) \tag{5.4}$$

where s is the number of switching; t_s is the switching time

Boundary Conditions:

$$\frac{\partial C_{i,j}}{\partial x} = \frac{u_j}{D_T}(C_{i,j} - C_{i,j}^{in}) \qquad \text{for } x = 0 \text{ at } t > 0 \tag{5.5}$$

$$\frac{\partial C_{i,j}}{\partial x} = 0 \qquad \text{for } x = L \text{ at } t > 0 \tag{5.6}$$

$C_{i,j}^{in}$ are subject to the material balances at the column conjunctions, which will be determined by the following node model.

- **The Node Model for an SMB system**

The flow and integral mass balance equations at each node are given in the following equations, according to the sketch in Figure 5.3, under the assumptions that the dead volume by the switching devices, connecting tubes, and other parts is negligible.

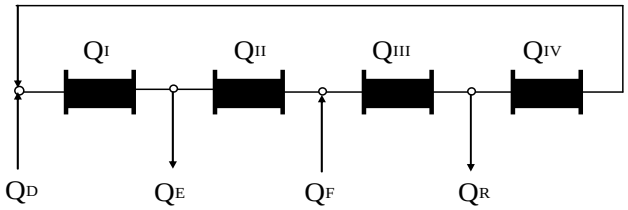

Figure 5.3 *Flow diagram of 4 section SMB system*

Desorbent Node (eluent):

$$Q_I = Q_{IV} + Q_D; \quad C_{i,I}^{in} Q_I = C_{i,IV}^{out} Q_{IV} + C_{i,D} Q_D \tag{5.7a}$$

Extract draw-off node:

$$Q_{II} = Q_I - Q_E; \quad C_{i,E} = C_{i,II}^{in} = C_{i,I}^{out} \tag{5.7b}$$

Feed node:

$$Q_{III} = Q_{II} + Q_F; \quad C_{i,III}^{in} Q_{III} = C_{i,II}^{out} Q_{II} + C_{i,F} Q_F \tag{5.7c}$$

Raffinate draw-off node:

$$Q_{IV} = Q_{III} - Q_R; \quad C_{i,R} = C_{i,IV}^{in} = C_{i,III}^{out} \tag{5.7d}$$

Other nodes:

$$C_{i,j}^{in} = C_{i,j-1}^{out} \tag{5.7e}$$

Q_I, Q_{II}, Q_{III}, Q_{IV} : volumetric flow rate through the corresponding sections

Q_D : the desorbent flow rate

Q_F : the feed flow rate

Q_E : the extract flow rate

Q_R : the raffinate flow rate

$C_{i,j}^{in}$, $C_{i,j}^{out}$: the concentrations of component i at the outlet and the inlet of section j.

Thus, an SMBC model is constructed by all the single column models connected in series by boundary conditions. The dominating parameters of the interstitial velocity u_j and the inlet concentration of each column are restricted by node models. It is a distributed parameter system in which the dependent variables vary with axial position and time. The number of model equations is enlarged in folder with the number of columns involved and the components to be separated. For a typical eight column binary operation, the SMBCP model has 16 PDEs from Equation (5.1), 16 ODEs from Equation (5.2) and 20 AEs from Equations (5.3) and (5.7). Although for specific cases there exist analytical solutions to a single column model, it is impossible to obtain analytical solutions for a SMB system with all these highly coupled equations.

5.2 Numerical Computing

Since it is almost impossible to solve the system model analytically, numerical computing of the system model becomes crucial for system analysis, optimisation, and control design. In our study, we will investigate the potential of wavelet collocation methods for solving SMB models numerically. The effectiveness of this method will be compared with finite difference and high resolution methods through two case studies.

5.2.1 From PDEs to ODEs

The spatial discretisation of Equation (5.1) and its boundary conditions for column model are performed using finite difference, wavelet collocation and high resolution methods to transform partial differential equations to ordinary equations for each spatial mesh point (or collocation point).

Let $y_{i,j}$ be the approximation of $C_{i,j}$, for all methods, we have ***Initial conditions*** describing the status of the column at the beginning of the switching:

$$y_{i,j}^{[s]}(0,x) = y_{i,j}^{[s-1]}(t_s, x) \tag{5.8}$$

For simplicity, in the following expression we will use y to stand for $y_{i,j}$. Each of the equation should be applied to components *A* and *B* for N_{column} column number.

(1) Finite difference discretisation using upwind-1 method

$$\frac{dy(x_k,t)}{dt} = \frac{D_T}{\Delta x^2} y(x_{k+1},t) - (\frac{u}{\Delta x} + \frac{2D_T}{\Delta x^2}) y(x_k,t) + (\frac{D_T}{\Delta x^2} + \frac{u}{\Delta x}) y(x_{k-1},t) - \frac{1-\varepsilon_T}{\varepsilon_T} k_{eff} [q^*(x_k,t) - q(x_k,t)] \quad (5.9)$$

Where: $k = 2 \cdots N-1$, $\Delta x = x_{k+1} - x_k$, N is the number of mesh points.

The boundary conditions are treated using the False Boundary Method, which gives:

$$\frac{dy(x_1,t)}{dt} = \frac{D_T}{\Delta x^2} y(x_3,t) - (\frac{D_T}{\Delta x^2} + \frac{u^2}{D_T} + \frac{u}{\Delta x}) y(x_2,t) + (\frac{u^2}{D_T} + \frac{u}{\Delta x}) y^{in}(x_1,t)] - \frac{1-\varepsilon_T}{\varepsilon_T} k_{eff} [q^*(x_1,t) - q(x_1,t)] \quad (5.10)$$

and

$$\frac{dy(x_N,t)}{dt} = (\frac{D_T}{\Delta x^2} + \frac{u}{\Delta x})[y(x_{N-1},t) - y(x_N,t)] - \frac{1-\varepsilon_T}{\varepsilon_T} k_{eff} [q^*(x_N,t) - q(x_N,t)] \quad (5.11)$$

(2) Wavelet collocation discretisation

The compactly supported orthonormal wavelets is constructed to approximate the function to the interval of [0,1]. Let $z = x / L$,

$$\frac{dy(z_k,t)}{dt} = -\frac{u}{L} \sum_{j=0}^{2^J} y(z_j,t) T_{k,j}^{(1)} + \frac{D_T}{L^2} \sum_{j=0}^{2^J} y(z_j,t) T_{k,j}^{(2)} - \frac{1-\varepsilon_T}{\varepsilon_T} k_{eff} [q^*(z_k,t) - q(z_k,t)] \quad (5.9')$$

where $k = 2 \cdots N-1$, $N = 2^J + 1$ is the number of collocation points; J is the resolution level; $T_{k,j}^{(1)}$ and $T_{k,j}^{(2)}$ are the first and second derivatives, respectively, for the autocorrelation function of the scaling function.

The left boundary condition is

$$\sum_{j=0}^{2^J} y(z_j,t) T_{1,j}^{(1)} = \frac{uL}{D_T} [y(z_1,t) - y^{in}(z_1,t)] \quad (5.10')$$

And the right boundary condition is

$$\sum_{j=0}^{2^J} y(z_j,t)T^{(1)}_{2^J,j} = 0 \qquad (5.11')$$

(3) High resolution method

Applying the high resolution method to the model equation gives the following ODEs:

$$\frac{dy(z_k,t)}{dt} = \frac{D_T}{\Delta z}\left(\frac{\partial y}{\partial z}\Big|_{z_{k+1/2}} - \frac{\partial y}{\partial z}\Big|_{z_{k-1/2}}\right) - \frac{u}{\Delta z}[y(z_{k+1/2},t) - y(z_{k-1/2},t)]$$

$$-\frac{1-\varepsilon_T}{\varepsilon_T}k_{eff}[q^*(z_k,t) - q(z_k,t)] \qquad (5.9'')$$

where $k = 1\cdots N$. The expression of each part in this equation is defined as in Chapter 3.3; and again specified here.

$$\frac{\partial y}{\partial z}\Big|_{1/2} = \frac{-8C^{in} + 9y(z_1,t) - y(z_2,t)}{3\Delta z + 8D_T/u}$$

$$y(z_{1/2},t) = \frac{3u\Delta z C^{in} - 9D_T y(z_1,t) + D_T y(z_2,t)}{3u\Delta z + 8D_T}$$

$$y(z_{3/2},t) = \frac{y(z_1,t) + y(z_2,t)}{2}$$

$$\frac{\partial y}{\partial z}\Big|_{N-1/2} = \frac{y(z_N,t) - y(z_{N-1},t)}{\Delta z}$$

$$\frac{\partial y}{\partial z}\Big|_{N+1/2} = 0$$

$$y(z_{N+1/2},t) = y(z_N,t) + \frac{1}{2}\left[y(z_N,t) - y(z_{N-1},t)\right]$$

For $i = 2,\cdots,N-1;\ \kappa \in [0,1]$

$$\frac{\partial y}{\partial z}\Big|_{z_{k+1/2}} = \frac{y(z_{k+1},t) - y(z_k,t)}{\Delta z}$$

$$\left.\frac{\partial y}{\partial z}\right|_{z_{k-1/2}} = \frac{y(z_k,t) - y(z_{k-1},t)}{\Delta z}$$

$$y(z_{k+1/2},t) = y(z_k,t) + \frac{1+\kappa}{4}\left[y(z_{k+1},t) - y(z_{k/2},t)\right] + \frac{1-\kappa}{4}\left[y(z_k,t) - y(z_{k-1},t)\right]$$

$$y(z_{k-1/2},t) = y(z_{k-1},t) + \frac{1+\kappa}{4}\left[y(z_k,t) - y(z_{k-1},t)\right] + \frac{1-\kappa}{4}\left[y(z_{k-1},t) - y(z_{k-2},t)\right]$$

5.2.2 The Calculation Procedure

Numerical simulations in this thesis have been conducted using *Matlab* on a personal computer with an Intel's Pentium IV 3.00GHz processor. The program code attached below is the integration solver for the numerical solution of 4 section SMB (2:2:2:2) Transport-Dispersive Model. The IVP integrator is Alexander Semi-implicit Method (third-order Runge-Kutta). Function "model" returns the expression of ordinary differential equations, which are generated from original partial differential equations through spatial discretisation technique (finite difference, wavelet collocation and high resolution). Since all the related algorithms have been given in the previous section, detailed program for "model" is also omitted here.

Using an 8 column SMB bi-separation system as example, partial differential equations are defined as: 1-8 for component A in liquid phase; 9-16 for component B in liquid phase; 17-24 for component A in solid phase; and 15-32 for B in solid phase. As a result of discretisation (N mesh points/collocation points for each column), the "model" will contain 32xN ordinary equations. To compromise the large number of ODEs, a big integration stepsize should be chosen to release the computational pressure. This program indeed worked very well with a sparse integration step.

Cyclic steady state is assumed to be reached after 12 cycles (96 switches), or the relative error defined by Equation (5.15) is less than 0.001. However, this can always be set up by user according to specific applications.

```
%-----------------------------------------------------------------
** Input process parameters **

** Constructing wavelet basis **

[D0,D1,D2]=Basis(nJ,WL,MB);
```

```
** Dimension defined **

** Calculate global variables **

** Specify the parameters for integrator **

for isw=1:100       % isw: number of switch

%start the integration
   for k=1:n-1

    %define stage time
    t1=t(k)+gama*h;
    t2=t(k)+c*h;
    t3=t(k)+h;

    %solve stage equation using Newton's Method
    x1=xc(:,k); %initial guess for Newton algorithm
    x2=xc(:,k);
    x3=xc(:,k);

    % ===========first stage equation f(x1)===============
    for iterations=1:Nmax
        g1=model(x1,m);
        f=x1-xc(:,k)-gama*h*g1;
        if norm(f)<tol, break, end

        %calculate jacobian of g1 using numerical differentiation
        steptub=(1+x1)*1e-7;
        for jj=1:dimc
            xh=x1;
            xh(jj)=x1(jj)+steptub(jj);
            gh=model(xh,m);
            jac(:,jj)=(gh-g1)/steptub(jj);
        end

        %calculate Jacobian of f
        J=eye(dimc)-h*gama*jac;

        %Newton estimate update
        x1=x1-J\f;
    end
    if (iterations==Nmax),error('Maximum iterations reached'),end

   % ===========second stage equation f(x2)===============
    for iterations=1:Nmax
        g2=model(x2,m);
        f=x2-xc(:,k)-(c-gama)*h*g1-gama*h*g2;
        if norm(f)<tol, break, end
        steptub=(1+x2)*1e-7;
        for jj=1:dimc
            xh=x2;
            xh(jj)=x2(jj)+steptub(jj);
            gh=model(xh,m);
            jac(:,jj)=(gh-g2)/steptub(jj);
        end
        J=eye(dimc)-h*gama*jac;
        x2=x2-J\f;
```

```
    end
    if (iterations==Nmax),error('Maximum iterations reached'),end

    % =============third stage equation f(x3)==================
    for iterations=1:Nmax
        g3=model(x3,m);
        f=x3-xc(:,k)-b1*h*g1-b2*h*g2-gama*h*g3;
        if norm(f)<tol, break, end
        steptub=(1+x3)*1e-7;
        for jj=1:dimc
            xh=x3;
            xh(jj)=x3(jj)+steptub(jj);
            gh=model(xh,m);
            jac(:,jj)=(gh-g3)/steptub(jj);
        end
        J=eye(dimc)-h*gama*jac;
        x3=x3-J\f;
    end
    if (iterations==Nmax),error('Maximum iterations reached'),end

    %calculate overall slope estimate
    gk=b1*g1+b2*g2+gama*g3;

    %calculate new point at next time step
    xc(:,k+1)=xc(:,k)+h*gk;

  end

** calculate boundary points **

** Calculate average concentration at extract and raffinate ports **

** Calculate relative error **

   if REr(isw)<0.001,break,end

** Reset initial conditions after switching **

end
% -------------------------------------------------------------------
```

5.3 Case Study 1: Fructose-Glucose Separation (Beste et al. 2000)

The separation of fructose-glucose in de-ionized water used in Beste *et al*. (2000) and Lim and Jorgensen (2004b) is taken as one of our case study systems. The SMBCP has 8 columns with the configuration of 2:2:2:2. The operating conditions and model parameters are summarised in Table 5.1. The transport-dispersive-LDF model is selected to represent the column dynamics. Thus, the model consists of 16 PDEs, 16 ODEs and 20 AEs connecting all the variables together.

Numerical simulations have been performed in this work using both finite difference and wavelet collocation methods for spatial discretisation. The same integrator, the Alexander semi-implicit method (third-order Runge-Kutta), is adopted so that the results can be compared on the effectiveness of different spatial discretisation methods. For the trials of finite difference, the number of mesh along one column length has been chosen as *Nx = 33* and *65*, which are equivalent to the collocation points generated by wavelet level of *J = 5* and *J = 6*. Simulations using wavelet collocation were conducted on the level *J = 4, 5,* and *6*. The boundary conditions are treated using polynomial interpolation proposed by Liu et al. (2000) with the degree *M* of *1, 2,* and *3*. The number of mesh along the time axis is 5 points in each switching period for all the trials. The reason for less mesh point is that this semi-implicit integrator has a built-in Newton iteration mechanism for all its three stage equations.

Table 5.1 *Parameters of the fructose-glucose separation*

Symbol	**Value**	**Symbol**	**Value (Sp. A-fructose)**	**Value (Sp. B-glucose)**
L (cm)	52.07	$k_{eff,i}$ (min^{-1})	0.72	0.9
D (cm)	2.6	$C_{i,feed}$ (g/L)	363	322
ε_T	0.41448	$q_A^* = 0.675C_A$ $q_B^* = 0.32C_B + 0.000457C_AC_B$		
t_s (min)	16.39			
Q_F (ml/min)	1.67			
	Zone I	Zone II	Zone III	Zone IV
Q (ml/min)	15.89	11.0	12.67	9.1
D_T (cm^2/min)	1.105	0.765	0.881	0.633

Results and Analysis

First of all, some definitions are given, which will be used to quantitatively evaluate the performance of each method in this case study. We defined the exit port average concentration within one switching as:

$$\bar{y} = \frac{y(z,t_1) + 2\sum_{i=2}^{N_t-1} y(z,t_i) + y(z,t_{N_t})}{2(N_t - 1)} \tag{5.12}$$

where N_t is the total time step of integration for one switching period.

The product purity and yield are defined by equations:

$$Purity_i = \frac{\bar{y}_i}{\sum_{j=1}^{N_{comp}} \bar{y}_j} \tag{5.13}$$

$$Yield_i = \frac{\bar{y}_i Q_{exit}}{C_i^{in} Q_{Feed}} \tag{5.14}$$

$i = component$; N_{comp} is the number of components need to be separated.

Figures 5.4, 5.5, 5.6 illustrate the numerically solved concentration distribution along the total columns length at the middle of 80th switching, under the wavelet resolution level of *4, 5, 6* and boundary treatment degree of *1, 2, 3*. Although simulation using wavelet approach has been conducted under different levels, the results from lower levels can fit equivalently well with the experimental data, especially at the feeding port, where the concentration front experiences a sudden change. Higher level (*J=6*) wavelet demands much more computational time while giving a similar prediction performance.

As pointed out in Section 4.3, the effect of *M* is very hard to explain. In our case, *M=1* when *J=4* and *M=2* when *J=5* gave the best approximations. There is no particular difference for *J = 6*.

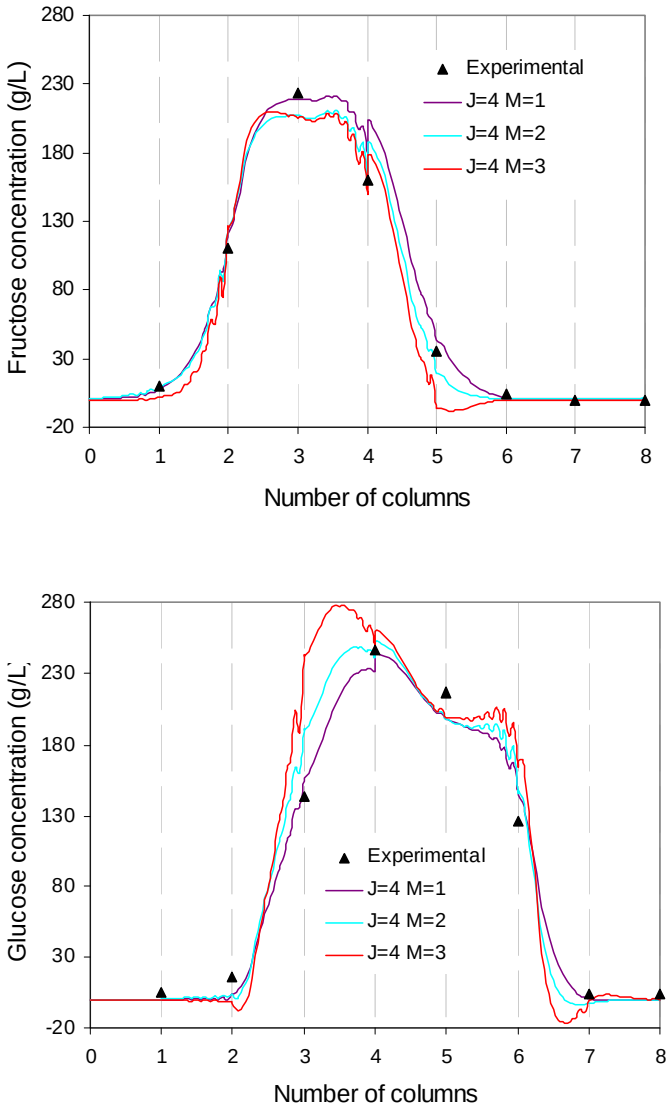

Figure 5.4 *Concentration distribution at the middle of 80th switch (W: J=4)*

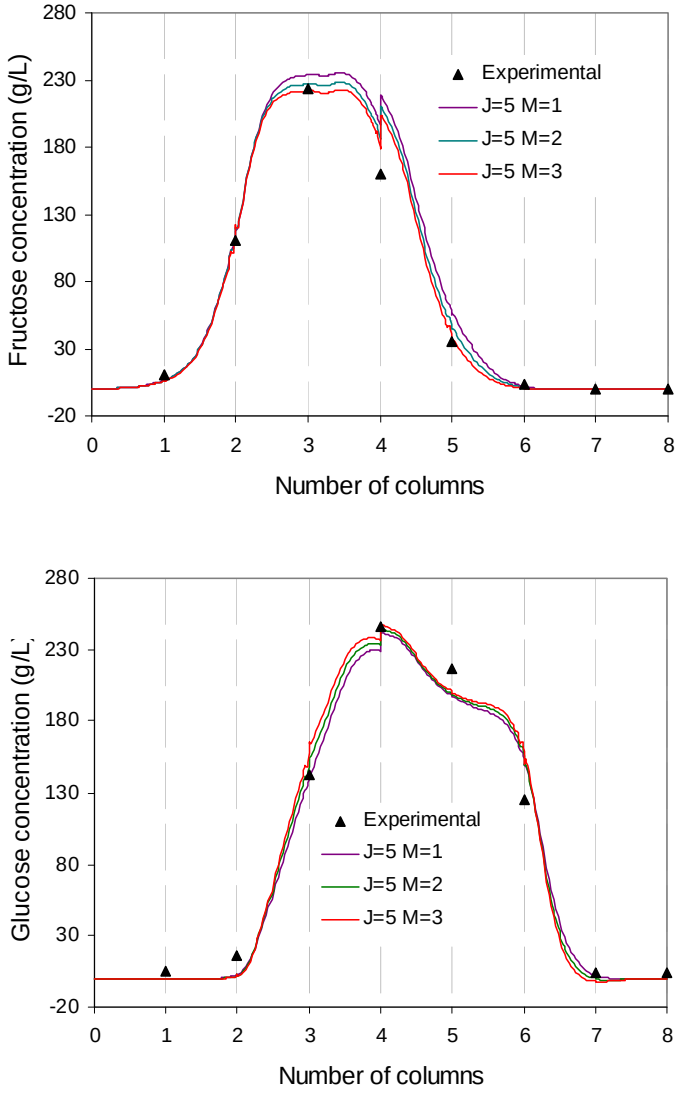

Figure 5.5 *Concentration distribution at the middle of 80th switch (W: J=5)*

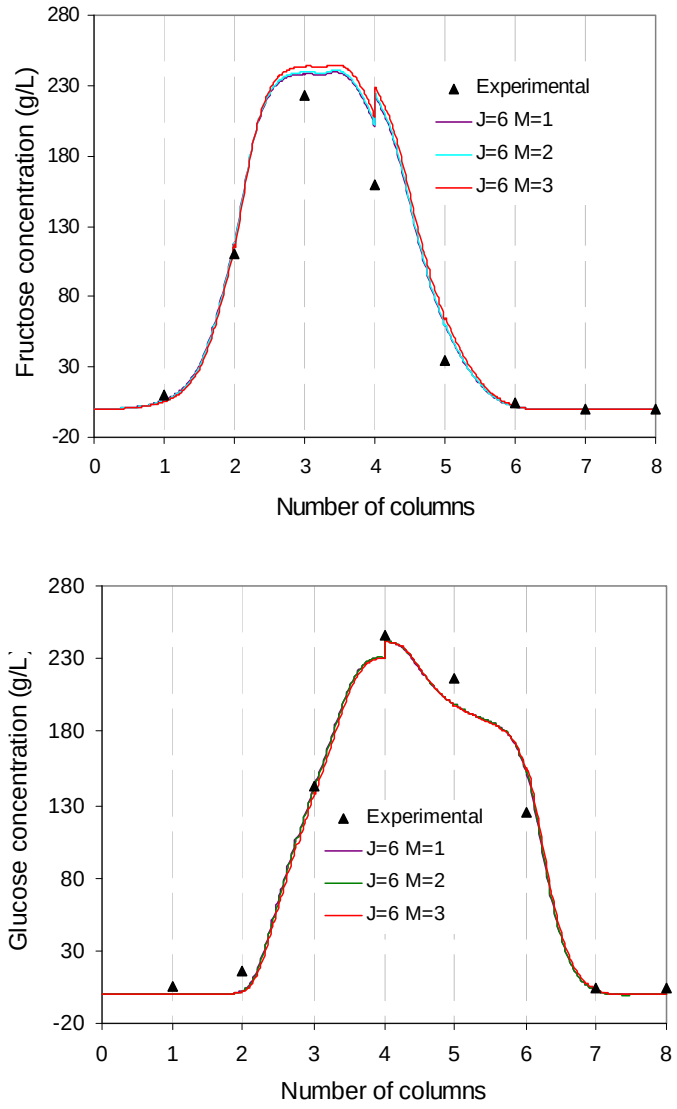

Figure 5.6 *Concentration distribution at the middle of 80th switch (W: J=6)*

To compare the simulation with experimental data (Beste *et al*., 2000), we show the results from both finite difference and wavelet collocation in Figure 5.7. The two methods produced almost identical profile; however, as far as computational cost is concerned, wavelet takes remarkably less time for each switching period (5sec for $J = 4$; 16sec for $J = 5$; 285sec for $Nx = 65$ of the FD method in this study).

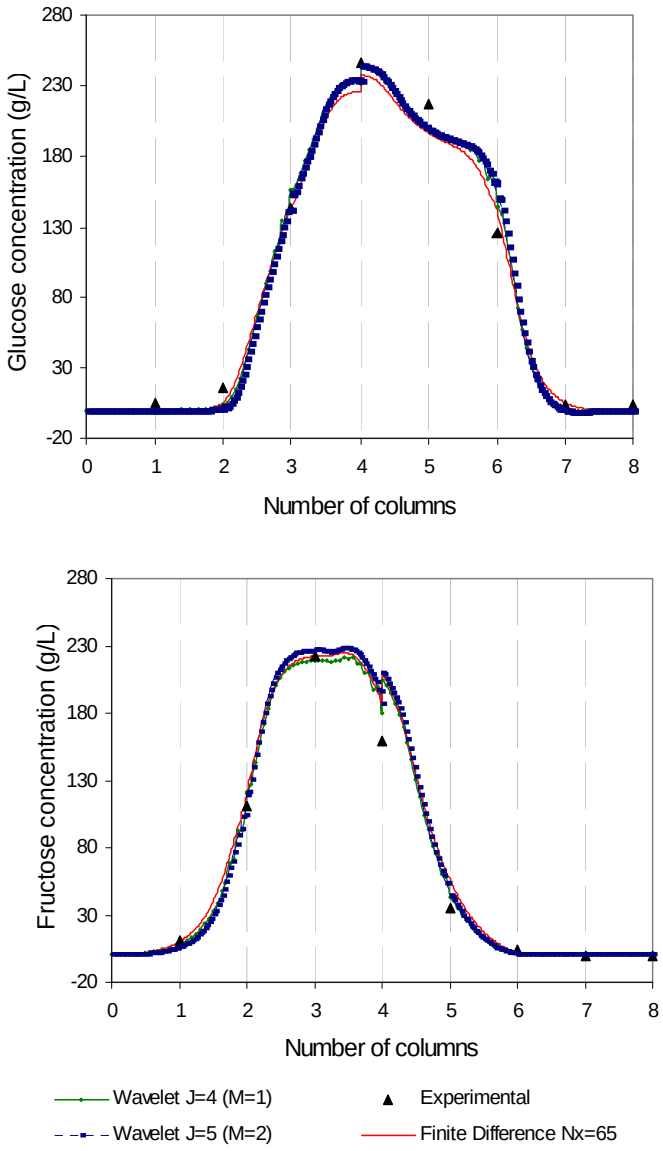

Figure 5.7 *Comparison of numerical solution from wavelet-collocation and finite difference methods with experimental data.*

From the time profile of average concentration in Figure 5.8, numerical simulation from wavelet reaches steady state faster than the solution from finite difference. Furthermore, the product purity and yield are used as criterion for the evaluation of separation quality. They were calculated as average during a switching period. Table 5.2 lists the result from our simulation, reported experimental data, and other published simulation results based on the same case study. The numerical solution using wavelet is very close to the results reported in Lim and Jorgensen (2004b), which was carried out on Sun Ultra Spark I platform using the Method of Line.

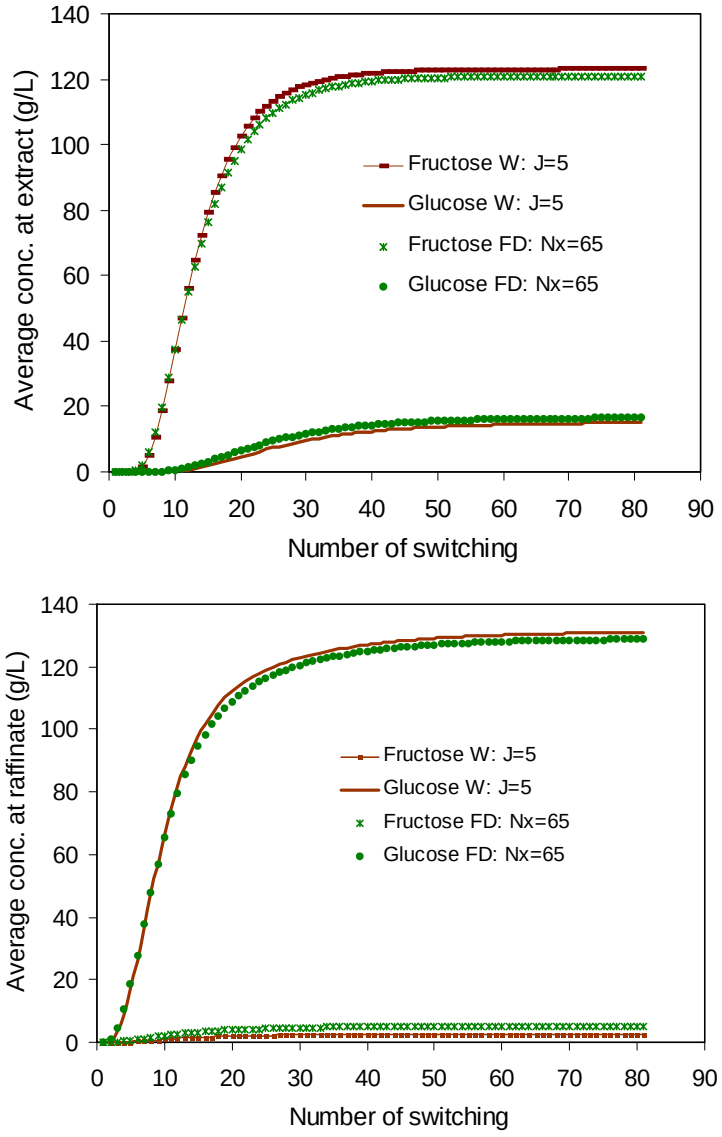

Figure 5.8 *Time profile of average concentration at the extract and raffinate ports*

Table 5.2 *Separation quality analysis (average at 73th switching unless Ns is specified)*

	Purity (%)		Yield (%)		Elapsed Time (for 80 switches)
	Extract	Raffinate	Extract	Raffinate	
#Experimental (Beste et al. 2000)	81.6	92.9	96.4	80.4	-
Finite Difference Nx = 65	88.0	96.2	97.6	85.5	6h (P4 3.00GHz)
Wavelet J = 4 (M = 1)	88.0	97.8	98.9	85.1	6min (P4 3.00GHz)
Wavelet J = 5 (M = 2)	89.2	98.0	99.3	86.9	21min (P4 3.00GHz)
#Simulation(MOL) (Beste et al. 2000)	89.4	97.9	98.3	86.9	4-5h (Sun Spark I)
#CE/AE at Ns = 40 (Lim et al. 2004b)	97.8	98.3	89.5	97.3	-

 # denote the results from references

As for the computing demand and efficiency, the reported calculation time for the Method of Line (MOL) on Sun Ultra Spark I platform is 4-5 hours. The numerical simulations of this project have been conducted on a personal computer with an Intel's Pentium IV 3.00GHz processor, and thus the computation times cannot be compared with that from the Sun Ultra Spark I platform. However, we have simulated both the finite difference method and wavelet collocation method on the same personal computer, and therefore the computation times can be directly compared with each other.

It is seen from Table 5.2 that the finite difference method consumes a few hours to get the results, while the wavelet method requires only 6min to 21min. This indicates that the computing performance of the wavelet method is encouraging. The track of purity and yield at extract and raffinate ports shown in Figure 5.9 present a good convergence property for both methods.

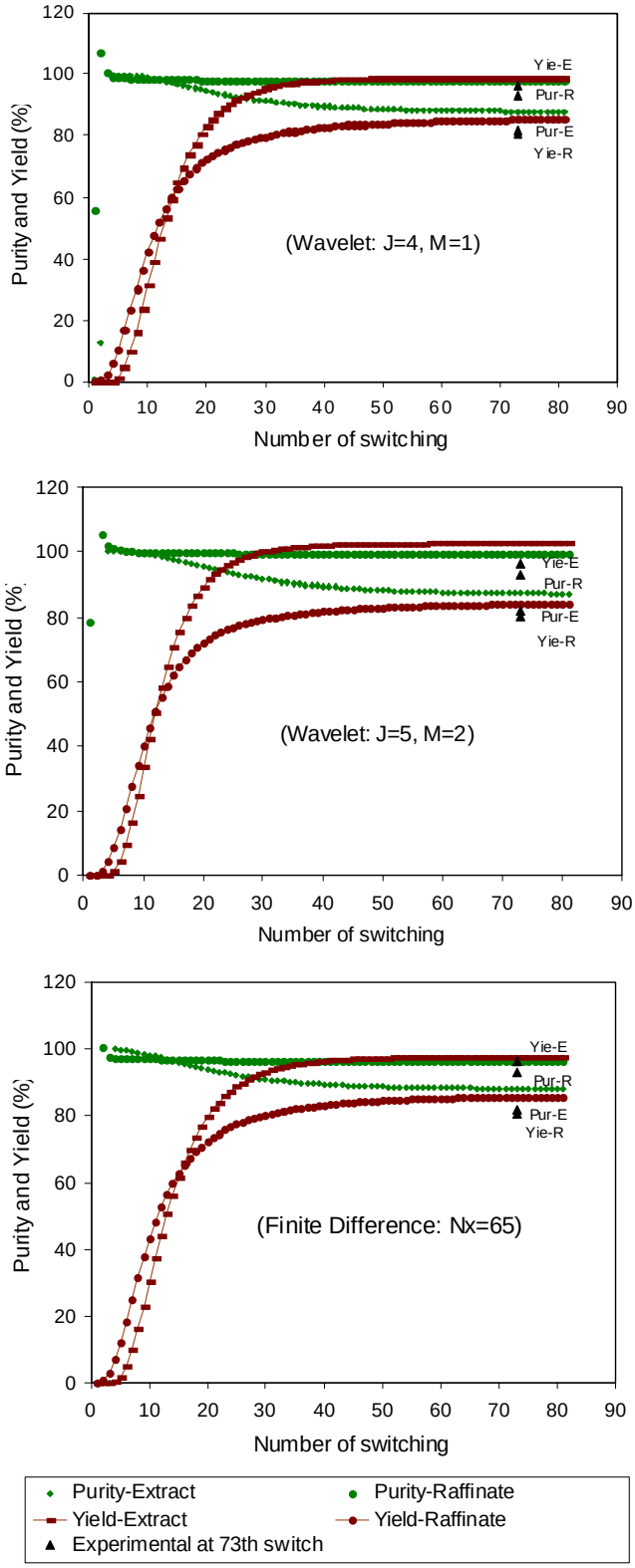

Figure 5.9 *Time profile of purity and yield at exit ports*

5.4 Case Study 2: Bi-naphthol Enantiomers Separation (Pais et al., 1997)

The separation of Enantiomers of 1,1'-bi-2-naphthol in 3,5-dinitrobenzoyl phenylglycine bonded to silica gel columns reported by Pais *et al*. (1997) is taken as our second case study system. The SMBCP also has 8 columns with the configuration of 2:2:2:2. System parameters and operation conditions are listed in Table 5.3.

Table 5.3 *System parameters and operating conditions*

Symbol	Value	Symbol	Value (Sp. A)	Value (Sp. B)
L (cm)	10.5	$k_{eff,i}$ (min^{-1})	6.0	6.0
D (cm)	2.6	$C_{i,feed}$ (g/L)	2.9	2.9
ε_T	0.4	$q_A^* = \frac{2.69C_A}{1+0.00336C_A+0.0466C_B} + \frac{0.1C_A}{1+C_A+3C_B}$		
t_{switch} (min)	2.87			
Q_F (ml/min)	3.64	$q_B^* = \frac{3.73C_B}{1+0.00336C_A+0.0466C_B} + \frac{0.3C_B}{1+C_A+3C_B}$		
	Zone I	**Zone II**	**Zone III**	**Zone IV**
Q (ml/min)	56.83	38.85	42.49	35.38
D_T (cm^2/min)	0.141	0.096	0.105	0.088

As the Peclet number is close to *2000* in this application, the finite difference method will not be adopted for solving the model equations numerically due to the reason given in Chapter 4. Therefore, numerical simulations have been performed using both the high resolution and wavelet collocation methods for spatial discretisation. The same integrator, the Alexander semi-implicit method as described in Section 3.4, is used so that the results on the effectiveness of different spatial discretisation methods can be compared.

For the trials of the high resolution method, the number of mesh points along one column length has been chosen to be *Nz =17* and *33*, which are equivalent to the collocation points generated by wavelet level of *J=4* and *J=5*, respectively. Simulations using wavelet collocation method are conducted on the level *J= 4*, *5*, and *6*, respectively. The boundary conditions are treated using polynomial interpolation with the degree *M=1*. The number of mesh points along the time axis is 5 points each switching period for all the trials.

Results and Discussion

Here, we will use relative error as a criterion to look at the convergence of proposed algorithms. It is defined by Minceva et al. (2003) between the average concentration of each component in the extract and raffinate stream for the successive switches.

$$Err = \left|1 - \frac{E_{A,s-1}}{E_{A,s}}\right| + \left|1 - \frac{E_{B,s-1}}{E_{B,s}}\right| + \left|1 - \frac{R_{A,s-1}}{R_{A,s}}\right| + \left|1 - \frac{R_{B,s-1}}{R_{B,s}}\right| \tag{5.15}$$

where $E_{A,s}$ stands for average concentration of *A* in the Extract stream for this switch and it is defined by Equation (5.12). *R* is for raffinate stream.

Figures 5.10 and 5.11 illustrate the calculated concentration distributions against experimental data, along the total columns length at the middle of 80th switching, which is taken to be steady state.

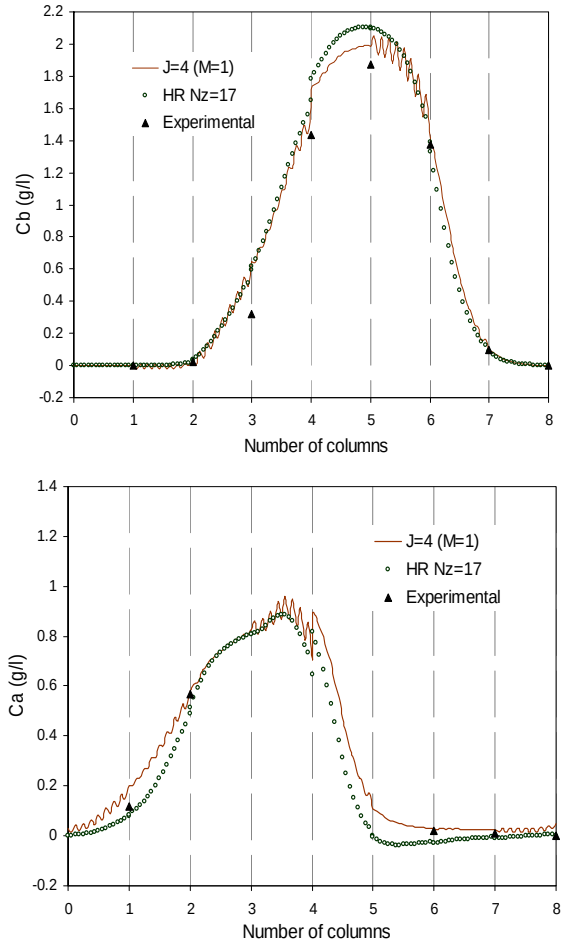

Figure 5.10 *Concentration distributions at cyclic steady state*

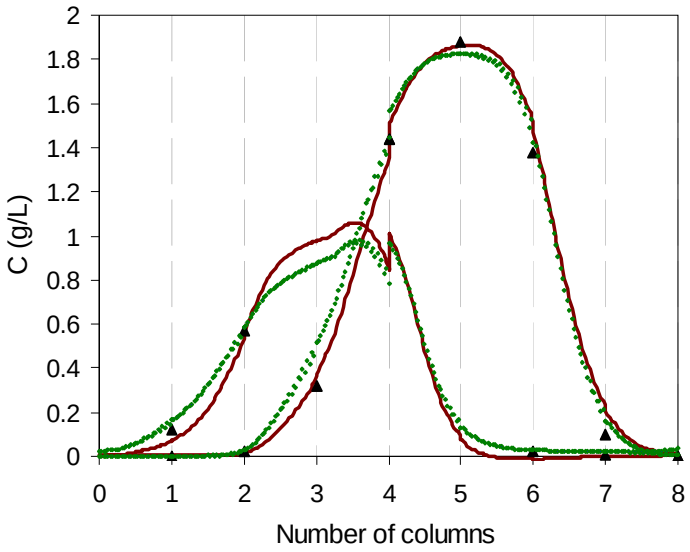

High Resolution - HR 33, line (red)
Wavelet Collocation - J=5, dash line (green)

Figure 5.11 *Concentration distributions at cyclic steady state*

It is seen that, *J=4* (wavelet collocation) or *Nz=17* (high resolution) are not good enough to predict the real value. Furthermore, wavelet collocation presents certain degree of oscillation. However, with the increasing density of spatial mesh point, wavelet collocation with *J=5* or high resolution with *Nz=33* (Figure 5.12), the approximations are getting better with high resolution method produces much closer results. As far as computational cost is concerned, using the same number of spatial mesh points, wavelet takes less time for each switching period (16sec for *J=5*) because less iteration (2) is required during the solving of Jacobi matrices. While for high resolution, it needs 24.8sec for one switching calculation where 4 iterations are required. Nevertheless, the results from the high resolution method are much closer to the reported experimental data.

Further analysis is carried out by examining the relative error produced by wavelet *J=5* and high resolution *Nz=33*. Figure 5.12 gives the relative error from wavelet collocation with different interpolation degrees, which is accomplished by two scaling down sub figures. A common observation is the abrupt point at the cycle transaction point ($s \times 8$ switch). The cause of this is not clear at the moment.

As demonstrated in Figure 5.13, high resolution also has consistent and better convergence performance.

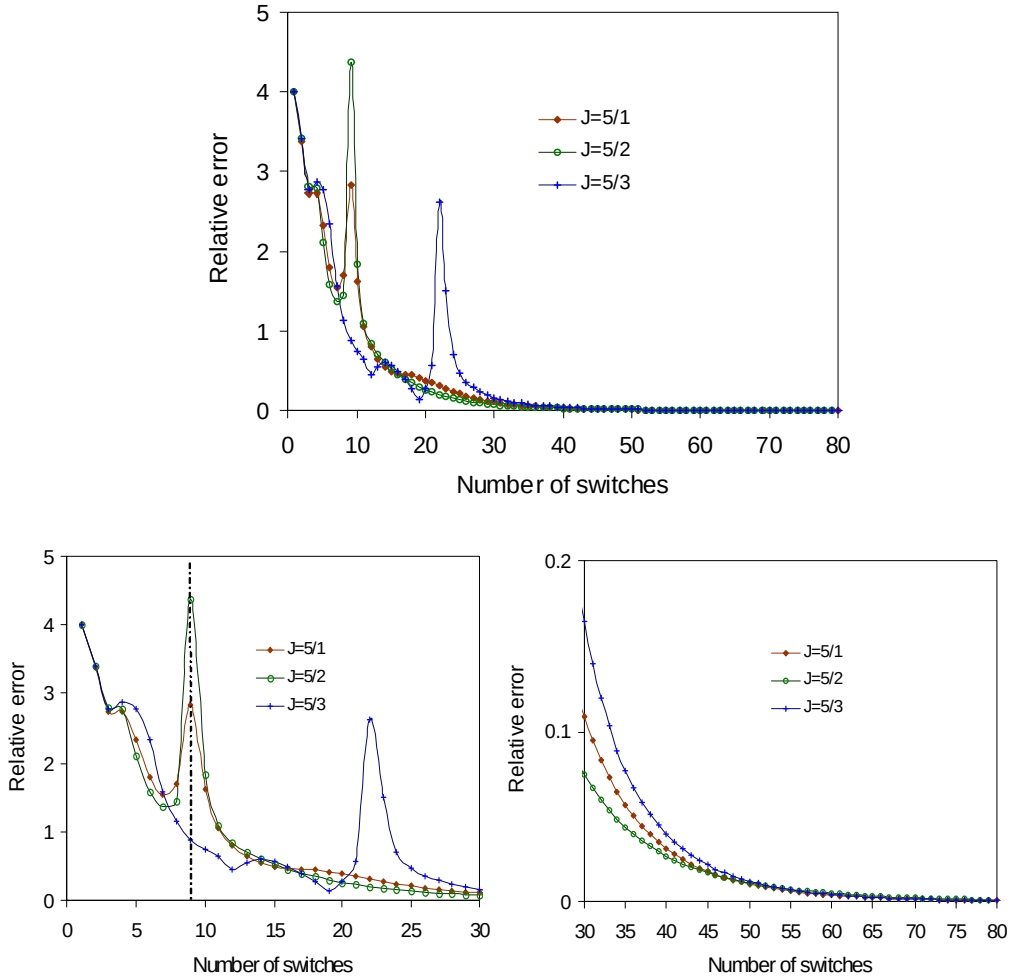

Figure 5.12 *Relative error from wavelet collocation method*

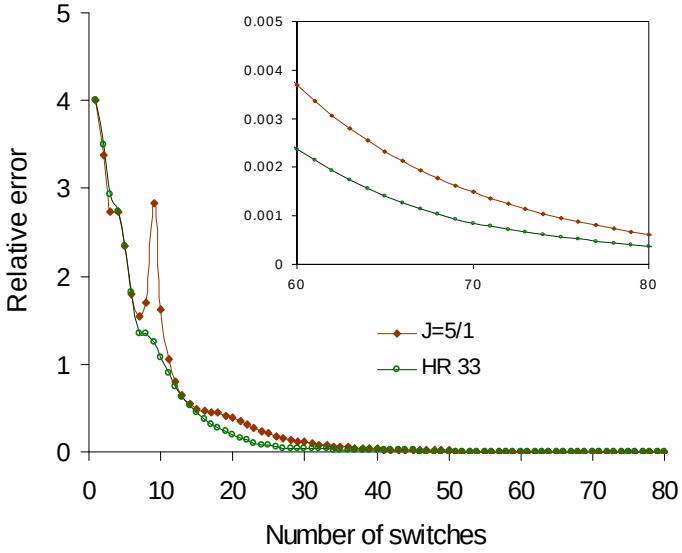

Figure 5.13 *Comparison of relative error*

5.5 Summary

This chapter has explored some upfront discretisation techniques for the solution of complicated dynamic system models with sharp variations. Recently developed wavelet based approaches and high resolution methods have been successfully used for solving models of simulated moving bed chromatographic separation processes.

This application shows that both of the methods are good candidacies for the numerical solution of this kind of complex models. They have produced encouraging results in terms of computation time and prediction accuracy on steep front. High resolution presents better stability at achieving steady state and closer approximation to experimental data. Wavelet based methods have the advantage of capturing system dynamics at low resolution levels, therefore, requires less computational efforts. The attempts made in this research prove that it is not always necessary to use a sophisticated mathematical tool if an algorithm with its basic structure can solve the problem.

This investigation provides a powerful numerical computing framework for solutions of complicated SMBCP model, as well as for many other complex industries. It is surely beneficial for online optimisation and real-time control.

Nomenclature

$C_{i,j}$: liquid phase concentrations of component *i* in column *j*

$C_{i,j}^{in}$, $C_{i,j}^{out}$: concentration of component *i* at the outlet or the inlet of column *j*

D: column diameter

$T_{i,j}^{(1)}$; $T_{i,j}^{(2)}$: the first and second order derivative for the autocorrelation function of scaling function

D_T: total diffusion coefficient

Err: relative error of numerical solution

J: wavelet resolution level

k_{eff}: effective mass transfer coefficient

L: column length

M: interpolation degree of boundary treatment in wavelet-collocation method

N_x: number of mesh points in finite difference method

N_z: number of subintervals in high resolution method

Pur: product purity

Q_I, Q_{II}, Q_{III}, Q_{IV}: volumetric flow rate through the corresponding sections

Q_D: desorbent flow rate

Q_E: extract flow rate

Q_F: feed flow rate

Q_R: raffinate flow rate

$q_{i,j}$: solid phase concentration of component *i* in column *j*

$q*$: equilibrium concentration in interface between two phases

s: number of switching

t: time coordinates

t_s: switching time

u_j: interstitial velocity in column *j*

x: axial coordinate

Yie: production yield

y: approximation of concentration of *C*

$\bar{y}$: average concentration at the exit port within one switching

ε_T: total porosity

CHAPTER 6
ACCELERATING THE STEADY STATE DETERMINATION

For the two strategies of modelling of SMB process, the equivalent true moving bed (E-TMB) is designed to operate under steady state and dynamic simulated moving bed under cyclic steady state. Since dynamic SMB modelling involves the solution of a set of partial differential equations and algebraic equations, it brings the difficulty in solution procedure and requires much more computational time. On the other hand, because the TMB model is represented by a set of ordinary differential and algebraic equations, it tends to be used for initial design and optimisation of the SMB process. However, E-TMB is a rather severe idealization of the simulated countercurrent process, it is restricted to the case of three or more columns per zone with linear isotherms and no reaction is involved. Comparative simulations (Strube & Schmidt-Traub, 1998) also suggested that since E-TMB models do not include the transient regime of the quasi-stationary, periodic steady state of SMB processes and not consider the upper and lower bounds of the retention time, an SMB optimisation based on E-TMB model will lead to a miscalculated operating condition.

The determination of cyclic steady state from dynamic SMB modelling thus becomes important although there is a challenge in numerical procedure. In recent years, attention has been paid to accelerating the calculation of the cyclic steady state for control and optimisation of SMB processes. There are essentially two approaches to determine the steady state of a cyclic operation, the dynamic simulation approach and the direct prediction approach. The former is implemented through successive substitution, while the latter is employed through implementing the periodic boundary conditions into the problem formulation. In this research, we have made an effort to implement a fast integration scheme based on the concept of “Quasi-Envelope”; this is a totally new attempt in such an application.

6.1 The Concept of "Quasi-Envelope"

The original idea of "Quasi-Envelope" is related to the solving of differential equations that have highly oscillatory solutions. It can be traced back to as early as 1957, when astronomers firstly introduced the so called multi-revolution methods for calculating the orbits of artificial satellites. The "Quasi-Envelope" method was proposed by Petzold (1981), who was inspired by the observation that when a nearly periodic function is sampled at multiples of the period (or near-period) of the oscillation, the resulting sequence of points changes slowly. It aimed at finding that slow change behaviour of the solution without having to closely follow the oscillation details. In the following section, we will firstly present how the problem is formulated in mathematical descriptions.

6.1.1 Highly Oscillatory ODE and Its Quasi-Envelope

Given an initial value problem

$$y' = f(y,t),\ y(0) = y_0 \tag{6.1}$$

where $y(t)$ is periodic or near periodic function with a period of T. A typical solution is shown in Figure 6.1.

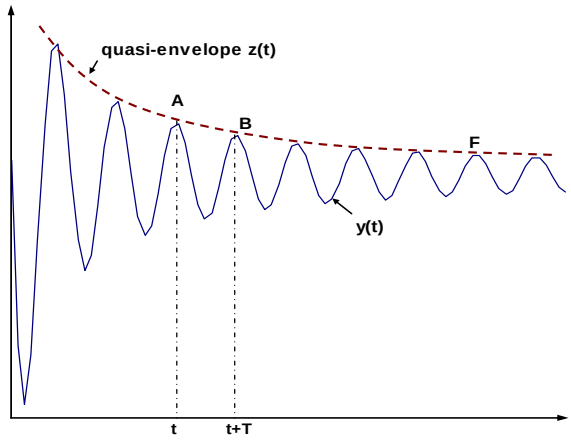

Figure 6.1 *Sinusoidal wave and its quasi-envelope*

We ignore the details of every oscillation represented by $y(t)$, instead, we look at the peak in each period. When the oscillation is very fast, a smooth curve $z(t)$, which passes through these multiples of period, can be defined, so called the quasi-envelope. Using $z(t)$ to

represent the quasi-envelope of original function $y(t)$, according to the definition, it has the following properties:

(1) The state on $z(t)$ can be found at discrete points, one cycle time apart. Those points should agree with the solution to the original problem, especially, $z(0) = y(0)$, and in general, $z(nT) = y(nT)$, where n is an integer.

Since this is a slowly varying function compared to oscillation, it can be followed in large steps H to approximate the value at intervals $H >> T$. More precisely, the property of the quasi-envelope determines that the value at multiples of the period agrees with the solution to the original equation. Starting with any of the points, the point-wise solution to the original problem can be recovered through integration using that particular point as initial condition. For example, if we know $z(t)$ at point A, then the curve underneath A-B can be found through one cycle integration to $y(t)$.

(2) $z(t)$ is a fictitious curve, thus the derivatives of z with respect to time cannot be found through mathematical operation. Derivatives of z is a must for any of the numerical computations. By assumption, since $y(t)$ is nearly periodic, the values of $z(nT)$ should change slowly. Derivatives of z with respect to time may be approximated by the change of function $z(t)$ during one period T:

$$z'(t) \approx g(z) = \frac{z(t+T) - z(t)}{T} \tag{6.2}$$

Petzold's algorithm is analogous to Gear's multivalue or multistep algorithm but using the above difference quotients instead of derivatives. Multivalue methods require several pieces of information about the dependent variable at time t_{n-1} to compute the equivalent pieces of information at t_n. If we use the values of the dependent variable and its derivative at k different mesh points $t_{n-1}, t_{n-2}, \cdots, t_{n-k}$, they are commonly called Multistep methods; in this cases, k-step methods. This method consists of two processes, the prediction and correction. The most popular multistep combination is the explicit Adams-Bashforth predictor and the implicit Adams-Moulton corrector.

Denote H as the step size of integration for function $z(t)$, the multistep integration formulas can be represented by the following equations:

$$z_{n,(0)} = \sum_{j=1}^{k} [\alpha_j(r) z_{n-j} + H\beta_j(r) g_{n-j}] \quad \text{(Adams-Bashforth prediction)} \tag{6.3}$$

where: $r = T / H$.

The prediction process does not make use of the original differential equation, so a correction process is imposed to correct the approximate value. The amount by which $z_{n,(0)}$ does not satisfy the real value is:

$$G(z_n) = g(z_n) - g_n \tag{6.4}$$

Thus, we have the following Adams-Moulton correction formula,

$$z_{n,(m+1)} = \sum_{j=1}^{k} [\alpha_j^*(r) z_{n-j} + H\beta_j^*(r) g_{n-j}] + H\beta_0^*(r) G(z_{n,(m)}) \tag{6.5}$$

Starting from the predictor, Equation (6.5) is calculated to correct the result from Equation (6.3). It is then repeated for $m = 1,2\cdots$ iterations until there is no further change in $z_{n,(m+1)}$. Because $z(t)$ is discretised at nT, where the quasi-envelope and original function are crossed, the state of z at this point also agree with the state of y. If we have $z(t_n)$ as starting, the afterwards state of $y(t)$ can be calculated by detailed integration. In other words, $z(t)$ provides a starting point for the integration of $y(t)$. If H is chosen as several times of T, say, from B directly to F in Figure 6.1, the above calculation will give the state of $z(t)$ several cycles away. Using this state as initial, we can reconstruct $y(t)$ for the next full cycle or more.

6.1.2 Implications to SMB Operations

As explained in Chapter 5, a simulated moving bed chromatographic process is a cyclic operation. It approximates the countercurrent flow by continuously cyclic port switching. The stationary regime of this process is cyclic steady-state (CCS), in which in each section an identical transient during each period between two valve switches takes place. The CSS state is practically reached after a certain number of valves switches, but the system states are still varying over time because of the periodic movement of the inlet and outlet ports along the columns. A typical time profile of concentration distribution along the total column length is depicted in Figure 6.2.

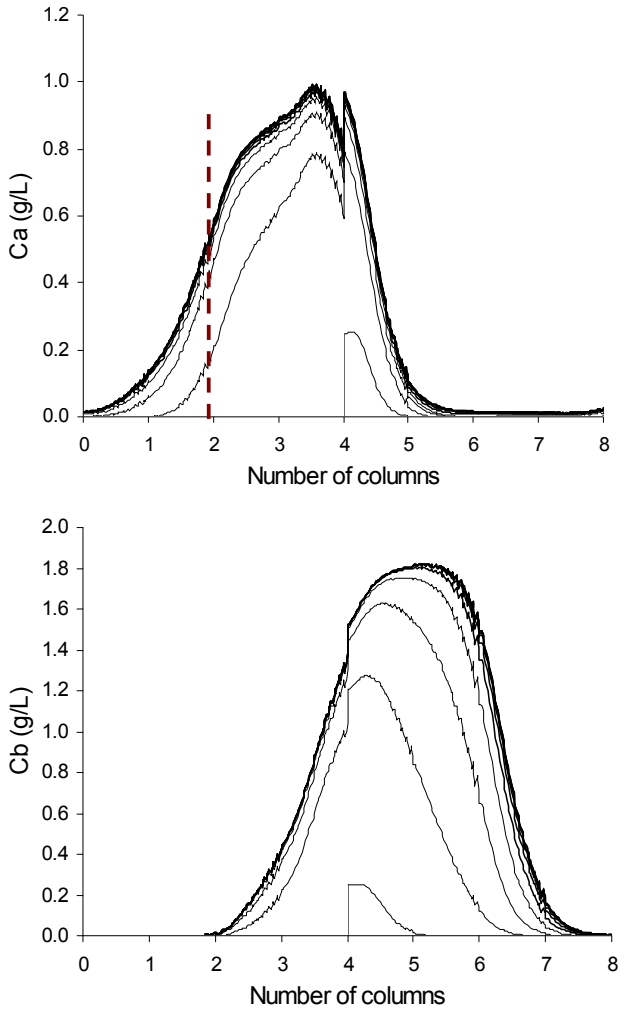

Figure 6.2 *Propagation of concentration wave in a binary separation*

It is hard to relate this process to oscillatory functions illustrated in Figure 6.1. Since this is a multivariable problem, let us look at the average concentration time profile (Figure 6.3) of a particular point along the column, e.g. at the extraction point, which is the cross section indicated by the dashed line in Figure 6.2.

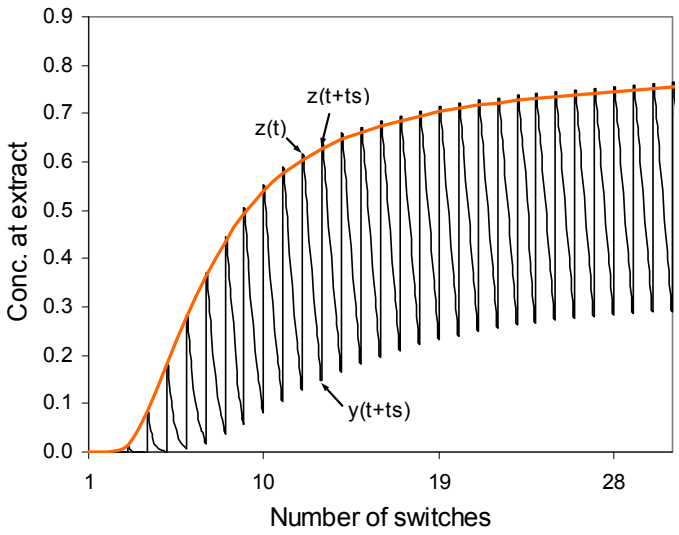

Figure 6.3 *Time profile of concentration at particular axial point*

As shown in Figure 6.3, each oscillation represents one switching period, starting from the top line and finishing at the bottom. Thus, it can be treated as a pseudo-oscillatory process. Compared to the oscillation, the underlying quasi-envelope is a slowly-varying function and can be defined by a smooth curve. For an SMB to reach steady state, it takes at least 10-12 cycles (for 8 column SMB, it is 80-96 switching). So the oscillation is highly condensed in terms of the process time constant.

The implication of Petzold's idea is obvious to SMB processes. Instead of traditional switch by switch (or cycle by cycle) integration, we can take advantage of quasi-envelope function as an express train to obtain the steady state faster by ignoring details of some of the switching period. Particularly, this is a process with known constant period (the switching time), which makes the application of Petzold's method to SMB simulation become straight forward.

6.2 The Algorithm and Implementation

The multistep method represented by Equations (6.3) and (6.5) uses current and previous points to predict the value at the next point. For stiff problems, Newton iteration is usually an essential part of a multistep stiff solver. However, multistep methods as we described above suffer from two serious difficulties. Since the formulas require results from equally spaced steps, adjusting the stepsize is difficult. Secondly, the starting and stopping problem also exist. For starting, we need not only the initial values but also several previous steps. For stopping, equal steps are unlikely to land directly on the desired termination point. To solve the above, especially for a variable step size, which is the key of this quasi-envelope method, Petzold has rewritten the algorithm in generalised Adams formula using multivalue methods. We will present the equations in the following section directly. Interested readers should refer to the original work (Petzold, 1981) and the book of C. William Gear (1971): Numerical Initial Value Problems in Ordinary Differential Equations.

6.2.1 Generalised Adams Formula from Multivalue Method

For multivalue methods, the basic data available to the integrator are the fist few terms of the Taylor series expansion of the solution at the current point t_n.

$$y_{n+1} = y_n + hy'_n + \frac{h^2}{2} y''_n + \cdots + \frac{h^k}{k!} y_n^{(k)}$$

This is contrast to multistep methods, where the data are the values of the solution at $t_{n-1}, t_{n-2}, \cdots, t_{n-k}$, as shown in Equations (6.3) and (6.5). The use of generalised Adams formula from multivalue method would allow the algorithm to easily adapt to a changing stepsize.

Define vector $\mathbf{w}_n$, so that $\mathbf{w}_n$ is a matrix of several pieces of information from t_n step only.

$$\mathbf{w}_n = [z_n, Hg_n, \frac{H^2}{2} g'_n \cdots, \frac{H^k}{k!} g_n^{(k-1)}]^T$$

Also, $\mathbf{w}'_n$ is defined as containing the information from previous several steps:

$$\mathbf{w}'_n = [z_n, Hg_n, Hg_{n-1} \cdots, Hg_{n-k-1}]^T$$

Where: $g_n = \dfrac{z(t_n + T) - z(t_n)}{T}$

Then, $\mathbf{w}_n$ and $\mathbf{w}_n^{'}$ can be related by the linear transformation:

$$\mathbf{w}_n = \mathbf{S}\mathbf{w}_n^{'} \tag{6.6}$$

The value of $\mathbf{S}$ is determined by the integration order. Petzold allows the integration order to vary from 1 to 11. For our purposes, the first-order method will not be used and much higher orders are also not applied considering stability of the algorithm. We will conduct our investigation on orders 2 and 3.

For second order (*k=3*) multivalue method, we have

$$z_n = z_n, \quad g_n = g_n, \quad g_{n-1} = g_n - Hg'_n$$

So, $$\mathbf{S} = \begin{bmatrix} 1 & 0 & 0 \\ 0 & 1 & 0 \\ 0 & 1/2 & -1/2 \end{bmatrix}$$

For third order (*k=4*) multivalue method,

$$z_n = z_n, \quad g_n = g_n, \quad g_{n-1} = g_n - Hg'_n + \frac{H^2}{2}g''_n, \quad g_{n-2} = g_n - 2Hg'_n + \frac{4H^2}{2!}g''_n$$

So, $$\mathbf{S} = \begin{bmatrix} 1 & 0 & 0 & 0 \\ 0 & 1 & 0 & 0 \\ 0 & 3/4 & -1 & 1/4 \\ 0 & 1/6 & -1/3 & 1/6 \end{bmatrix}$$

Then the generalised Adams prediction and correction method will be given by

$$\mathbf{w}_{n,(0)} = \mathbf{A}\mathbf{C}(R_n)\mathbf{w}_{n-1} \tag{6.7}$$

$$\mathbf{w}_{n,(m+1)} = \mathbf{w}_{n,(m)} + \mathbf{B}H_n\mathbf{G}(z_{n,(m)}) \tag{6.8}$$

with $R_n = H_n / H_{n-1}$ being the stepsize ratio for the consecutive integration step.

$\mathbf{C}(R_n) = diag[1, R_n, R_n^2, \cdots, R_n^k]$;

$$\mathbf{A}=\begin{bmatrix} 1 & 1 & 1-r & 1-\frac{3}{2}r+\frac{1}{2}r^2 & \cdots & \cdots \\ & 1 & 2 & 3 & & \\ & & 1 & 3 & & \\ & & & 1 & & \\ & & & & \ddots & \\ & & & & & 1 \end{bmatrix};$$

$\mathbf{B}=\mathbf{Sc}$;

$\mathbf{c}=[\beta_0^*(r),1,0,\cdots,0]^T$;

For second order (k=3), $\beta_0^*(r)=1-r$; and $\mathbf{B}=\begin{bmatrix}\beta_0^*(r)\\ 1\\ 1/2\end{bmatrix}$

For third order (k=4), $\beta_0^*(r)=\frac{5}{12}-\frac{6}{12}r+\frac{1}{12}r^2$; and $\mathbf{B}=\begin{bmatrix}\beta_0^*(r)\\ 1\\ 3/4\\ 1/6\end{bmatrix}$

$\mathbf{G}(z_{n,(m)})$ is defined by Equation (6.4), in vector:

$$\mathbf{G}(z_n)=\mathbf{g}(z_n)-\mathbf{g}_n \tag{6.9}$$

$\mathbf{g}_n$ is predicted value included in the vector $\mathbf{w}_n$.

In classical numerical method, $\mathbf{g}(z_n)$ is $\mathbf{z}'_n$, which can be calculated if the function of $z'(t)$ is given. In this technique, $g(z_n)$ is defined by

$$g(z_n)=\frac{z(t_n+T)-z(t_n)}{T}$$

$z(t_n+T)$ will be obtained through one cycle integrating on the original function using predicted z_n, so that,

$$\mathbf{g}(\mathbf{z}_n)=\frac{\mathbf{y}(t_n+T)-\mathbf{z}(t_n)}{T} \tag{6.10}$$

It can be seen that Equation (6.7) allows a variable stepsize. Changing the stepsize by a ratio R_n corresponds to multiplying $\mathbf{w}_{n-1}$ by the matrix $\mathbf{C}(R_n)$.

6.2.2 Periodic Integration Procedure

The time integration is conducted on the ODEs transformed from PDEs. For PDEs to ODEs, we have studied various spatial discretization techniques in the previous chapters. Here we will select wavelet collocation method and choose the same fructose-glucose separation as our case study. Since Chapter 5 has presented the simulation results from direct substitution, they can be used for performance evaluation purpose.

The complete solution algorithm is depicted in the following diagram.

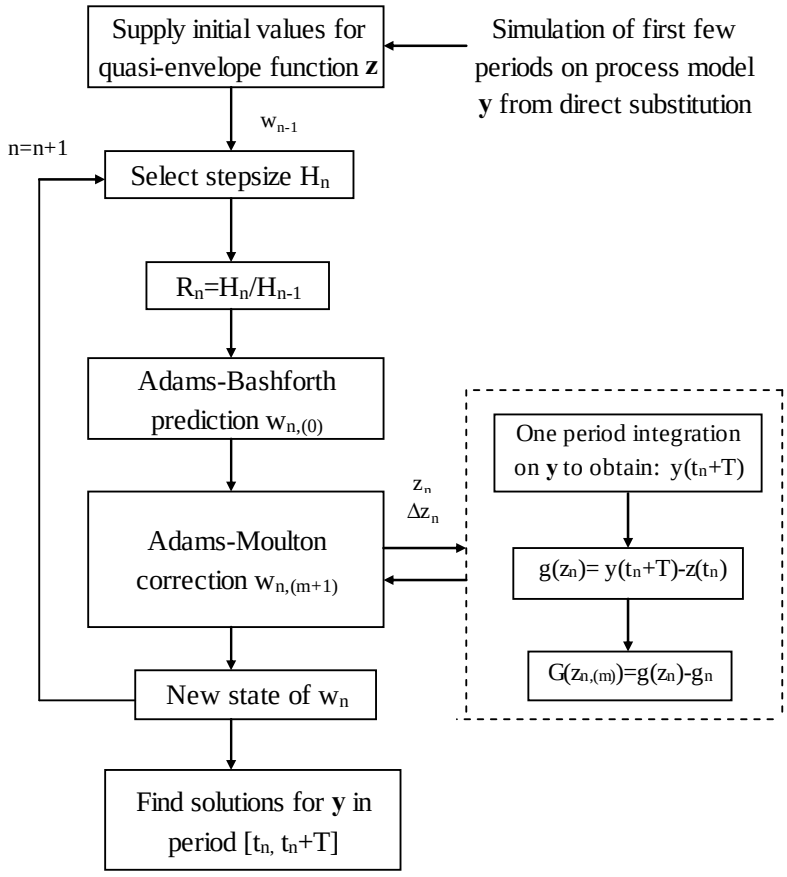

Figure 6.4 *Outline of the periodical integration algorithm*

The complete procedure involves two integration operations, one for the original function $y(t)$ and the other for the quasi-envelope function $z(t)$. The above proposed multivalue method applies to the integration of $z(t)$, called "outer integration". However, during which, the corrector also requires a one cycle evaluation of $y(t)$, named "inner integration". Based

on the previous work, we conclude that the Alexander semi-implicit method works well for this specific application and thus kept that for inner integration.

The implementation of the above algorithm is detailed in the following steps:

Step 1: The integration routine starts by taking several steps with step size equal to one switching time. Cares must be taken to ensure that the initial evaluations should provide sufficiently accurate information for $z(t)$ to start the integration.

$z(0) = y(0);$ $\quad$ $z(1) = y(H);$

$g(0) = y(T) - y(0);$ $\quad$ $g(1) = y(H+T) - y(H);$

$g'(0) = 0;$ $\quad$ $g'(1) = \dfrac{g(1) - g(0)}{H};$

$g''(0) = 0;$ $\quad$ $g''(1) = \dfrac{3!}{H^3}[z(1) - z(0) - Hg(1) + \dfrac{H^2}{2} g'(1)]$

$g''(1)$ is derived from third order Taylor expansion.

Step 2: Calculate the prediction of $\mathbf{w}_{n,(0)}$ using Equation (6.7)

Step 3: Using Newton iteration to calculate $\mathbf{w}_{n,(m+1)}$ from Equation (6.8) until it meets the convergence requirement.

One of the correction steps is:

$$\mathbf{w}_{n,(m+1)} = \mathbf{w}_{n,(m)} + (H_n / T)\mathbf{B}[\mathbf{I} - (H_n / T)\beta_0^*(r)\mathbf{\Phi}]^{-1}\mathbf{G}(z_{n,(m)}) \qquad (6.11)$$

Step 4: Choosing next stepsize and repeat from Step 2.

The major part of the program is attached below.

```
%-----------------------------------------------------------------

** Input process parameters **

** Construct wavelet basis **

[D0,D1,D2]=Basis1(nJ,WL,MB);
```

```
** Dimension defined for w **

** Specify the parameters for outer integrator **

** Set the starting state for z(t) **

%start the outer integration

for i=3:30   % number of outer integration step, start from t=T+8T

** Select H(i) **

   R=H(i)/H(i-1);
   r=T/H(i); h1=H(i)/T;h2=H(i)^2/(2*T);h3=H(i)^3/(6*T);
%------------ predictor-----------------------------------%
    c=[1;R;R^2;R^3];
    A=[1,1,1-r,1-3/2*r+r^2/2;0,1,2,3;0,0,1,3;0,0,0,1];
    a=A*diag(c);
% -----------first order---------------------------------
   wp(:,i)=wp(:,i-1)+a(1,2)*h1*gp(:,i-1);
   gp(:,i)=a(2,2)*gp(:,i-1);
% -----------second order--------------------------------
   wp(:,i)=wp(:,i-1)+a(1,2)*h1*gp(:,i-1)+a(1,3)*h2*dg(:,i-1);
   gp(:,i)=a(2,2)*gp(:,i-1)+a(2,3)*H(i)/2*dg(:,i-1);
   dg(:,i)=a(3,3)*dg(:,i-1);
%-------------third order--------------------------------
   wp(:,i)=wp(:,i-1)+a(1,2)*h1*gp(:,i-1)+a(1,3)*h2*dg(:,i-1)
           +a(1,4)*h3*ddg(:,i-1);
   gp(:,i)=a(2,2)*gp(:,i-1)+a(2,3)*H(i)/2*dg(:,i-1)
           +a(2,4)*H(i)^2/6*ddg(:,i-1);
   dg(:,i)=a(3,3)*dg(:,i-1)+a(3,4)*H(i)/3*ddg(i,i-1);
   ddg(:,i)=a(4,4)*ddg(:,i-1);

%----------corrector - Newton iteration-----------------%
   % initial guess for Newton algorithm
    x1=wp(:,i);        %wp=z
    x2=gp(:,i);        %gp=g/T
    x3=dg(:,i);        %dg=g'/T
    x4=ddg(:,i);       %ddg=g''/T

    for iter=1:Nmax
        g1=-x1+inner(x1);
        f=x2-g1;
        NRM=norm(f)
        if NRM<tol, break, end

   %calculate jacobian of g1 using numerical differentiation
        steptub=(1+x1)*1e-7;
        for jj=1:dim
            xh=x1;
            xh(jj)=x1(jj)+steptub(jj);
            gh=-xh+inner(xh);
            jac(:,jj)=(gh-g1)/steptub(jj);
        end

   %calculate Jacobian of f
        J=eye(dim)-H/T*beta*jac;
        JF=-J\f;

   %Newton estimate update
```

```
   % -------------second order-------------------
         x1=x1+h*beta*JF;
         x2=x2+JF;
         x3=x3+JF/H;

   %------------- third order--------------------
         x3=x3+JF/2/H;
         x4=x4+JF*9/H^2;
    end
    if (iter==Nmax),error('Maximum iterations reached'),end

wp(:,i)=x1;
gp(:,i)=x2;
dg(:,i)=x3;
ddg(:,i)=x4;
end

%-------------------------------------------------------------------
```

The function *inner* conduct one period integration using the methods developed in Chapter 5.

The above procedure is very standard for a multistep numerical integration. The trouble is in the evaluation of Jacobian matrix $\mathbf{\Phi}$ for the Newton algorithm. The construction of Jacobian requires call for inner integration. The computation time is the dimension of $\mathbf{w}$ multiply the time used for the evaluation of a single switch. For SMB model, the dimension of $\mathbf{w}$ can be enormous. This is one of the problems we addressed in this investigation.

There is another concern when using Petzold's algorithm. The advantage of using quasi-envelope is to take longer stepsize so that one can obtain the steady state quickly. In direct substitution, the semi-implicit integrator typically requires 3-4 iteration in Newton algorithm. If we could keep a low number of Newton iteration, while moving in a larger stepsize $H >> T$, that will surely save our computing time. However, because $z(t)$ is a fictitious curve without an exact expression, the prediction can become unstable for quite a while, which means more steps will be needed when performing Adams-Moulton correction. This is another challenge we will face when applying Petzold's algorithm to SMB simulation.

6.3 Application to SMB Cyclic Processes

The separation of fructose-glucose in de-ionized water used in Beste *et al*. (2000) has been taken as one of our case study systems in Chapter 5.3. The SMBCP has 8 columns with the configuration of 2:2:2:2. This process will be used here for the study of applying the concept of quasi-envelope to the fast integration of SMB cyclic operation. The inner integrator block adopted the previously developed PDE solver, that is, wavelet collocation methods for spatial discretization using $J = 4$ ($M = 1$), and the Alexander semi-implicit method (3rd order Runge-Kutta) for time integration. All the programming parameters are kept the same as those in Chapter 5 Section 3. The outer integration is based on the generalised Adams prediction and correction method.

Simulation result from Section 5.3 for the concentration at extract using successive substitution (switch by switch) is illustrated in Figure 6.5.

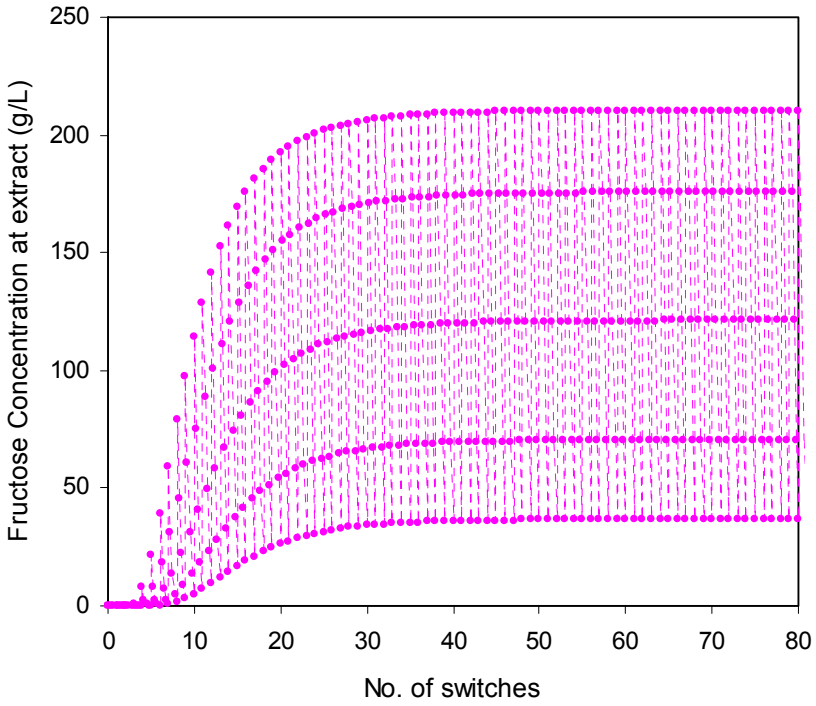

Figure 6.5 *Discrete concentration profile at extract.*

6.3.1 Determining the Initial Point for Quasi-Envelope

To apply the quasi-envelope concept, let us zoom in the above figure by looking at the behaviour between 10-20 switches. From Figure 6.6, it is clearly seen that this is a regular oscillation process and the starting state for each period constructs a fairly smooth curve. Our aim is to find out this starting state via a pseudo smoother function so that the real process can be reconstructed for any given starting conditions.

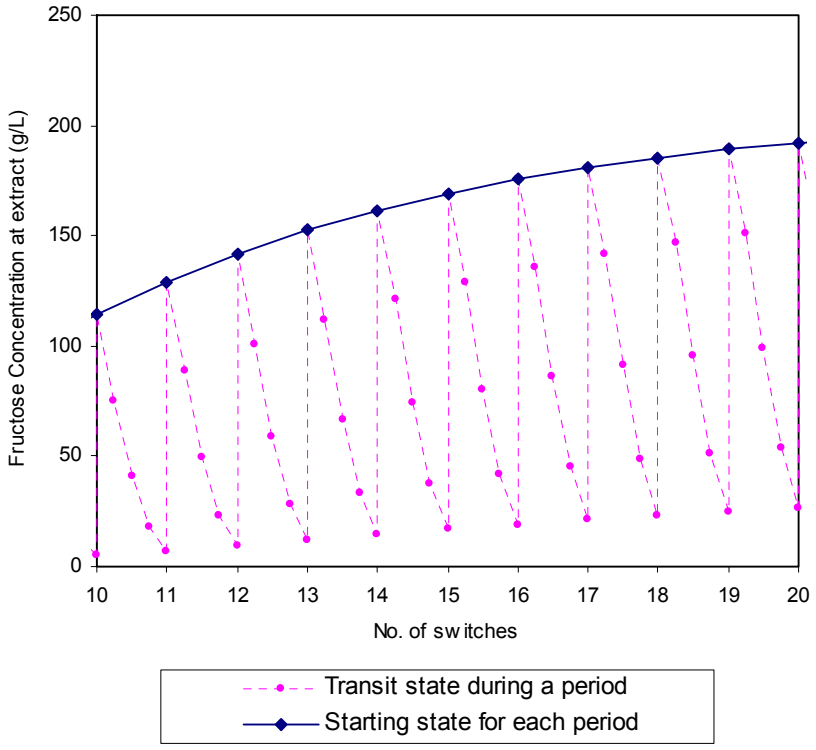

Figure 6.6 *Concentration time profile at extract.*

For preliminary study, we will choose a constant time step, $H = 8T$, as a start.

As pointed out previously, the initial state provided to the quasi-envelope is very important to ensure sufficient accuracy. Determining initial state can be done by taking several steps of detailed integration with step size equal to one switching time. Since the step size for quasi-envelope is set as one cycle (8T), we will firstly conduct one cycle detailed integration by direct substitution. The start-up operation is graphically illustrated in Figure 6.7.

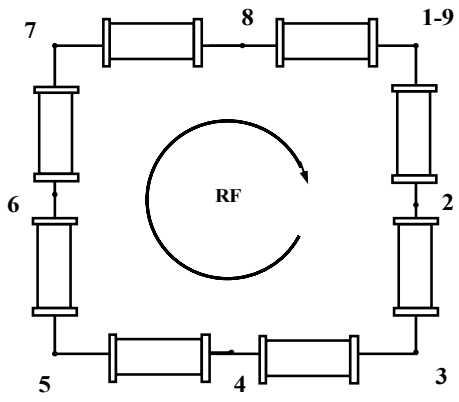

Figure 6.7 *Position of the feeding port for consecutive switches.*
(State 1 is the initial position; state 2 resulted from the first switch, and so on)

The number indicates the position of feed port, state 1 is the initial position, state 2 resulted from the first switch, and so on. After the 8th switch, it goes back to the original position, so state 1 and 9 correspond to the same operating conditions. This procedure produces the concentration profile at extract port as presented in Figure 6.8.

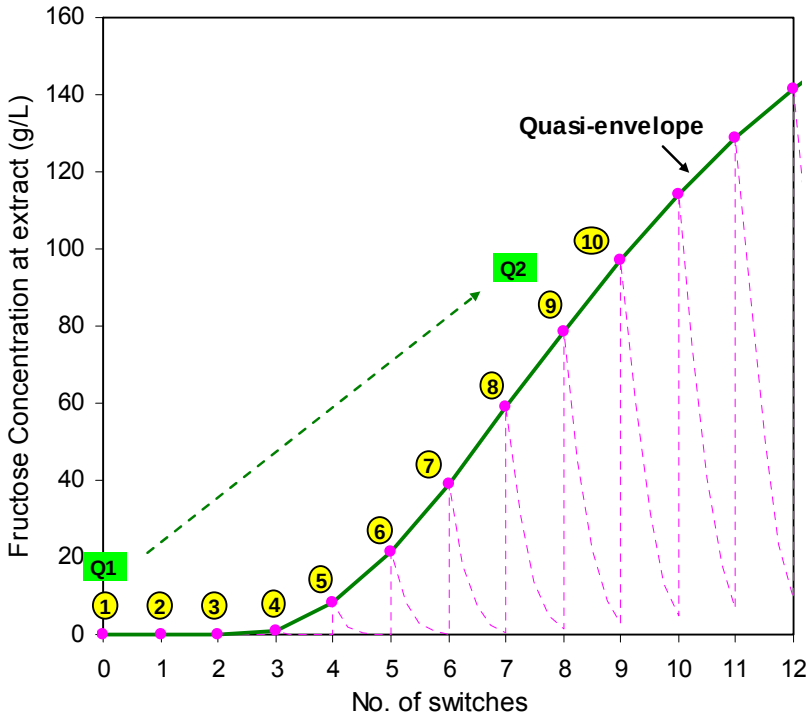

Figure 6.8 *Concentration profile at extract for the start-up.*
(1 to 10: the starting state of the real process within each switch; Q1 and Q2: the first two points for quasi-envelope, which are 8T apart).

The number in the circle corresponds to the positions of the feeding port in Figure 6.7, also indicates the starting state of the real process within each switch. The number in the square, Q1 and Q2 are the first two points for quasi-envelope, which are 8T apart. Because we assumed constant time step for quasi-envelope, the next point will be another 8 switches away. This is implemented by the following program.

```
%Set the starting state for z(t)
for k=1:9
   wc(:,k+1)=inner(wc(:,k));  %set up initial for quasi-envelope
end
wp(:,1)=wc(:,1);
wp(:,2)=wc(:,9);
gp(:,1)=wc(:,2)-wc(:,1);
gp(:,2)=wc(:,10)-wc(:,9);
dg(:,2)=(gp(:,2)-gp(:,1))/H;
ddg(:,2)=(T*(wp(:,2)-wp(:,1))-H*gp(:,2)+H^2/2*dg(:,2))*6/H^3;
```

This calculation will provide quasi-envelope function $z(t)$ the starting state Q1 and Q2, which are obtained from 9 steps of inner integration. From there, approximation of $z(t)$ will start.

6.3.2 Comparison of the QE Prediction with the Results from Successive Substitutions

It can be seen from the algorithm that during the correction, the evaluation of Jacobian matrix $\mathbf{\Phi}$ for the Newton iteration requires call for inner integration. The inner integration should be calculated many times because dimension of $\mathbf{w}$ is significantly high for an 8 column binary separation process, which is almost the basic configuration for SMB systems**.** Higher number of columns is expected. One of the solutions for the problem is to evaluate $\mathbf{\Phi}$ initially and thereafter only if the corrector iteration convergence is too slow (Toftegard & Jorgensen, 1989). If $\mathbf{\Phi}$ must be re-evaluated often, a Broyden update may be used.

In our study, we will evaluate the Jacobian matrix based on the point where the maximum prediction error occurs. This is implemented as:

```
steptub=(1+x1)*1e-7;
tt=find(max(abs(f)));
xt=x1; xt(tt)=x1(tt)+steptub(tt); xtc=inner(xt);
for jj=1:dim
    xh=x1;
    xh(jj)=x1(jj)+steptub(jj);
    gh=-xh+xtc;
    jac(:,jj)=(gh-g1)/steptub(jj);
end
```

This will lift the call of inner integration out of the construction of Jacobian matrix loop. So the number of using *inner* is equal to the number of Newton Iteration in the Adams correction step, which will significantly release the computational effort. Simulation results are given in Figures 6.9 and 6.10 using the second order multivalue method.

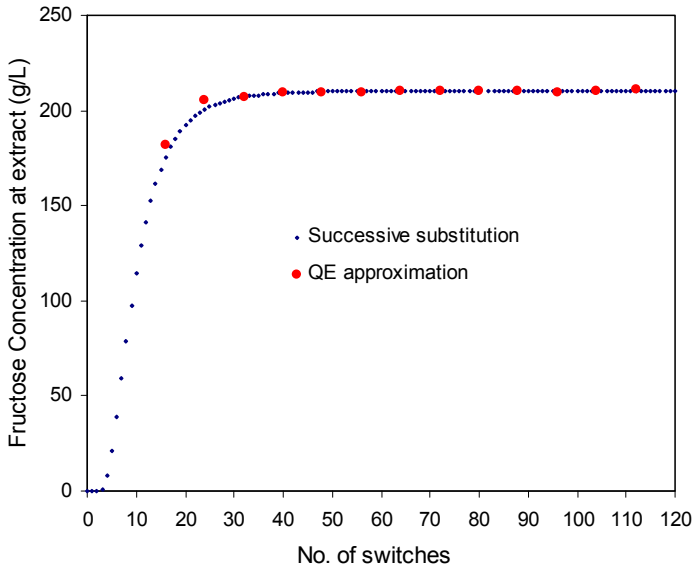

Figure 6.9 *The concentration state at the beginning of switch.*

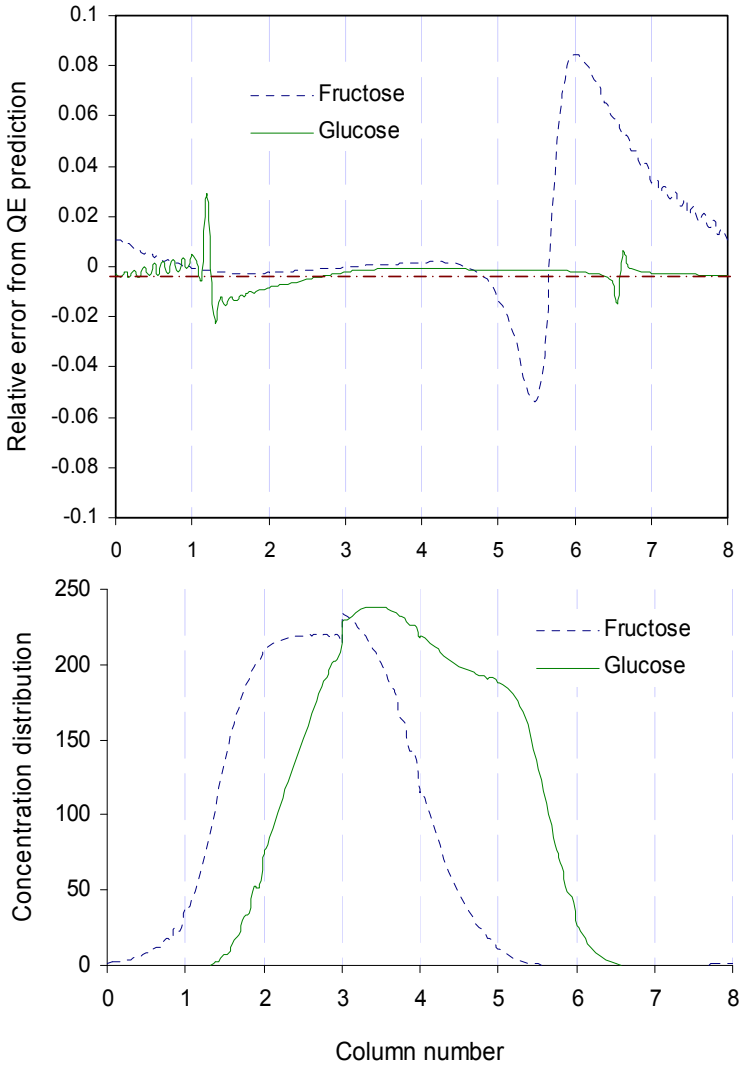

Figure 6.10 *Error distributions from QE prediction*

The discrete $z(t)$ is evenly distributed and the approximation is gradually getting very close to the one obtained from successive substitution. The successful reconstruction of concentration distribution at steady state proves that predicted starting state from this method can be safely used.

Recall that the sub-function *inner* runs evaluation of $y(t)$ for one switch. Thus, apart from accuracy, Newton iteration, which is required in the corrector, can be an important criterion for this proposed method. For sure the prediction of $z(t)$ should not take more iterations than successive substitution within two consecutive points. For example, if the integration step for $z(t)$ is $H = 8T$. In direct substitution, the state at $t_{n+1} = t_n + 8T$ can be obtained by running

inner 8 times. In quasi-envelope method, the prediction of $z(t_n)$ in each integration step should be restricted not to call *inner* more than 8 times, otherwise, this method lost its advantage over the direct substitution.

For this trial, the Newton iteration required during correction is depicted in Figure 6.11. Although the prediction accuracy of starting state is promising (as shown in Figure 6.9), the correction step requires too many iteration at the first few cycles.

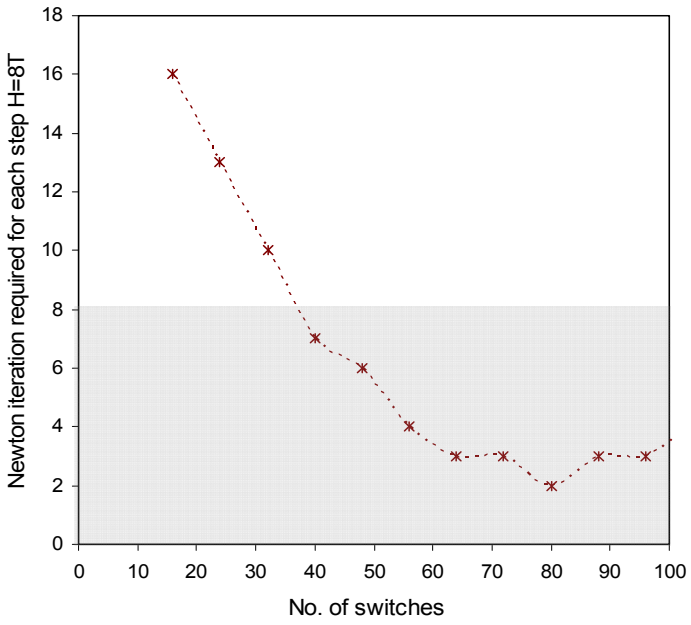

Figure 6.11 *Newton iterations required for second order multivalue method.*

The question is: how to keep the number of iterations within the shade area (less than 8 in this case)? Putting this in general, for each time step H_n, it should be less than H_n / T, or in total, less than the number of switches required to reach the steady state. We will investigate on this issue in the following sections.

6.4 Improvement of the Algorithm

In this Section, we will aim at ultimately using the quasi-envelope concept to achieve faster integration in the simulation of SMB operation. This is considered from the following aspects:

- *When should the QE line start to be used, e.g. choosing the first point of Q1?*
- *How does a change stepsize affect the performance?*

6.4.1 The Time for Launching the Quasi-Envelope Concept

From Figure 6.11 of the last Section, one would naturally think that if Newton iteration used in the prediction of QE line is more than the number of switch during that particular step, it will be more realistic to directly use successive substitution. However, the advantage of QE method has also been demonstrated at the later cycles. Can we jump onto the express train somewhere during the operation?

Still using the previous constant integration stepsize, $H = 8T$, the first point of $z(t)$ is moved forward for one cycle (8T). It can be seen from Figure 6.12 that as a result, we are gradually restricting the number of correction steps into the desired zone.

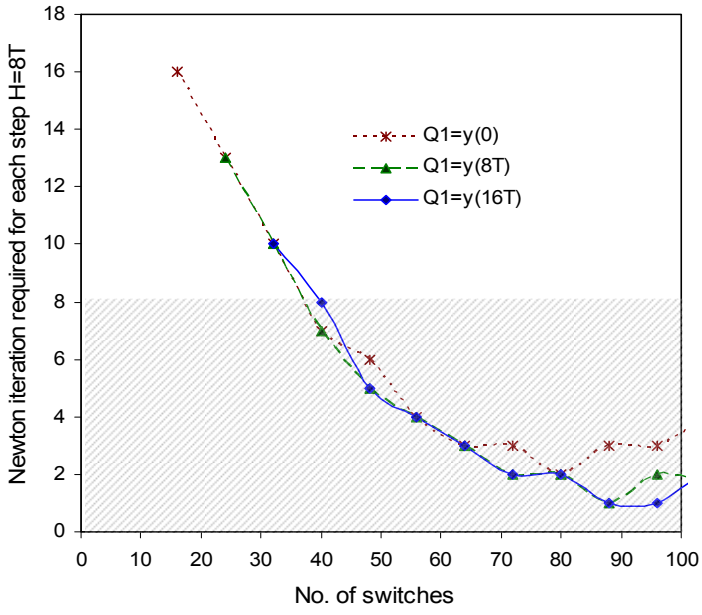

Figure 6.12 *Correction step required during the prediction of* $z(t)$ with $H=8T$

For $Q1 = y(0)$, the first predicted QE point is at 16th switch, for $Q1 = y(8T)$, the first prediction of QE is at the start of 24th switch, and so on. For the case of $Q1 = y(16T)$, we actually run initial 24 switches by successive substitution to give $z(t)$ the starting two points. Table 6.1 is given below to help the understanding of this mechanism.

Table 6.1 *Prediction result from different Q1 location (H=8T).*

No. switch	Required correction steps			Predicted starting state (g/L)			Starting state from Successive substitution (g/L)
	Q1=y(0)	Q1=y(8T)	Q1=y(16T)	Q1=y(0)	Q1=y(8T)	Q1=y(16T)	
0							0.00
8							78.70
16	16			181.55			175.64
24	13	13		205.62	202.66		200.53
32	10	10	10	206.77	207.35	207.44	207.13
40	7	7	8	209.39	208.88	208.94	209.19
48	6	5	5	209.70	209.59	209.56	209.90
56	4	4	4	209.80	209.86	209.88	210.17
64	3	3	3	210.27	210.05	210.09	210.27
72	3	2	2	210.52	210.28	210.22	210.32
80	2	2	2	210.28	210.44	210.28	210.33
88	3	1	1	209.87	210.44	210.25	210.34
96	3	2	1	209.80	210.18	210.15	210.34
Switch/Step Ratio	88/70	80/49	72/36				

Here, the Switch/Step ratio "80/49" stands for total of 49 correction steps in the outer integration to predict 80 switches in real process operation. The higher this ratio the better the performance is. It is apparent that the call for inner integration is significantly reduced when QE is launched after the first few cycles.

To evaluate the accuracy, we compared the predicted starting state with the calculated starting state from successive substation using absolute relative error as criterion. This is shown in Figure 6.13. It can be kept under 0.2% if the quasi-envelope is launched after the first two cycles.

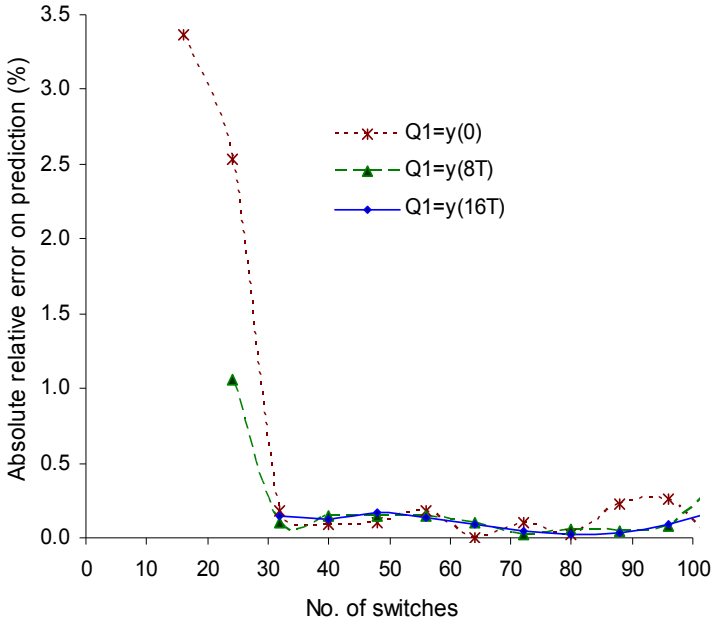

Figure 6.13 *Absolute relative error for QE prediction with H=8T*

Similar results can be obtained with constant stepsize of $H = 6T$ (Figure 6.14a) and $H = 10T$ (Figure 6.14b). Detailed prediction results and accuracy evaluation are given in Table 6.2, Figure 6.15, Table 6.3, and Figure 6.16, respectively.

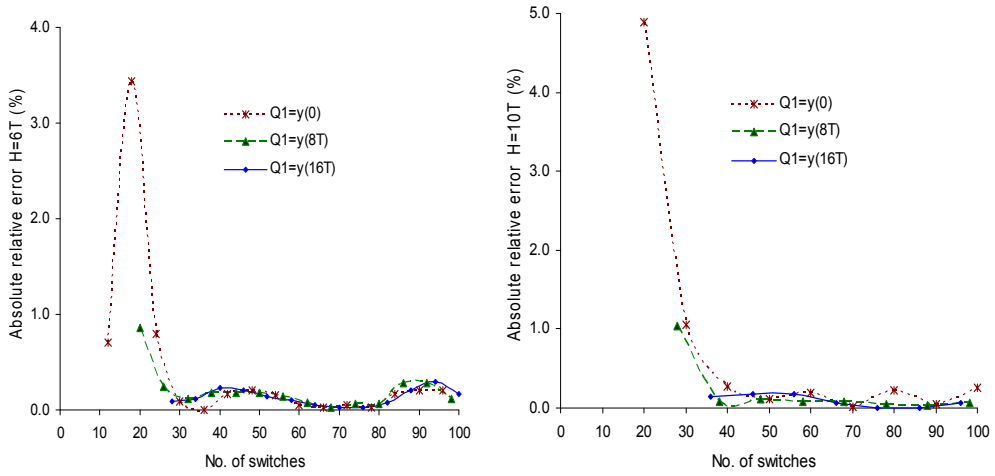

(a) ***(b)***

Figure 6.14 *Absolute relative error for QE prediction with (a) H=6T; (b) H=10T*

Table 6.2 *Prediction results from different Q1 location (H=6T).*

Q1=y(0)				Q1=y(8T)				Q1=y(16T)			
N_s	N_{cret}	QE Predict	SS Calculate	N_s	N_{cret}	QE Predict	SS Calculate	N_s	N_{cret}	QE Predict	SS Calculate
0											
6				8							
12	13	140.61	141.61	14				16			
18	11	191.81	185.44	20	10	193.93	192.28	22			
24	9	202.13	200.53	26	8	203.51	203.01	28	7	204.98	204.81
30	7	206.32	206.14	32	6	206.88	207.13	34	6	207.53	207.77
36	5	208.43	208.44	38	5	208.50	208.87	40	4	208.72	209.19
42	4	209.09	209.44	44	3	209.27	209.64	46	4	209.37	209.79
48	3	209.48	209.90	50	4	209.62	210.00	52	2	209.76	210.07
54	3	209.82	210.13	56	1	209.87	210.17	58	3	210.00	210.21
60	2	210.12	210.23	62	3	210.09	210.26	64	1	210.17	210.27
66	2	210.35	210.29	68	2	210.36	210.3	70	2	210.26	210.31
72	2	210.42	210.32	74	2	210.44	210.32	76	1	210.27	210.32
78	2	210.27	210.33	80	2	210.19	210.33	82	2	210.16	210.33
84	3	209.99	210.33	86	2	209.74	210.34	88	2	209.90	210.34
90	3	209.92	210.34	92	3	209.73	210.34	94	2	209.72	210.34
96	3	209.92	210.34	98	3	210.58	210.34	100	2	209.99	210.34
	90/72				**84/54**				**78/38**		

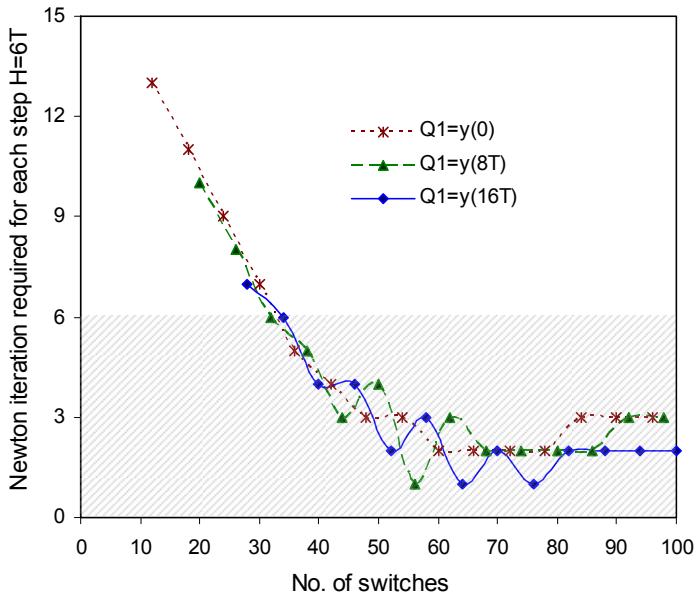

Figure 6.15 *Correction step required during the prediction of* $z(t)$ with *H=6T*

Table 6.3 *Prediction results from different Q1 location (H=10T).*

Q1=y(0)				Q1=y(8T)				Q1=y(16T)			
N_s	N_{cret}	QE Predict	SS Calculate	N_s	N_{cret}	QE Predict	SS Calculate	N_s	N_{cret}	QE Predict	SS Calculate
0											
10				8							
20	19	201.67	192.28	18				16			
30	15	208.31	206.14	28	15	206.92	204.81	26			
40	10	208.61	209.19	38	12	208.71	208.87	36	12	208.76	208.44
50	8	210.23	210.00	48	8	209.67	209.9	46	9	209.42	209.79
60	6	209.81	210.23	58	6	210.04	210.21	56	6	209.82	210.17
70	4	210.28	210.31	68	4	210.13	210.3	66	5	210.14	210.29
80	3	210.78	210.33	78	2	210.23	210.33	76	2	210.32	210.32
90	3	210.44	210.34	88	3	210.28	210.34	86	2	210.33	210.34
100	4	209.79	210.34	98	2	210.19	210.34	96	2	210.22	210.34
	90/72				**80/52**				**70/38**		

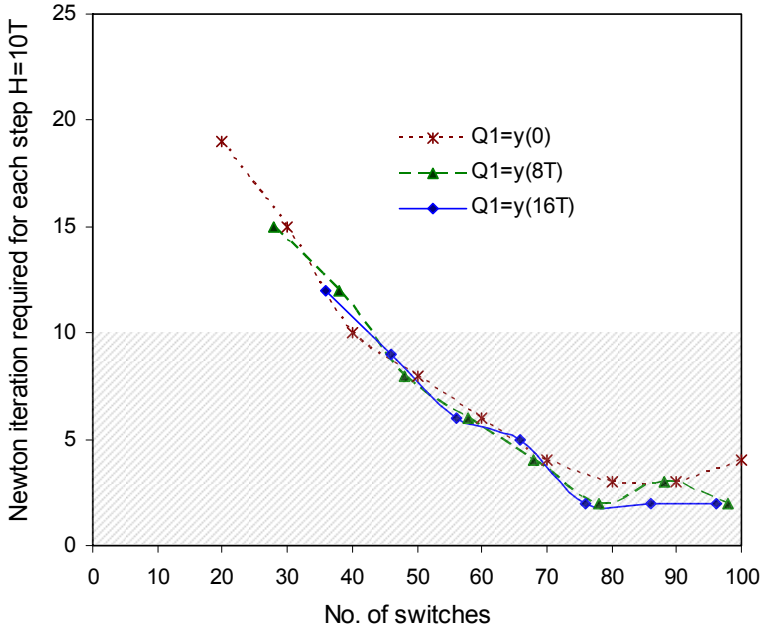

Figure 6.16 *Correction step required during the prediction of* $z(t)$ with *H=10T*

To look at the impact of stepsize and starting point, we draw a summary figure of their switch/step ratios in Figure 6.17. The ratio is based on the minimum switch required to reach a steady state.

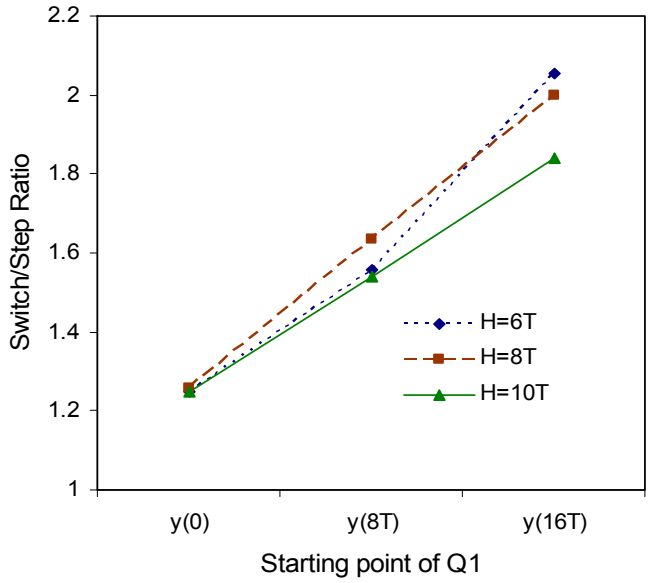

Figure 6.17 *The Switch/Step ratio from QE integration*

From these trials, the following conclusions can be made:

- If choosing $z(0) = y(0)$, the multivalue algorithm would require similar computational effort (total number of correction steps) to achieve the steady state prediction of $z(t)$, regardless of the integration stepsize.
- If using constant stepsize, launching QE later is helpful when the quasi-envelope displays steep change at the start-up period.
- The quasi-envelope method would be of great advantage to predict the long term SMB operating states.

6.4.2 Investigation of a Changing Stepsize

As shown in Figure 6.5, the shape of the quasi-envelope which we approximated is rather an exponential function than a linear one. The derivation of this algorithm in Section 6.2 has taken into account a variable stepsize. It has been pointed out (Davis, 1984) that variable step-size can be useful for controlling the local truncation error and improving efficiency during solution of a stiff problem. We will explore this possibility in our application to see if it helps with the improvement of performance, nevertheless, attentions will be given on the cost of computation.

There are two ways under consideration: the judicious choice of the stepsize and the adaptive determination of the stepsize.

For the later, adaptive stepsize strategies rely on the local or global estimation error. It involves the choosing of step-size for one step, the adopted approximation algorithm and its accuracy order, definition of test criteria and an expression for the step size to use for the next step or to repeat the rejected step. No matter which method was used, the basic mechanism is to execute one step and to perform the test. If the test succeeds, the step is accepted; otherwise, it is rejected. However, during this execute-test procedure, extra work is inevitably required on the top of the standard numerical method.

Alternatively, it is possible to specify analytically how the step size should be varied if one has knowledge of the process being studied. This would eliminate the test procedure. However, before using any stepsize strategies, we conducted a few trials by changing stepsize with an increment of one T for each integration step, or with a pre-defined pattern set up as below:

Case 1: *Q1 = y(0)*, stepsize: 6,6,6,8,8,8,10,10,10..…..

Case 2: *Q1=y(16T)*, stepsize: 6,6,6,10,10,10,……

The results are shown in Figure 6.18a and Figure 6.18b.

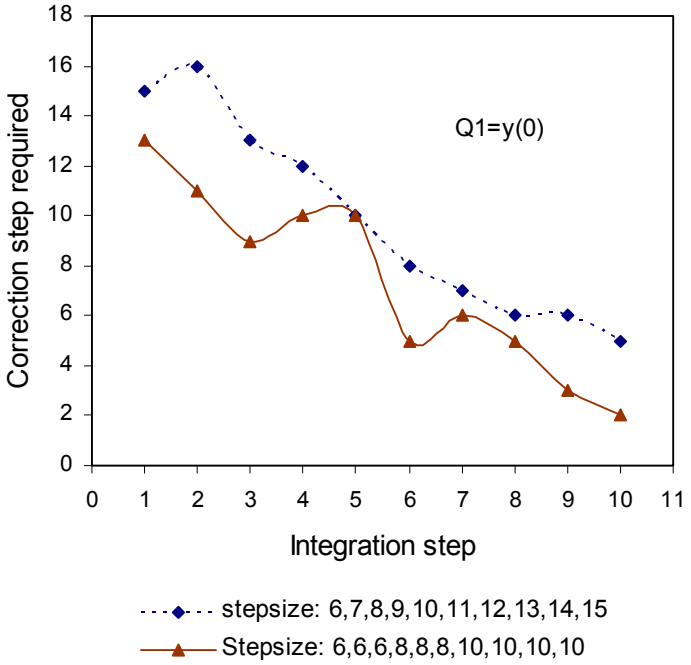

Figure 6.18a *Outer integrator performance under changing stepsize Q1=y(0)*

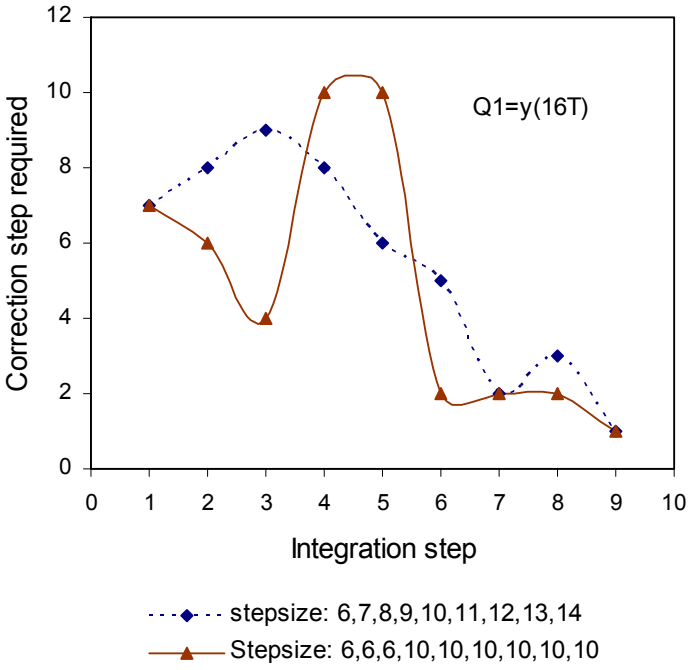

Figure 6.18b *Outer integrator performance under changing stepsize Q1=y(16T)*

Both cases show the increasing work load where the stepsize change is occurred. In general, it produces slow convergence compared to the constant stepsize strategy. This is not strange. When iteration processes used for solving the implicit relations arisen in ODE-IVP methods, it only starts to converge rapidly after a certain number of iterations. We have observed this from all the trials in this Section. This characteristic obviously prevents us from frequently changing a stepsize, unless other iteration method is imposed to achieve faster convergence right from the beginning. There are many modifications to this method in the aim of improving global convergence property. However, it is beyond the scope of this study and will be further investigated in future.

6.5 Concluding Remarks

Earlier determination of steady state is needed for the evaluation of the SMB performance and control strategies can be decided ahead. In this study, we have successfully applied the concept of Quasi-Envelope in order to achieve a faster prediction of this state. The view of SMB operation as a highly oscillatory process brought a totally new approach of achieving the steady state. It has been considered that, for such a cyclic operation, stationary conditions prevail when the cycle time is much less than the characteristic process time, in this case, the time required achieving cyclic steady state. This scheme provides an indirect prediction via a pseudo smooth function and avoids the detailed calculation of transit equations. The computational time spent on the determination of steady state can be reduced by half.

The standard Newton's method has simple structure and quadratic convergence behaviour that have attracted researchers for many decades and it is still a stand-alone method for solving nonlinear equations/systems. Related computational cost comes from two contributions, respectively due to the Jacobian updates and due to the successive iterations. In the implicit stages of multistep method, the corrector will be solved iteratively by generating a sequence of iterates. Unfortunately, this iteration process only starts to converge rapidly after a certain number of iterations. In particular, iteration methods whose error amplification matrix is non-normal often exhibit such behaviour. In order to take full advantage of the proposed concept for the approximation of cyclic operation, further investigations on the iteration methods will be helpful, e.g. the parallel iteration or via L-U decomposition.

Nomenclature

g: first-order derivative of z

H: step size for integration

$Q1$: the initial state of z

R_n: stepsize ratio for the consecutive integration step

T: duration of one cycle

$\mathbf{w}_n$: matrix of several pieces of information from t_n step only

y: original function

z: Quasi-envelope function

$\alpha; \beta$: coefficients in multistep integration formula

$\mathbf{\Phi}$: Jacobian matrix for the Newton algorithm

CHAPTER 7
CONCLUSIONS AND RECOMMENDATIONS

Simulated moving bed chromatography represents a type of chemical engineering processes and exhibits non-linear, non-ideal, multivariable-coupling, and hybrid system dynamics with significant time delay. Given the value of the products and operating costs, the effort in SMBCP modelling has big impact for industries and will be translated into significant monetary benefits. However, developing techniques for solving SMBCP models is challenging due to the high order model equations with complexity.

Survey on the previous work reveals that, in the mathematical modelling of SMBC processes, the numerical procedure can be investigated from two aspects: one is the discretisation technique to circumvent the steep gradients encountered, and the other is how to rapidly obtain the solution at stationary state for any arbitrary initial condition.

The overall aim of this project was to develop or apply frontier techniques for numerical computing of SMB chromatographic processes model, and to provide a practically useful tool for achieving the model solution which is useful for real-time control and online optimisation. To achieve this overall aim, studies have been carried out in:

(1) SMBCP dynamics analysis and model selection to identify various SMBCP models and their dynamic properties in representing the adsorption process;

(2) Numerical solution to investigate a powerful numerical computing framework for solutions of complicated SMBCP model using frontier spatial discretisation techniques;

(3) Fast simulation to develop an effective integration procedure for the simulation of cyclic operation of SMBCP with sufficient stability and robustness.

Conclusions and recommendations are addressed below around these three investigated aspects.

7.1 CONCLUSIONS

This thesis makes significant contribution to the numerical solution and simulation of SMBCP models through systematic and comprehensive study on model selection, discretisation technique and integration scheme. The first contribution lies in the systematic model analysis to characterise their complexity and dynamic behaviours so that a proper model type can be selected to meet particular application requirement. Contribution also goes to the comprehensive investigation of different numerical methods for the solution of PDEs representing particular problems. Furthermore, this is the first time to apply wavelet based approaches, as well as high resolution methods, to solving complex SMBCP models. The fourth contribution goes to the development of effective integration techniques for fast steady state determination of SMBC operation. This is the first time that a completely new concept is introduced to avoid the direct substitutions traditionally used in the simulation of SMB process.

(I) *Model Dynamic Analysis and Simplification*

1) Among the three broad classes of models, the equilibrium theory and plate models are not adequate for the realistic modelling and application because of its empirical nature cannot be related to first principles. The statistical model was used for simple calculation of estimates of the variance of chromatographic band profiles and to study the mechanism of band broadening. The solutions of PDEs which describe the mass balance and the mass transfer kinetics are the basis of model predictive control.

2) In terms of SMB modelling approach, equivalent true moving bed model (TMB) is a rather severe idealization of the simulated countercurrent process and is restricted to the case of three or more columns per zone with linear isotherms and no reaction is involved Since TMB models do not include the transient regime of the quasi-stationary, periodic steady state of SMB processes and do not consider the upper and lower bounds of the retention time, an SMB optimisation based on TMB model will lead to a miscalculated operating condition. However, dynamic SMB modelling gives the essential information for a better understanding of chromatographic processes. It is a crucial aid to develop control strategies and to analysis the stability of SMB processes concerning malfunctions.

3) Selection of column model is vital in dynamic SMB modelling. This determines the complexity of the model representation and, thereafter, the computational intensity. In summary, a column model can be chosen from the following three types:

Ideal model. Both mass transfer resistance and axial dispersion are neglected.

Dispersive model. Mass transfer resistance and axial dispersion are modelled. The model has a compromise between accuracy and computational efficiency.

General rate model. The following effects are modelled: convection, axial dispersion, pore diffusion, solid and liquid phase mass transfer, multi-component adsorption, and homogenously/heterogeneously catalysed reactions.

The effort on model development for process control can be made in two aspects: obtaining the sufficiently accurate model with simple representation and good robustness, and development of computationally efficient algorithms for solving the model equations which ultimately capture the process dynamics. This requires that the chosen of model is detailed enough to describe the complexity of the process dynamics and on the other hand is suitable for simulation and real time control.

4) The Transport-Dispersive-Equilibrium column model based on the absorption equilibrium isotherm and a linear driving force (LDF) approach for mass transfer from bulk to solid phase offers a realistic representation of industrial processes and proves a good compromise between accurate and efficient solutions of these models.

(II) *Discretisation Technique Solving PDEs with Singularity*

1) In the prediction of transit behaviour of wave propagation, comparisons of the numerical solutions from finite difference, wavelet and high resolution methods with analytical solutions revealed that all the proposed methods work well when the PDEs system has low Peclet number. The high resolution method provides an accurate numerical solution for the PDEs in question with moderate value of Pe. The wavelet collocation method is capable of catching up steep changes in the solution, and thus can be used for numerically solving PDEs with high singularity.

2) For similar degree of discretisation, wavelet does show its advantage of using less collocation points to obtain a reasonable prediction. Analysis on error distributions further proves this property. For the finite difference method, the error exists at every section of the wave, e.g., front, peak and tail, especially; the peak presents the largest error. For the wavelet method, the error is located at the front and tail, but not around the peak, which is actually the turning point of error sign. This reflects the capability of the wavelet method in capturing steep change very well.

3) From the case study of glucose-fructose separation process which has relatively simple isotherm representations, two selected methods (wavelets and finite difference) produce

almost identical profiles; however, as far as computational cost is concerned, wavelet-based algorithm takes remarkably less time for each switching period.

4) Applications of wavelet based approaches and high resolution methods to a dynamic SMB model for an enantiomers separation process shows that both of the methods are good candidates for the numerical solution of this complex model. They have provided encouraging results in terms of computation time and prediction accuracy on steep front. However, high resolution methods would be more preferable in this case because of better stability at achieving steady state and closer approximation to experimental data.

5) Although simulation using wavelet-based approach has been conducted under different levels, the results from lower levels (J = 4 & 5) can fit equivalently well with the experimental data, especially at the feeding port, where the concentration front experiences a sudden change. Higher level (over J = 6) demands much more computational time while giving a similar prediction performance.

6) In terms of the two approaches (wavelet collocation and high resolution) mainly investigated here, wavelet based methods have the advantage of capturing system dynamics at low resolution levels, therefore, requires less computational efforts, however, prior knowledge of wavelet is required in order to take advantage of this kind of method. High resolution presents better stability at achieving steady state, closer approximation to experimental data, and is easy for implementation.

7) This research shows that both methods are good candidates for the numerical solution of this type of complex models.

(III) *Fast Determination of Steady State for Cyclic Operation*

1) Earlier determination of steady state is useful for the control and optimisation of SMB processes. In this study, we have successfully applied the concept of Quasi-Envelope in order to achieve a faster prediction of this state. Although the algorithm was originally proposed for the approximation of highly oscillatory ordinary equations, it is proved to be a worthwhile tool for the simulation of SMB separation process.

2) If the starting state of Quasi-Envelope is chosen the same as original function, the multivalue algorithm would require similar computational effort (total number of correction steps) to achieve the steady state prediction, regardless of the integration stepsize.

3) If using constant stepsize, launching QE later is helpful when quasi-envelope displays steep change at the start-up period.

4) A changing stepsize produces slow convergence compared to the constant stepsize strategy, thus increasing the work load where the stepsize change is occurring. It coincides with the observation that, when iteration processes used for solving the implicit relations arise in ODE-IVP methods, it only starts to converge rapidly after a certain number of iterations. It requires other iteration method being imposed to achieve faster convergence right from the beginning.

5) This scheme provides an indirect prediction via a pseudo smooth function and avoids the detailed calculation of transit equations. The computational cost for the determination of steady state is ultimately reduced. Nevertheless, through further refinement of the proposed algorithm, potential applications can be seen to other chemical engineering processes with inherent cyclic behaviour.

In conclusion, the research tasks outlined in Chapter 1 have been fully completed and we have presented the main results in the relevant chapters of the thesis.

7.2 RECOMMENDATIONS

With the increasing recognition of the significance of the SMB chromatographic process technology by various industries, systematic investigations become necessary into the modelling, solutions and simulation of the models. The results obtained in this study are encouraging for their applications to other complicated industrial systems. Further investigation is recommended into various aspects of the discussed numerical computing method to improve their capability for numerically solving difficult PDEs.

1) Further work is recommended in this area to provide model validation. Using actual experimental data from real SMB case will strengthen the results obtained in this study.

2) It is realised from this study that wavelet based methods should be used with caution because overestimation of wave peak is observed in our simulation results as well as in previous work. Unlike the finite difference and high resolution methods, wavelet based methods do not follow the rule of the more points the better the approximation. The selection of wavelet resolution level is highly related to specific problem. This property affects the reliability of wavelet-based method in the approximation of PDEs. Structural insight for the algorithm mechanism might be necessary to make it become a generically useful tool.

3) We have also noted that the selection of the interpolating degree for boundary treatment in the adopted wavelet-based method appears very important since it could affect the numerical solution significantly. No report has been found so far in the open literature on

how to systematically adjust this parameter. Further investigation should be carried out to clarify this issue.

4) The standard Newton's method has simple structure and quadratic convergence behaviour, which have attracted researchers for many decades. It is still a stand-alone method for solving nonlinear equations/systems. However, to improve global convergence property, one has to pay attention to the two computational cost associated contributions, the Jacobian updates and successive iteration. In order to take full advantage of the proposed quasi-envelope concept for the determination of steady state of cyclic operation, further investigations on the iteration methods will be useful, e.g., the parallel iteration or via L-U decomposition.

5) Considering high dimensionality is always a problem for controller design and simulating the process model on-line, the development of control-relevant model reduction techniques is a worthwhile area for exploration. We have used wavelet-collocation method to derive a non-linear but high-order ordinary differential equation model to approximate the SMBCP dynamics. Then, the concept of inertial manifold can be applied to group the slow and fast subsystems in wavelet domain, resulting in a low-order ODE system that still accurately reproduces the dominant dynamics of the original system. The asymptotic validity of the ODE approximation can be established using the singular perturbation theory.

6) Future work can also be conducted in the development of model predictive control scheme based on the reduced model. Though model predictive control is now a fairly standard technique for model-based control, it is still challenging to design a non-linear version for optimal SMB operation with sufficient stability and robustness.

Effective control of an SMB process is a significant industrial problem at the frontier of engineering research. By application of the leading edge research techniques in applied mathematics, process modelling, and advanced control, a better understanding and implementation of the optimal SMB operation to achieve efficient and high purity separations could be achieved. The outcomes will be beneficial to many related industries. We look forward to making contributions to further development and advances in this area.

REFERENCES

1. Abel, S., Erdem, G., Mazzotti, M., Morari, M. & Morbidelli, M. (2004). Optimising control of simulated moving beds – linear isotherm. *Journal of Chromatography A*, 1033, 229-239.

2. Araújo, J. M. M., Rodrigues, R. C. R., & Mota, J. P. B. (2006). Use of single-column models for efficient computation of the periodic state of a simulated moving-bed process. *Industrial and Engineering Chemistry Research*, 45(15), 5314-5325.

3. Azevedo, D. C. S. & Rodrigues, A. S. (2000). Obtainment of high-fructose solutions from cashew (Anacardium occidentale) apple juice by simulated moving-bed chromatography. *Separation Science and Technology*, 35(16), 2561-2581.

4. Barreto Jr., A. G., José da Silva Jr., I., Garcia dos Santos, M. A., Vinicius de Veredas, & Santana, C. C. (2008). Modeling, simulation, and experimental evaluation of continuous chromatographic separation of ketamine enantiomers on MCTA. *Journal of Liquid Chromatography & Related Technologies*, 31(20), 3057-3076.

5. Bertoluzza, S. (1996). A wavelet collocation method for the numerical solution of partial differential equations. *Applied Computers and Harmonia Analysis*, 3, 1-9.

6. Bertoluzza, S., & Naldi, G. (1994). Some remarks on wavelet interpolation. *Journal of computational and applied mathematics,* 13(1), 13–32.

7. Bertoluzza, S., Canuto, C., & Urban, K. (2000). On the adaptive computation of integral wavelets. *Applied and Numerical Mathematics*, 34, 13-38.

8. Beste, Y. A., Lisso, M., Wozny, G., & Arlt, W. (2000). Optimisation of simulated moving bed plants with low efficient stationary phases: separation of fructose and Glucose. *Journal of Chromatography A,* 868, 169-188.

9. Bhatia, S. K. (1991). Analysis of catalytic reactor operation with periodic flow reversal. *Chemical Engineering Science*, 46(1), 361-367.

10. Biegler, L. T., Jiang L., & Fox, V. G. (2004). Recent advances in simulation and optimal design of pressure swing adsorption systems. *Separation and Purification Reviews*, 33(1), 1-39.

11. Bindal, A., Khinast J. G., & Ierapertritou M. G. (2003). Adaptive multiscale solution of dynamical systems in chemical processes using wavelets. *Computers and Chemical Engineering*, 27, 131-142.

12. Biressi, G., Ludemann-Hombourger, O., Mazzotti, M., Nicoud, R. M., & Morbidelli, M. (2000). Design and optimisation of a simulated moving bed unit: role of deviations from equilibrium theory. *Journal of Chromatography A*, 876, 3-15.

13. Blom, J. G., & Zegeling, P. A. (1994). Algorithm 731: a moving-grid interface for systems of one-dimensional time-dependent partial differential equations. *ACM Transactions on Mathematical Software*, 20, 194-214.

14. Borges da Silva, E. A., Souza, D. P., Ulson de Souza, A. A., Souza, S. M., Rodrigues, A. E. (2005). Analysis of the behaviour of the simulated moving bed reactor in the sucrose inversion process. *Separation Science and Technology*, 40, 2373-2389.

15. Briesen, H., & Marquardt, W. (2005). Adaptive multigrid solution strategy for the dynamic simulation of petroleum mixture processes. *Computers and Chemical Engineering*, 29(1), 139-148.

16. Chang, S. C., & To, W. M. (1991). *A New numerical framework for solving conservation laws-The method of space-time conservation element and solution element.* NASA TM 104495.

17. Ching, C. B. (1997). Parabolic intraparticle concentration profile assumption in modelling and simulation of nonlinear simulated moving-bed separation processes. *Chemical Engineering Science*, 53(6), 1311-1315.

18. Chu, K. H., & Hashim, M. A. (1995). Simulated countercurrent adsorption processes: a comparison of modelling strategies. *The Chemical Engineering Journal*, 56, 59-65.

19. Crittenden, B., & Thomas, W. J. (1998). *Adsorption technology & design*. Oxford: Butterworth-Heinemann.

20. Cruz, P., Mendes, A., & Magalhães, F. D. (2001). Using wavelets for solving PDEs: an adaptive collocation method. *Chemical Engineering Science*, 56, 3305-3309.

21. Cruz, P., Mendes, A., & Magalhães, F. D. (2002). Wavelet-based adaptive grid method for the resolution of nonlinear PDEs. *American Institute of Chemical Engineering Journal*, 48(5), 774-785.

22. Cruz, P., Santos, J. C., Magalhães, F. D., & Mendes, A. (2005). Simulation of separation processes using finite volume method. *Computers and Chemical Engineering*, 30, 83-98.

23. Davis, M. E. (1984). *Numerical Methods & Modelling for Chemical Engineers*. New York: John Wiley & Sons, Inc.

24. Dondi, F., & Remelli, M. (1986). The characteristic function method in the stochastic theory of chromatography. *The Journal of Physical Chemistry*, 90(9), 1885-1891.

25. Dondi, F., Munari, P., Remelli, M., & Cavazzini, A. (2000). Monte Carlo model of nonlinear chromatography. *Analytical Chemistry*, 72, 4353-4362.

26. Dorfi, E. A., & Drury, L. O. C. (1987). Simple adaptive grids for 1 - D initial value problems. *Journal of Computational Physics*, 69, 175-195.

27. Dünnebier, G., Fricke, J., & Klatt, K-U. (2000a). Optimal design and operation of simulated moving bed chromatographic reactors. *Industrial and Engineering Chemistry Research*, 39, 2290-2304.

28. Dünnebier, G., Weirich, I., & Klatt, K-U. (1998). Computationally efficient dynamic modelling and simulation of SMB chromatographic processes with linear isotherms. *Chemical Engineering Science*, 3(14), 2537-2546.

29. Dünnerbier, G., & Klatt, K-U. (2000b). Modelling and simulation of nonlinear chromatographic separation processes: a comparison of different modelling approaches. *Chemical Engineering Science*, 55, 373-380.

30. Eigenberger, G., & Butt, J. B. (1976). A modified Crank-Nicolson technique with non-equidistant space steps. *Chemical Engineering Science,* 31, 681-691.

31. Erdem, G., Morari, M., Amanullah, M., Mazzotti, M., & Morbidelli, M. (2006). Optimising control of an experimental simulated moving bed unit. *American Institute of Chemical Engineering Journal*, 52(4), 1481-1494.

32. Ernst, U. P., & Hsu, J. T. (1989). Study of simulated moving-bed separation processes using a staged model. *Industrial & Engineering Chemistry Research*, 28,1211-1221.

33. Francotte, E. R., & Richert, P. (1997). Applications of simulated moving-bed chromatography to the separation of the enantiomers of chiral drugs. *Journal of Chromatography A*, 769(1-2), 101-107.

34. Furzeland, R. M. (1990). A numerical study of three moving-grid methods fro one-dimensional partial differential equations which are based on the method of lines. *Journal of Computational Physics*, 89, 349-388.

35. Gear, C. W. (1971). *Numerical Initial value problems in ordinary differential equations*. New Jersey: Prentice-Hall, Inc.

36. Glowinski, R., Lawton, W., Ravachol, M., & Tenenbaum, E. (1990). Wavelet solutions of linear and nonlinear elliptic, parabolic, and hyperbolic problems in one space dimension. *Computing Methods in Applied Sciences and Engineering, Chapter 4*. R. Glowinski and A. Lichnewsky, eds., 55-120, SIAM, Philadelphia, PA.

37. Gridding, J. C. (1960). *Dynamics of chromatography*. New York: Marcel Dekker.

38. Gu, T. (1995). *Mathematical modelling and scale up of liquid chromatography*. New York: Springer.

39. Guiochon, G. (2002). Review: Preparative liquid chromatography. *Journal of Chromatography A*, 965, 129-161.

40. Guiochon, G., & Ghodbane, S. (1988). Computer simulation of the separation of a two-component mixture in preparative scale liquid chromatography. *Journal of Physical Chemistry*, 92, 3682-3686.

41. Gunawan, R., Fusman, I., & Braatz, R. D. (2004). High resolution algorithms for multidimensional population balance equations. *American Institute of Chemical Engineering Journal*, 50, 2738-2749.

42. Gupta, V. K., & Bhatia, S. K. (1991). Solution of cyclic profiles in catalytic reactor operation with periodic flow reversal. *Computers and Chemical Engineering*, 15(4), 229-237.

43. Hashimoto, K., Adachi, S., Noujima, H., & Maruyama, A. (1983). Models for the separation of glucose/fructose mixture using a simulated moving-bed adsorber. *Journal of Chemical Engineering in Japan*, 16, 400-406.

44. Hassan, M. M., Shamsur R. A. K. M., & Loughlin, K. F. (1995). Modelling of simulated moving bed adsorption system: a more precise approach. *Separations Technology*, 5(2), 77-89.

45. Henke, S., Kubát, M., & Bubník, Z. (2008). The new simulated moving bed pilot plant-modelling, simulation and application. *Journal of Food Engineering*, 87(1), 26-33.

46. Hu, S. S., & Schiesser, W. E. (1981). An adaptive grid method in the numerical method of lines. In R. Vichnevetsky & R. S. Stepleman (Eds.), Advances in Computer Methods for Partial Differential Equations (pp.305-311). IMACS: North-Holland.

47. Hu, S. S., & Sun, Y. Y. (1987). Mathematical modelling and optimum calculation of simulated moving bed absorption. *Simulation & Control B: Mechanical & Thermal Engineering, Materials & Resources, Chemistry*, 8(2), 1-12.

48. Huang, W., & Russell, R., D. (1996). A moving collocation method for solving time dependent partial differential equations. *Applied Numerical Mathematics*, 20, 101.

49. Jiang, G., & Shu, C. W. (1996). Efficient implementation of weighted ENO schemes. *Journal of Computational Physics*, 126, 202-228.

50. Jin, S. H., & Wankat, P. C. (2005). New design of simulated moving bed for ternary separations. *Industrial and Engineering Chemistry Research*, 441(6), 1906-1913.

51. Kaczmarski, K., Mazzotti, M., Storti, G., & Morbidelli, M. (1997). Modelling fixed-bed adsorption columns through orthogonal collocations on moving finite elements. *Computers and Chemical Engineering*, 21(6), 641-660.

52. Klatt, K-U., Hanisch, F., & Dünnebier, G. (2002). Model-based control of a simulated moving bed chromatographic process for the separation of fructose and glucose. *Journal of Process Control*, 12, 203-219.

53. Kloppenburg, E., & Gilles, E. D. (1999). A new concept for operating simulated moving-bed processes. *Chemical Engineering Technology*, 22, 813-817.

54. Koren, B. (1993) A robust upwind discretisation method for advection, diffusion and source terms, *CWI Report NM-R9308* April, Department of Numerical Mathematics.

55. Lapidus, L., & Amundson, N. R. (1952). Mathematics of adsorption in beds. VI. The effect of longitudinal diffusion in ion exchange and chromatographic columns. *Journal of Physical Chemistry*, 56, 984-988.

56. Leão, C. P., & Rodrigues A. E. (2004). Transient and steady-state models for simulated moving bed processes: numerical solutions. *Computers and Chemical Engineering*, 28, 1725-1741.

57. Lee, W. C., Tsai, G. J., & Tsao, G. T. (1993). Analysis of chromatography by plate theory. *Separation Technology*, 3, 178-197.

58. Lehoucq, S., Verhève, D., Wouwer, A. V., & Cavoy, E. (2000). SMB enantio-separation: process development, modelling and operating conditions. *American Institute of Chemical Engineering Journal*, 46(2), 247-256.

59. Leitold, A., Hangos, K. M., & Tuza, Z. (2002). Structure simplification of dynamic process models, *Journal of Process Control*, 12, 69-83

60. Li, S., & Petzold, L. (1997). Moving mesh methods with upwinding schemes for time-dependent PDEs. *Journal of Computational Physics*, 131, 368-377.

61. Lim, Y. (2004c). An optimisation strategy for nonlinear simulated moving bed chromatography: Multi-level optimisation procedure (MLOP). *Korean J. Chemical Engineering*, 21(4), 836-852.

62. Lim, Y., Chang, S. C., & Jorgensen, S. B. (2004a). A novel partial differential algebraic equation (PDAE) solver: iterative space-time conservation element/solution element (CE/SE) method. *Computers and Chemical Engineering*, 28, 1309-1324.

63. Lim, Y., Jorgensen, S. B. (2004b). A fast and accurate numerical method for solving simulated moving bed (SMB) chromatographic separation problems. *Chemical Engineering Science*, 59, 1931-1047.

64. Lim, Y., Lann, J. M., & Joulia, X. (2001a). Accuracy, Temporal performance and stability comparisons of discretisation methods for the numerical solution of partial differential equations (PDEs) in the presence of steep moving fronts. *Computers and Chemical Engineering,* 25, 1483-1492.

65. Lim, Y., Lann, J. M., & Joulia, X. (2001b). Moving mesh generation for tracking a shock or steep moving front. *Computers and Chemical Engineering,* 25, 653-633.

66. Liu, Y., Cameron, I. T., & Bhatia S. K. (2001). The wavelet-collocation method for adsorption problems involving steep gradients. *Computers and Chemical Engineering*, 25, 1611-1619.

67. Lu, Y., Wei, F., Shen, B., Ren, Q., & Wu, P. (2006). Modelling, simulation of a simulated moving bed for separation of phosphatidylcholine from soybean phospholipids. *Chinese Journal of Chemical Engineering*, 14(2), 171-177.

68. Mazzotti, M., Storti, G., & Morbidelli, M. (1994). Robust design of countercurrent adsorption separation processes: 2. Multicomponent systems. *American Institute of Chemical Engineering Journal*, 40(11), 1825-1842.

69. Mazzotti, M., Storti, G., & Morbidelli, M. (1996). Robust design of countercurrent adsorption separation processes: 3. Nonstoichiometric systems. *American Institute of Chemical Engineering Journal*, 42(10), 2784-2796.

70. Mazzotti, M., Storti, G., & Morbidelli, M. (1997). Robust design of countercurrent adsorption separation processes: 4. Desorbent in the feed. *American Institute of Chemical Engineering Journal*, 43(1), 64-72.

71. Miller, K., & Miller, R. N. (1981). Moving Finite Elements. I. *SIAM Journal of numerical Analysis*, 18, 1019-1032.

72. Minceva, M., & Rodrigues, A. (2002). Modelling and simulation of a simulated moving bed for the separation of p-xylene. *Industrial & Engineering Chemistry Research*, 41(14), 3454-3461.

73. Minceva, M., & Rodrigues, A. (2005). Two-level optimisation of an existing SMB for p-xylene. *Computers and Chemical Engineering*, 29(10), 2215-2228.

74. Minceva, M., Pais, L. S., & Rodrigues, A. (2003). Cyclic steady state of simulated moving bed processes for enantiomers separation. *Chemical Engineering and Processing*, 42, 93-104.

75. Molnar, Z., Nagy, M., Aranyi, A., Hanak, L., Argyelan, J., Pencz, I., & Szanya, T. (2005). Separation of amino acids with simulated moving bed chromatography. *Journal of Chromatography A*, 1075(1-2), 77-86.

76. Natarajan, S., & Lee, J. H. (2000) Repetitive model predictive control applied to a simulated moving bed chromatograph system. *Computers and Chemical Engineering*, 24, 1127-1133.

77. Nikolaou, M., & You, Y. (1994) Chapter 7: Use of wavelets for numerical solution of differential equations. In R. Motard & B. Joseph (Eds.), *Wavelet Applications in Chemical Engineering* (pp. 210-274). Kluwer: Academic Publisher.

78. Nilchan, S., & Pantelides, C. (1998). On the optimisation of periodic adsorption processes. *Adsorption*, 4, 113-147.

79. Pais, L. S., Loureiro, J. M., & Rodrigures, A. E. (1998). Modelling strategies for enantiomers separation by SMB Chromatography. *American Institute of Chemical Engineering Journal*, 44(3), 561-569.

80. Pais, L. S., Loureiro, J. M., & Rodrigures, A. E. (2000). Chiral separation by SMB Chromatography. *Separation and Purification Technology*, 20(1), 67-77.

81. Pais, L. S., Loureiro, J. M., Rodrigures, A. E. (1997). Separation of 1,1'-bi-2-naphthol Enantiomers by continuous chromatography in simulated moving bed. *Chemical Engineering Science,* 52, 245-257.

82. Petzold, L. R. (1981). An efficient numerical method for highly oscillatory ordinary differential equations. *SIAM J Numerical Analysis*, 18(3), 455-479.

83. Petzold, L. R. (1987). Observations on an adaptive moving grid method for one-dimensional systems of partial differential equations. *Applied Numerical Mathematics*, 3, 347-360.

84. Pynnonen, B. (1998). Simulated moving bed processing: escape from the high-cost box. *J. Chromatography A*, 827, 143-160.

85. Qamar, S., Elsner, M. P., Angelov, I. A., Warnecke, G., & Seidel-Morgenstern, A. (2006). A comparative study of high resolution schemes for solving population balances in crystallization. *Computers and Chemical Engineering*, 30, 1119-1131.

86. Revilla, M. A. (1986). Simple time and space adaptation in one-dimensional evolutionary partial differential equation. *International Journal for Numerical Methods in Engineering*, 23, 2263-2275.

87. Ruthven, D. M. (1984). *Principles of adsorption and adsorption process*. New York: John Wiley & Sons, Inc.

88. Ruthven, D. M., & Ching, C. B. (1989) Counter-current and simulated counter-current adsorption separation processes. *Chemical Engineering Science*, 44(5), 1011-1038.

89. Santiago, W., & Jorgensen, S. B. (1995). Efficient simulation of periodic cycled reactor operation. *Computers & Chemical Engineering*, 19, S483-S488.

90. Sanz-Serna, J. M., & Christie, I. (1986). A Simple adaptive technique for nonlinear wave problems. *Journal of Computational Physics*, 67, 348-360.

91. Saska, M., Wu, M. D., Clarke, S. J., & Iqbal, K. (1992). Continuous separation of sugarcane molasses with a simulated moving-bed adsorber: adsorption equilibria, kinetics, and application. *Separation Science and Technology*, 27(13), 1711-1732.

92. Schulte, M. (2001). Preparative enantio-separation by simulated moving bed chromatography. *Journal of Chromatography A*, 906, 399-416.

93. Schure, M. R., & Katti, A. M. (2006). Professor Georges A. Guiochon's 75th Birthday. *Journal of Chromatography A*, 1126(1-2), 2-5.

94. Song, I. H., Lee S. B., Rhee, H. K., & Mazzotti, M. (2006). Identification and predictive control of a simulated moving bed process: purity control. *Chemical Engineering Science*, 61, 1973-1986.

95. Spear M. Separations in Flux. http://www.chemicalprocessing.com (accessed Oct 2006).

96. Storti, G., Baciocchi, R., Mazzotti, M., & Morbidelli, M. (1995). Design of optimal operating conditions of simulated moving bed adsorptive separation units. *Industrial & Engineering Chemistry Research*, 34(1), 288-301.

97. Storti, G., Masi, M., Paludetto, R., Morbidelli, M., & Carrà, S. (1988). Adsorption separation processes: countercurrent and simulated countercurrent operations. *Computers and Chemical Engineering*, 12(5), 475-482.

98. Storti, G., Mazzotti, M., Morbidelli, M., & Carrà, S. (1993). Robust design of binary countercurrent adsorption separation processes. *American Institute of Chemical Engineering Journal*, 39(3), 471-492.

99. Strohlein, G., Mazzotti, M., & Morbidelli, M. (2005). Optimal operation of simulated-moving-bed reactors for nonlinear adsorption isotherms and equilibrium reactions. *Chemical Engineering Science*, 60(6), 1525-1533.

100. Strube, J., & Schmidt-Traub, H. (1998). Dynamic simulation of simulated-moving-bed chromatographic processes. *Computers and Chemical Engineering*, 22(9), 1309-1317.

101. Toftegard, B., & Jorgensen, S. B. (1989). An integration method for dynamic simulation of cycled processes. *Computers and Chemical Engineering,* 13(8), 927-930.

102. Toumi, A., & Engell, S. (2004). Optimisation-based control of a reactive simulated moving bed process for glucose isomerisation. *Chemical Engineering Science*, 59, 3777-3792.

103. Vasilyev, O. V., Paolucci, S., & Sen, M. (1995). A multilevel wavelet collocation method for solving partial differential equations in a finite domain. *Journal of Computational Physics*, 120, 33-47.

104. Wang, C., Klatt, K-U., Dünnerbier, G., Engell, S., & Hanisch, F. (2003). Neural network-based identification of SMB chromatographic processes. *Control Engineering Practice*, 11, 949-959.

105. Wang, X., & Ching, C. B. (2004). Chiral separation and modelling of the three-chiral-centre β-blocker drug nadolol by simulated moving bed chromatography. *Journal of Chromatography A*, 1035(2), 167-176.

106. Wankat, P. C. (1986). *Large scale adsorption and chromatography*. Boca Raton: CRC Press.

107. Wei, F., Shen, B., & Chen, M. (2006). From analytical chromatography to simulated moving bed chromatography: Resolution of omeprazole enantiomers. *Industrial & Engineering Chemistry Research*, 45(4), 1420-1425.

108. Wongso, F., Hidajat, K., & Ray, A. K. (2004). Optimal operating mode for Enantioseparation of SB-553261 racemate based on simulated moving bed technology. *Biotechnology and Bioengineering*, 87(6), 704-722.

109. Wouwer, A. V., Saucez, P., & Schiesser, W. E. (1998). Some user-oriented comparisons of adaptive grid methods for partial differential equations in one space dimension. *Applied Numerical Mathematics*, 26, 49-62.

110. Xie, Y., Chin, C. Y., Phelps, D. S. C., Lee, C. H., Lee, K. B., Mun, S., & Wang. L. (2005). *A five-zone simulated moving bed for isolation of six sugars from biomass hydrolyzate*. 2005 AIChE Annual Meeting and Fall Showcase, Conference Proceedings, 1675.

111. Yao, H. M., Tian, Y. C., & Tadé, M. O. (2008). Using Wavelets for Solving SMB Separation Process Models. *Industrial & Chemical Engineering Research*, 47, 5585-5593.

112. Yu, Q., & Wang, N. (1989). Computer simulations of the dynamics of multicomponent ion exchange and adsorption in fixed beds – gradient-directed moving finite elements method. *Computers and Chemical Engineering*, 13(3), 915-926.

113. Zhang, T., Tadé, M. O., Tian, Y. C., & Zang, H. (2008). High resolution method for numerically solving PDEs in process engineering. *Computers and Chemical Engineering*, 32, 2403-2408.

114. Zhang, Z. Y., Mazzotti, M., & Morbidelli, M. (2003a). PowerFeed operation of simulated moving bed units: changing flow-rates during the switching interval. *Journal of Chromatography A*, 1006, 87-99.

115. Zhang, Z. Y., Mazzotti, M., & Morbidelli, M. (2003b). Multiobjective optimisation of simulated moving bed and Varicol processes using a genetic algorithm. *Journal of Chromatography A*, 989, 95-108.

116. Zhong, G., & Guiochon, G. (1994). Theoretical analysis of band profiles in non-linear ideal countercurrent chromatography. *Journal of Chromatography A*, 688, 1-23.

117. Zhong, G., & Guiochon, G. (1996). Analytical solution for the linear ideal model of simulated moving bed chromatography. *Chemical Engineering Science*, 51(18), 4307-4319.

118. Zhong, G., & Guiochon, G. (1997a). Simulated moving bed chromatography. Effects of an axial dispersion and mass transfer under linear conditions. *Chemical Engineering Science*, 52(18), 3117-3132.

119. Zhong, G., & Guiochon, G. (1997b). Simulated moving bed chromatography: Comparison between the behaviours under linear and nonlinear conditions. *Chemical Engineering* Science, 52(23), 4403-4418.

120. Zhong, G., Smith, M. S., & Guiochon, G. (1997c). Effect of the flow rates in linear, ideal, simulated moving-bed chromatography. *American Institute of Chemical Engineering Journal*, 43(11), 2960-2969.